Nucleosynthesis of heavy elements in the Universe and their electromagnetic signatures

Gabriel Martínez-Pinedo

Masterclass 2018 EuNPC, Bologna, September 2, 2018

Origin elements

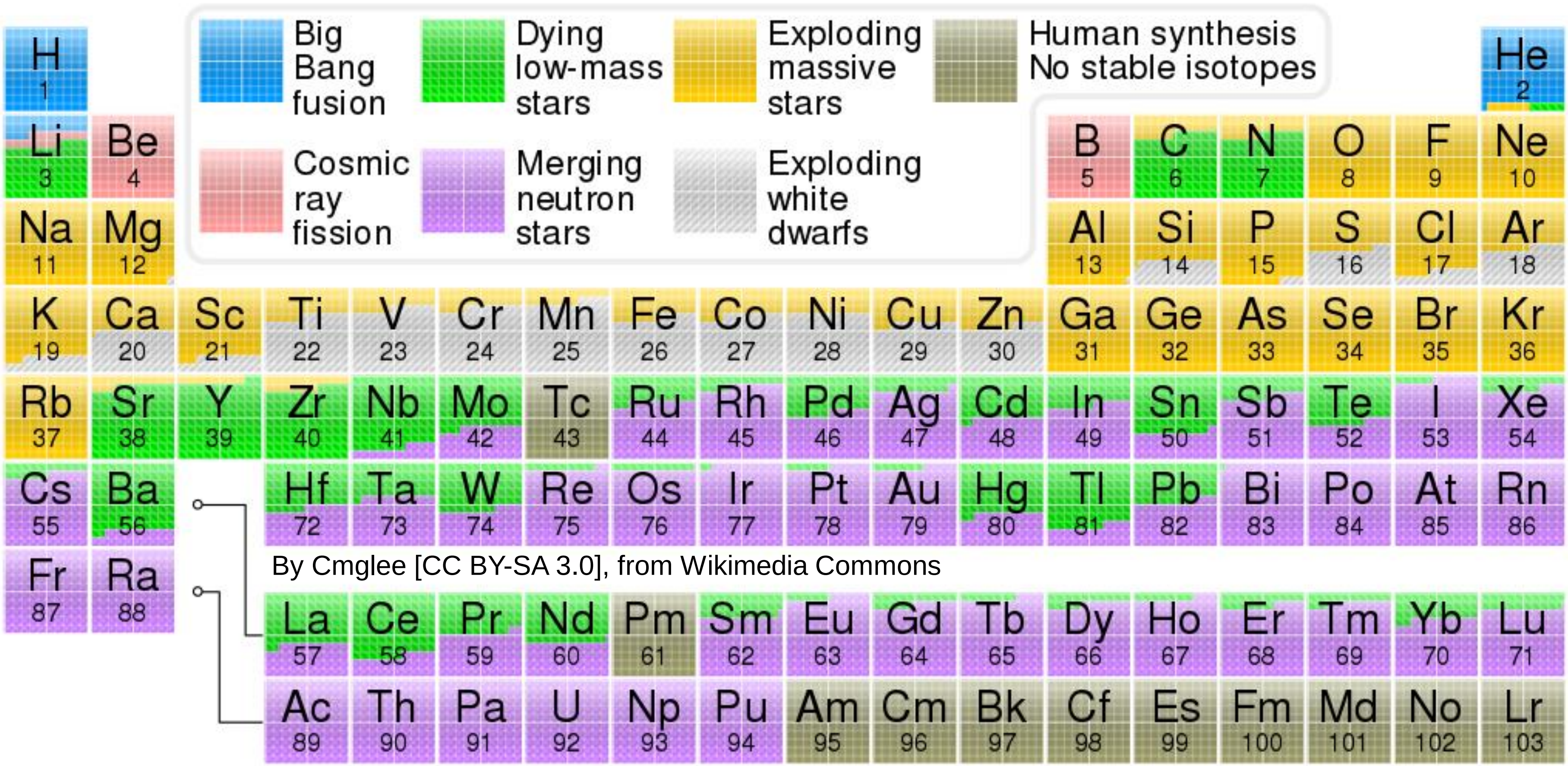

Elements consist of different isotopes with different astrophysical origins

Solar system abundances

Solar photosphere and meteorites:
chemical signature of gas cloud where the Sun formed

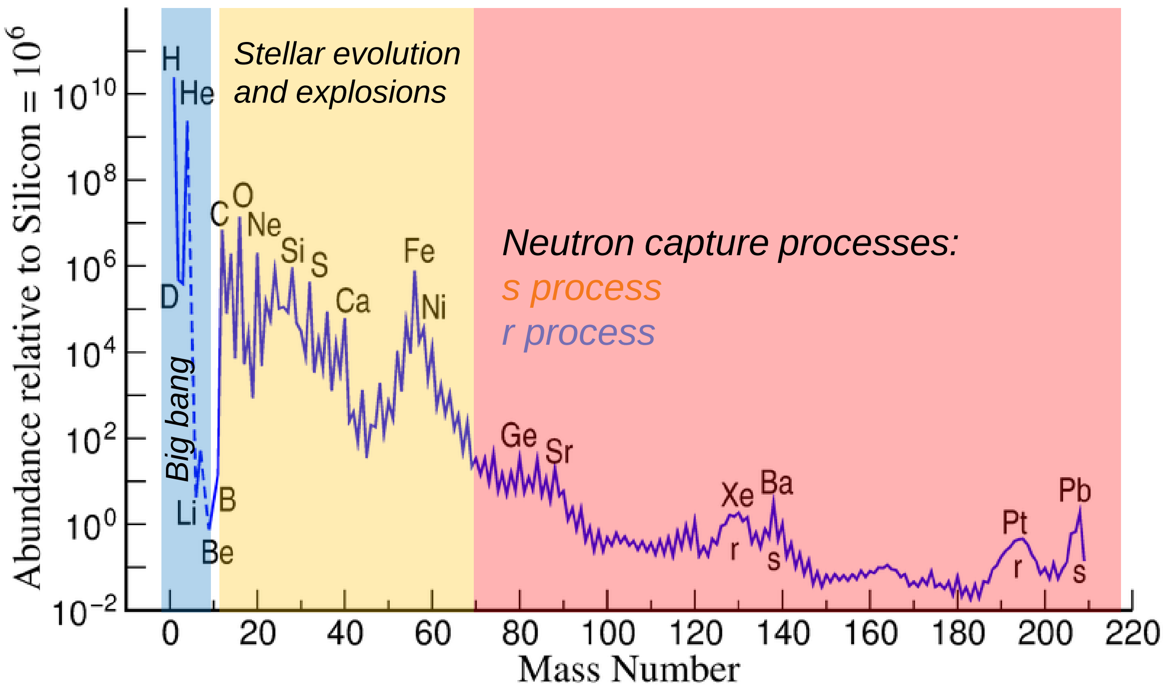

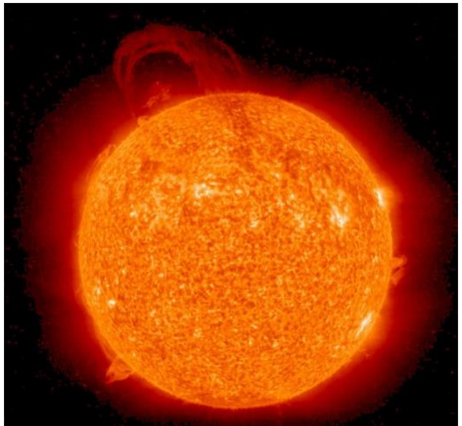

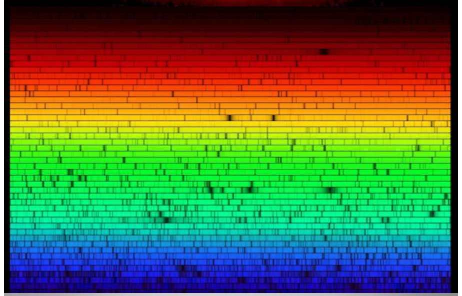

Signatures of nuclear structure and nuclear stability
Contributions of different nucleosynthesis processes

Nucleosynthesis processes

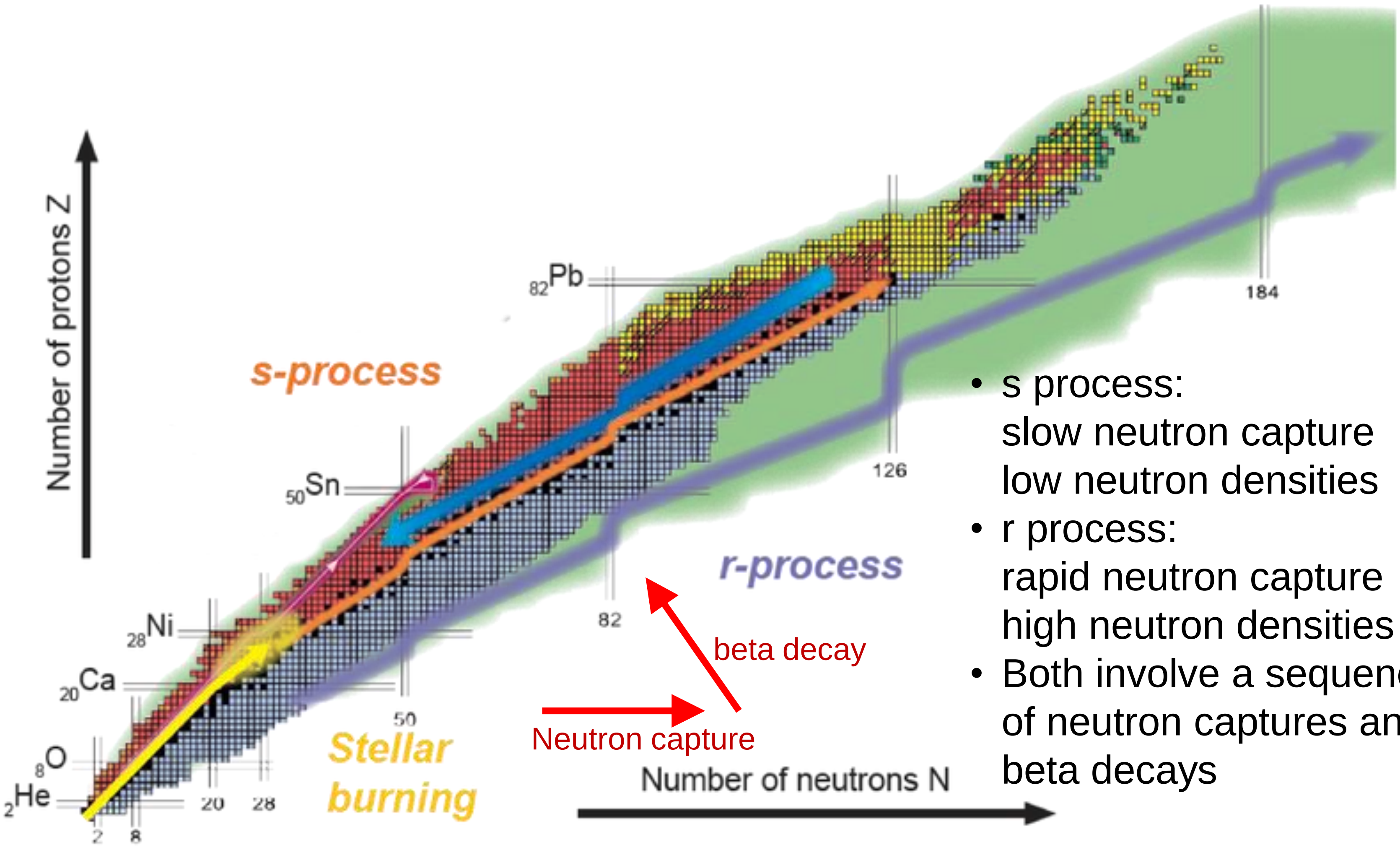

- s process:
  slow neutron capture
  low neutron densities
- r process:
  rapid neutron capture
  high neutron densities
- Both involve a sequence of neutron captures and beta decays

The s process

slow neutron capture

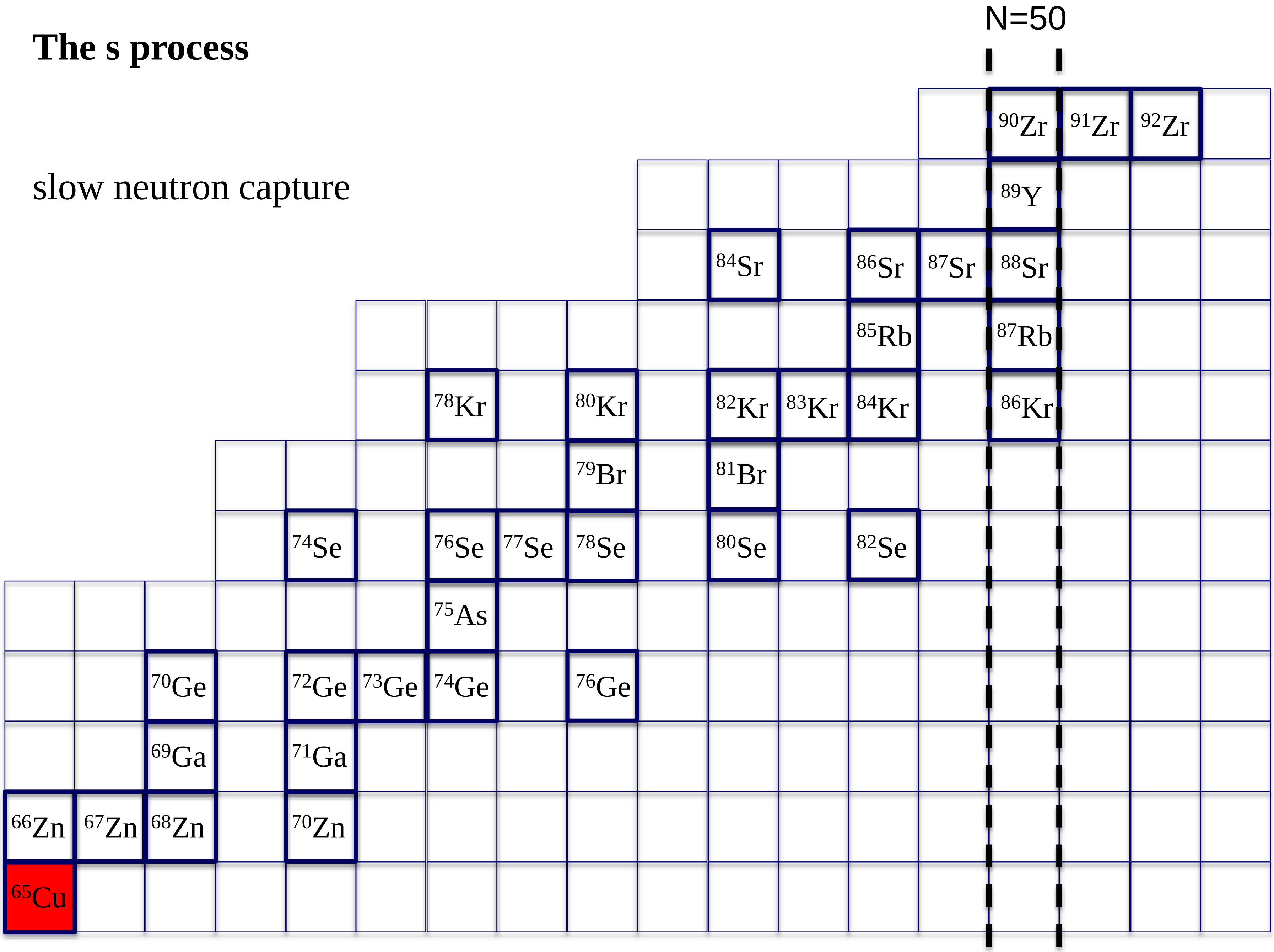

The s process

slow neutron capture

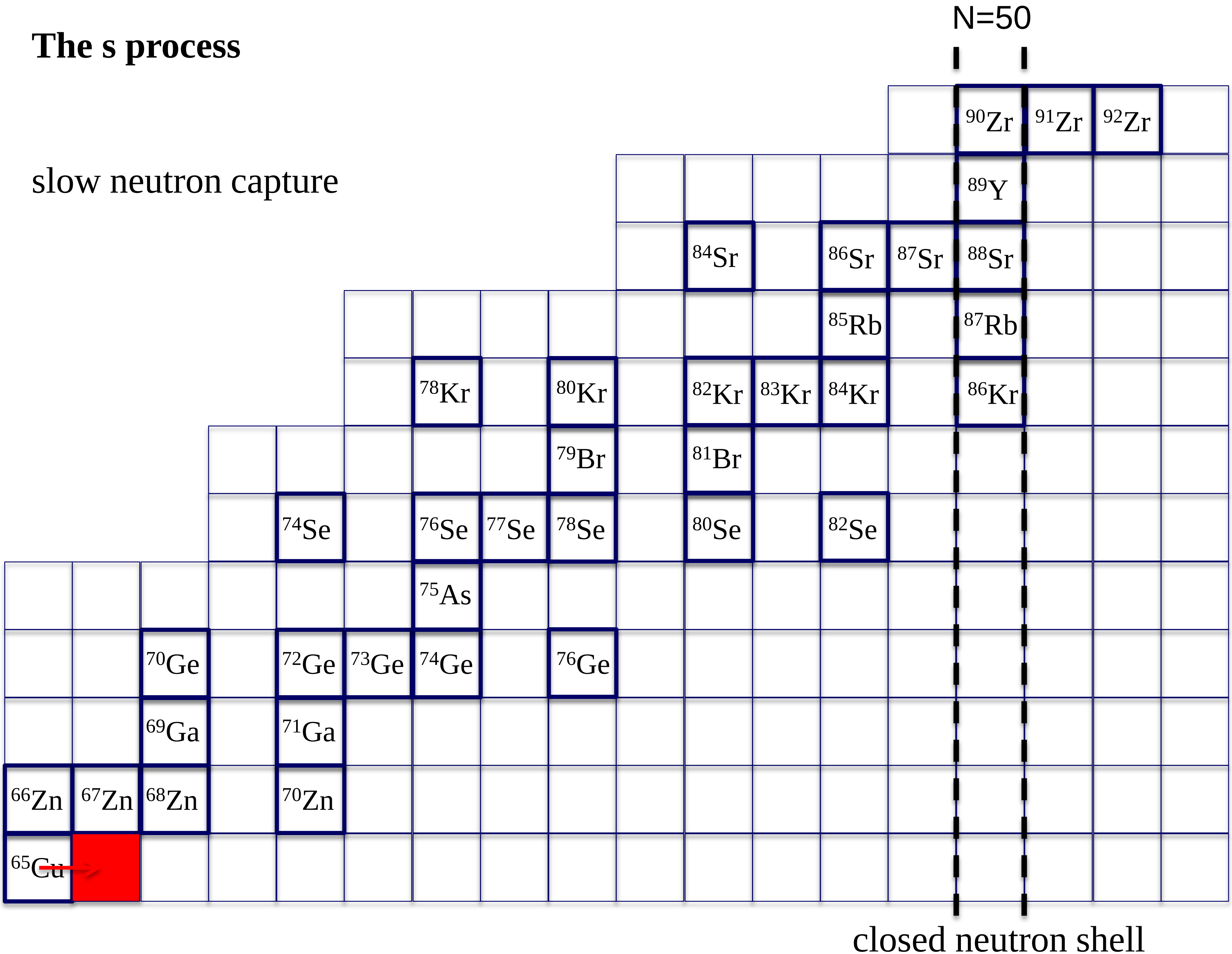

The s process

slow neutron capture

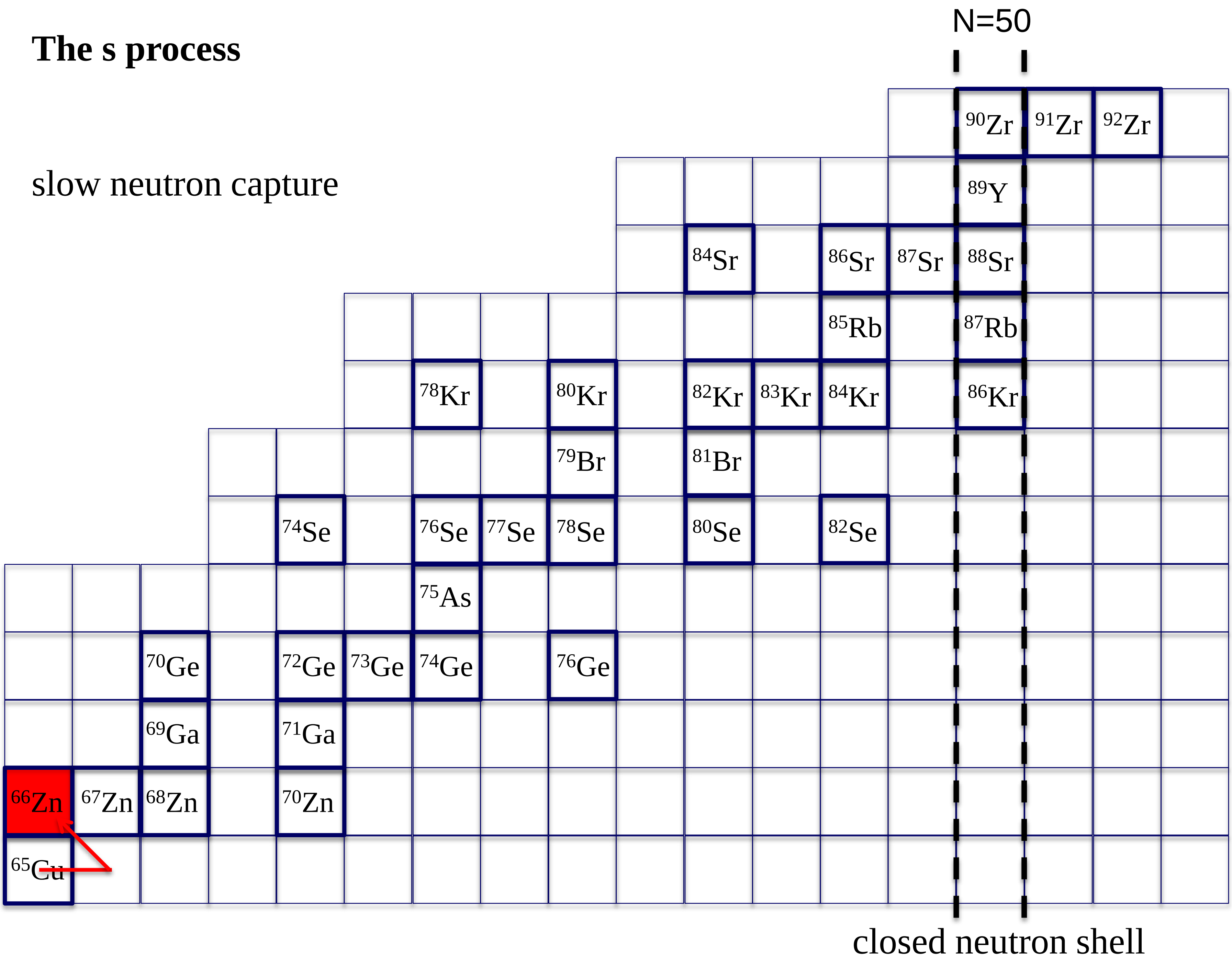

The s process

slow neutron capture

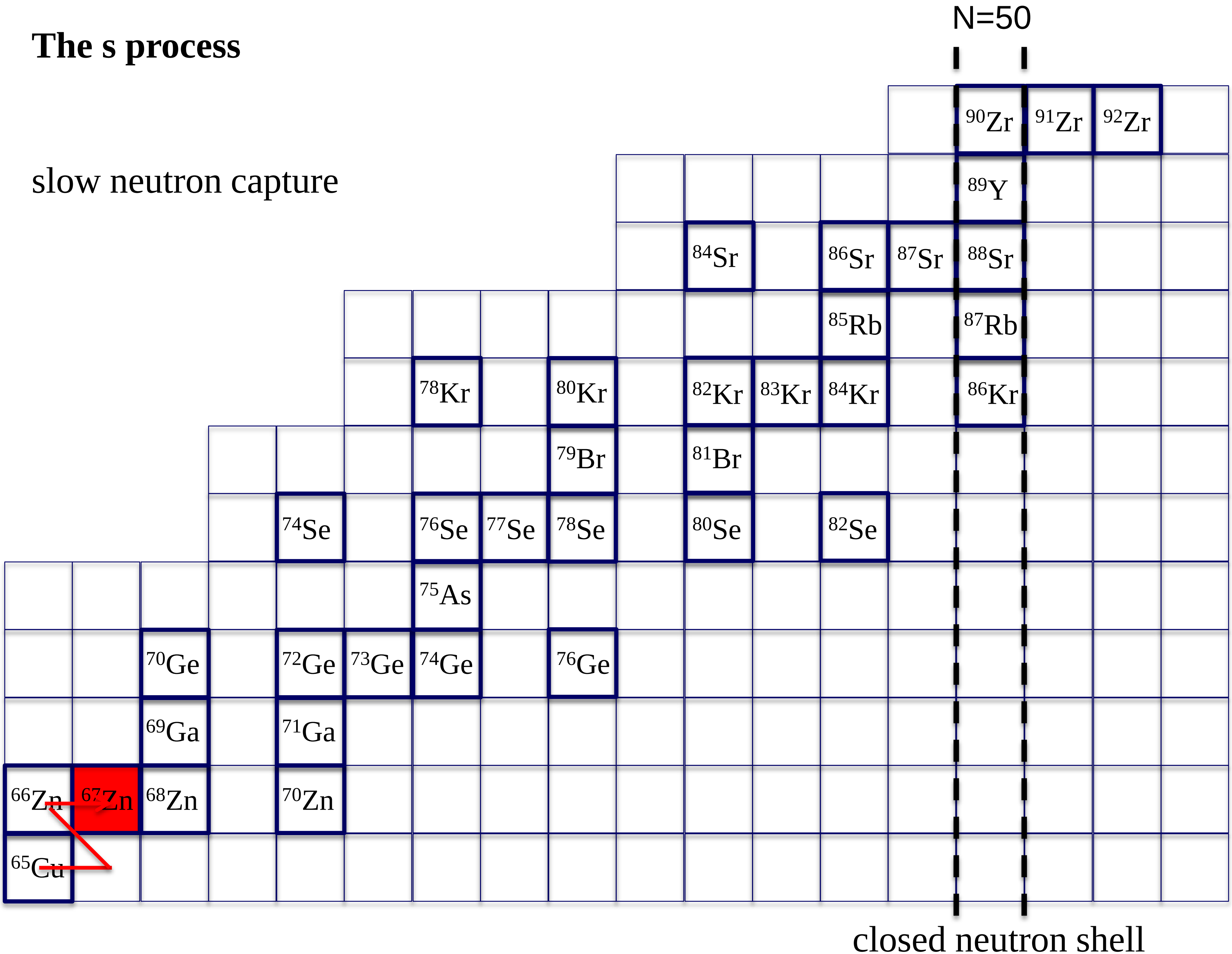

The s process

slow neutron capture

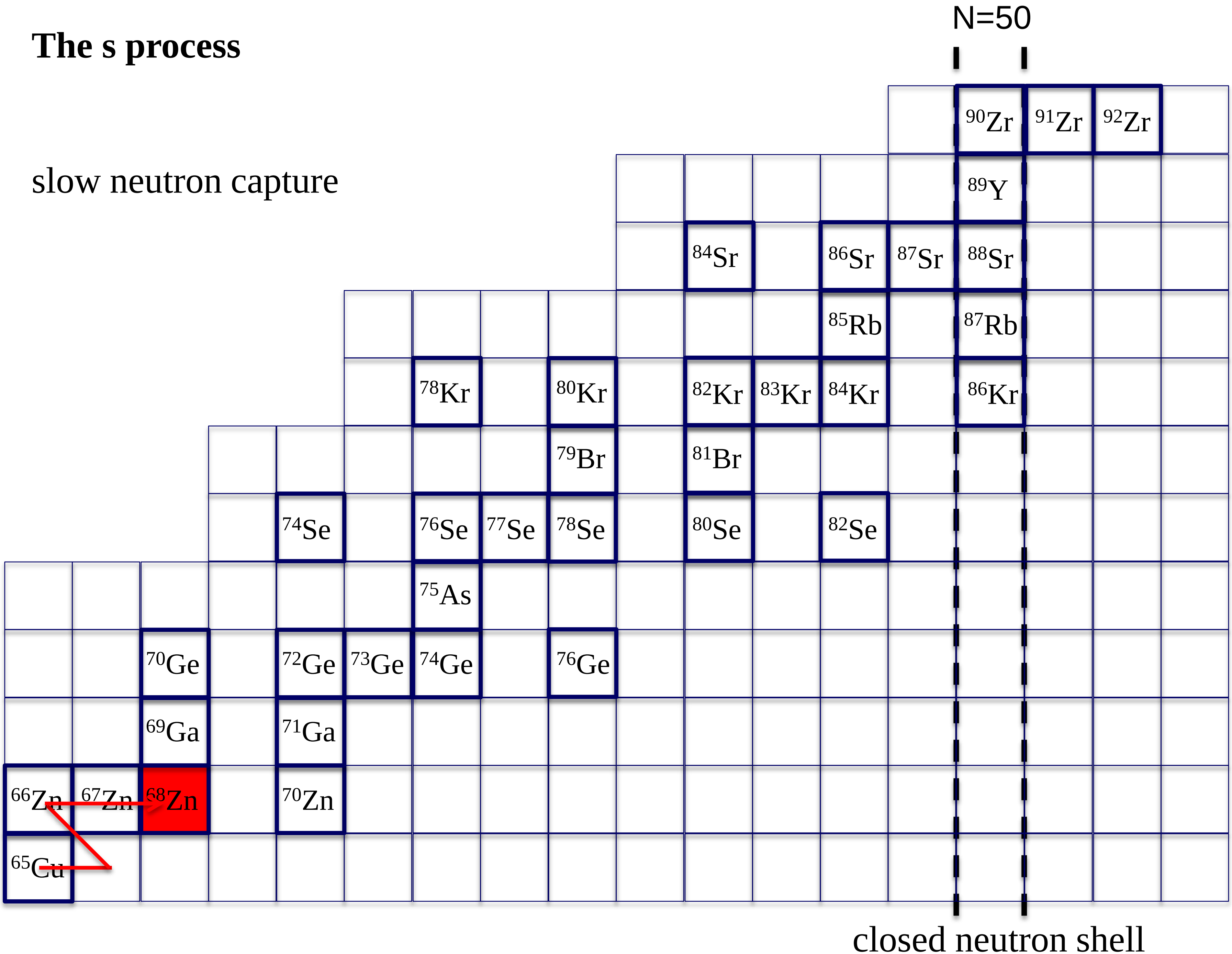

The s process

slow neutron capture

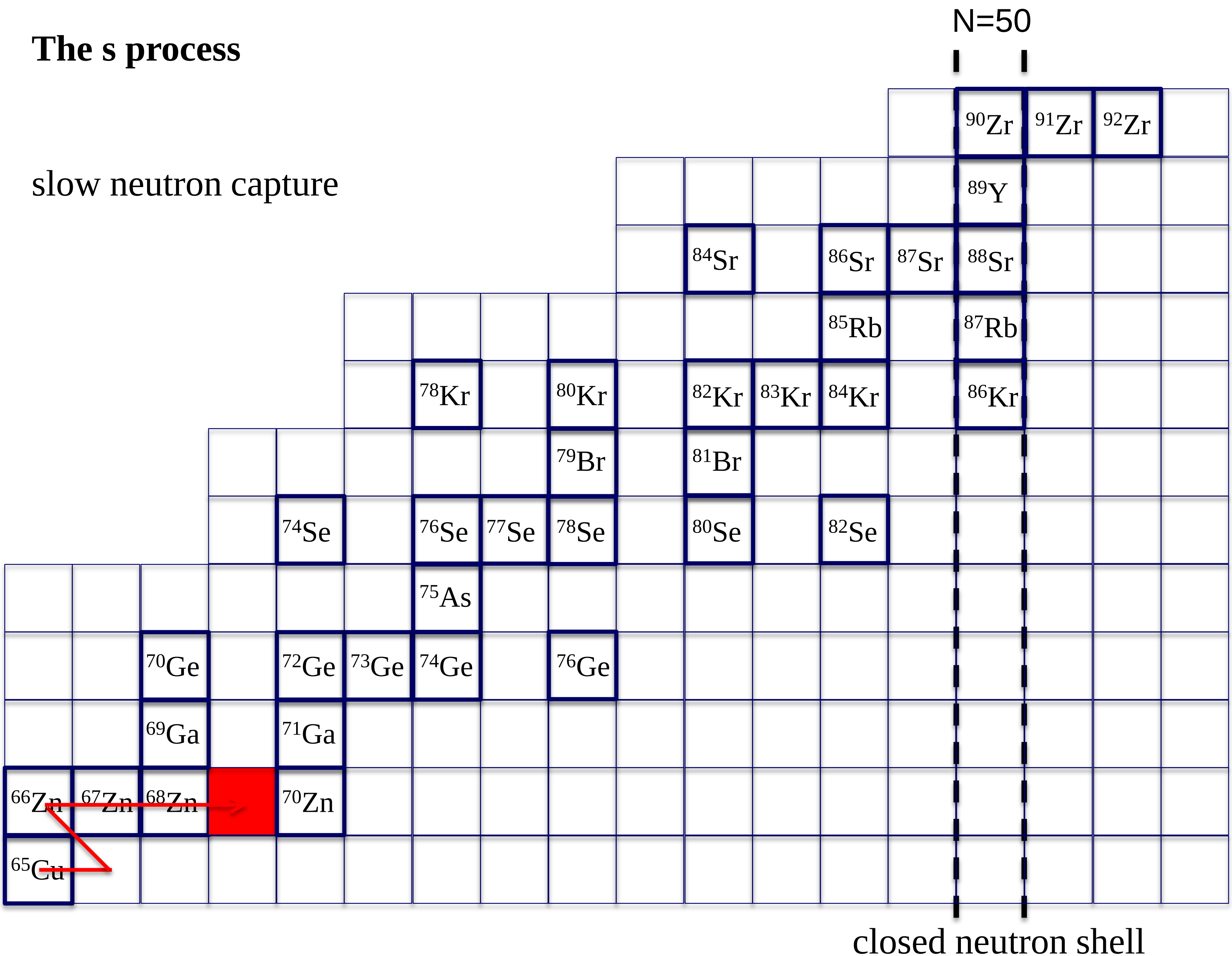

The s process

slow neutron capture

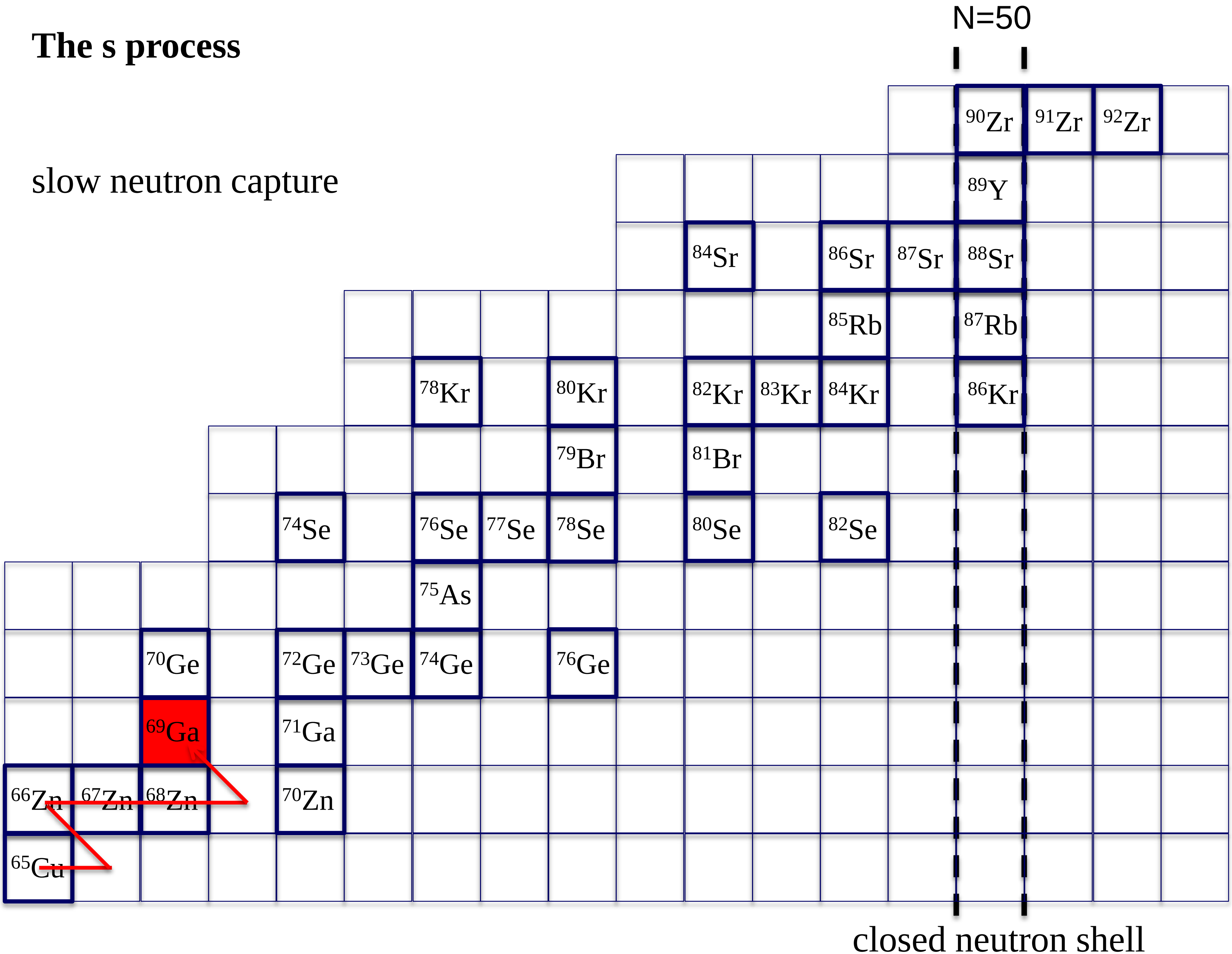

The s process

slow neutron capture

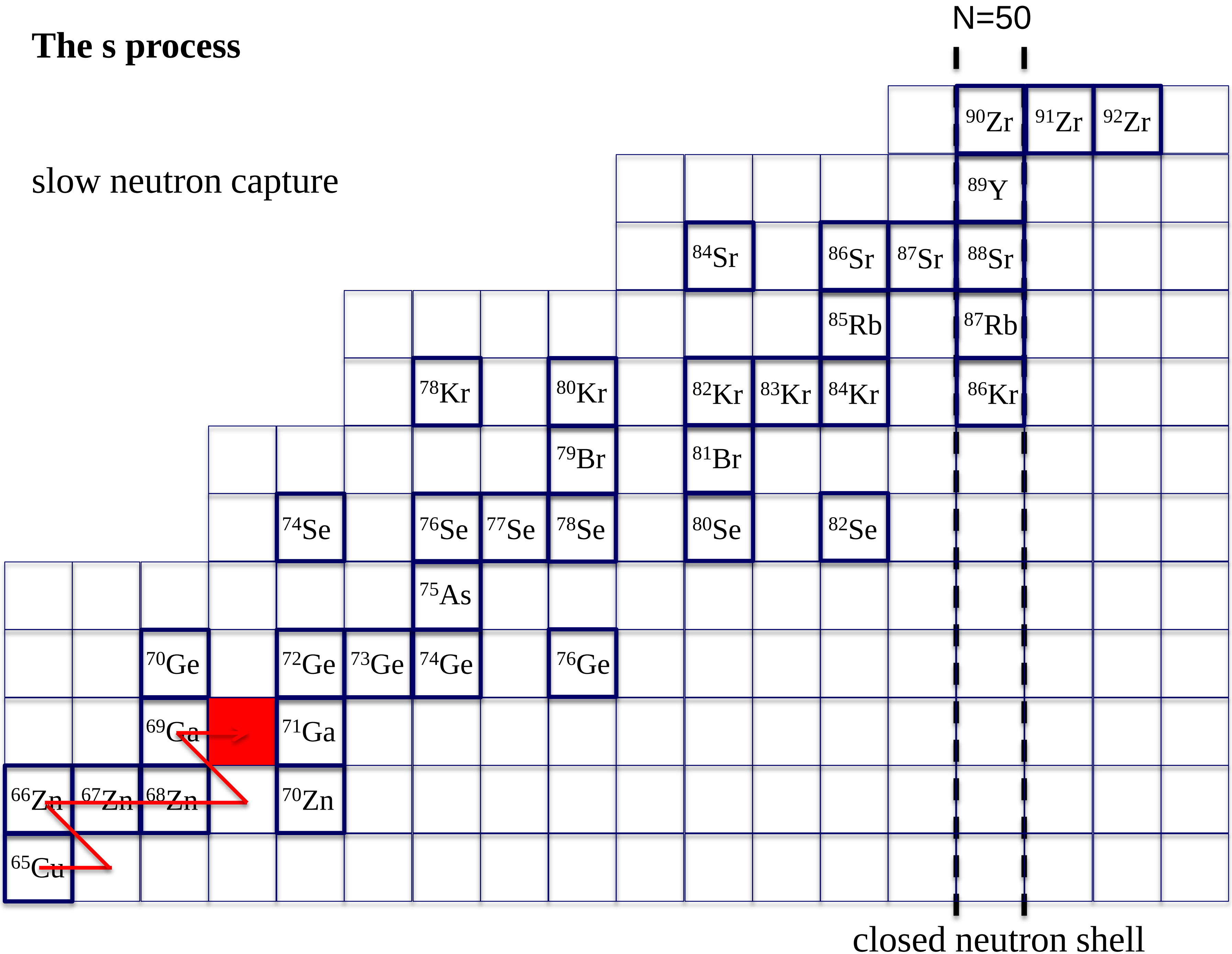

The s process

slow neutron capture

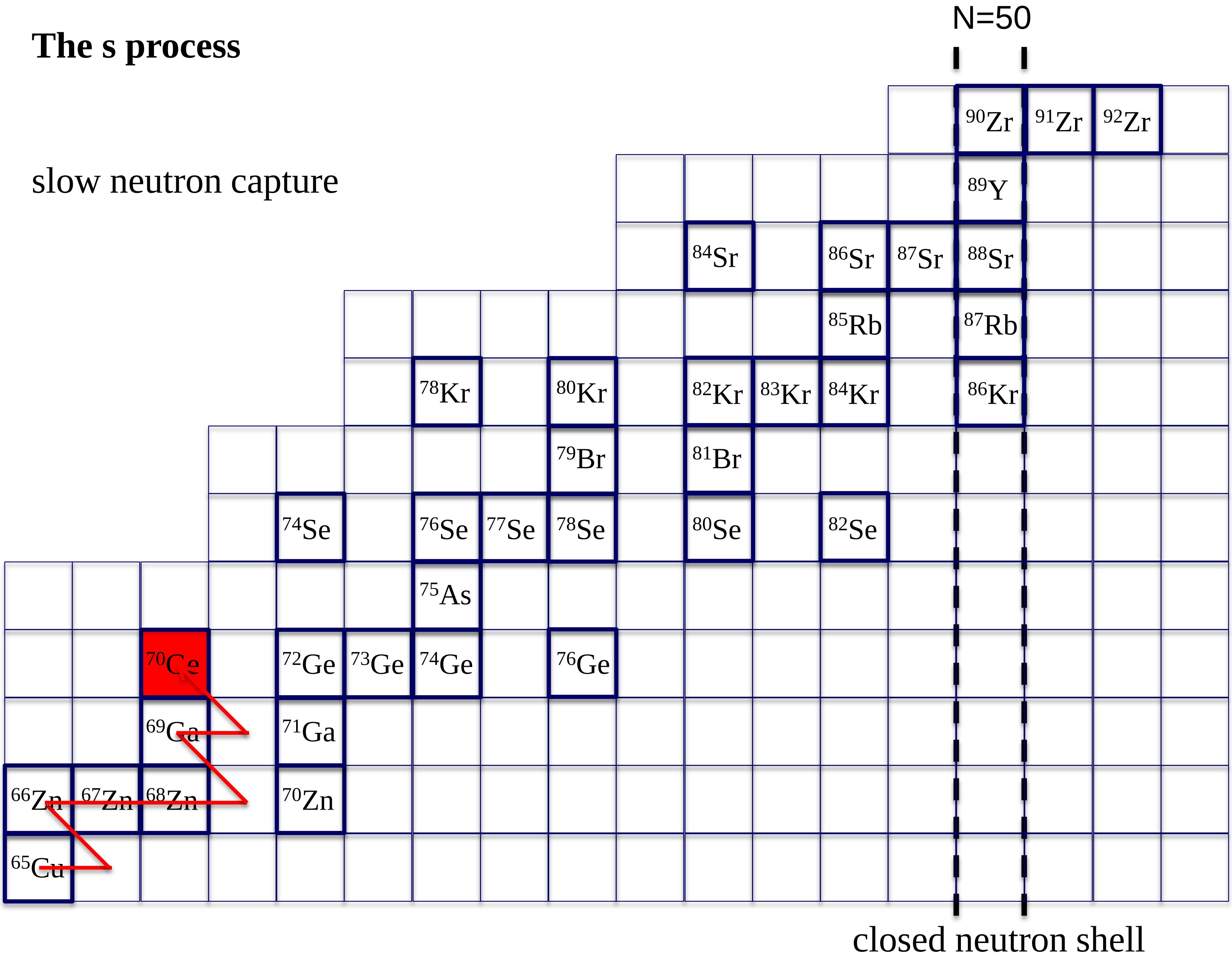

The s process

slow neutron capture

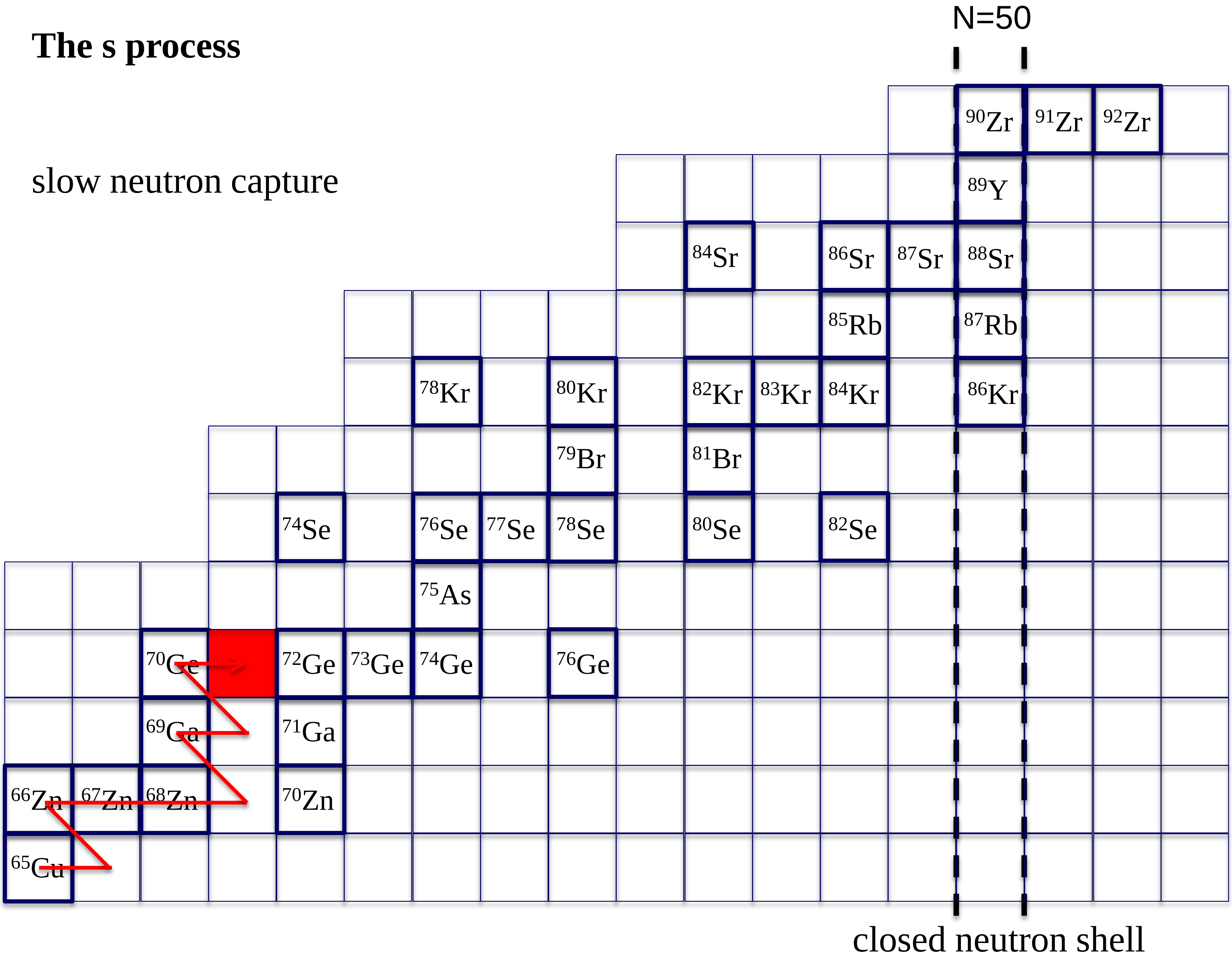

The s process

slow neutron capture

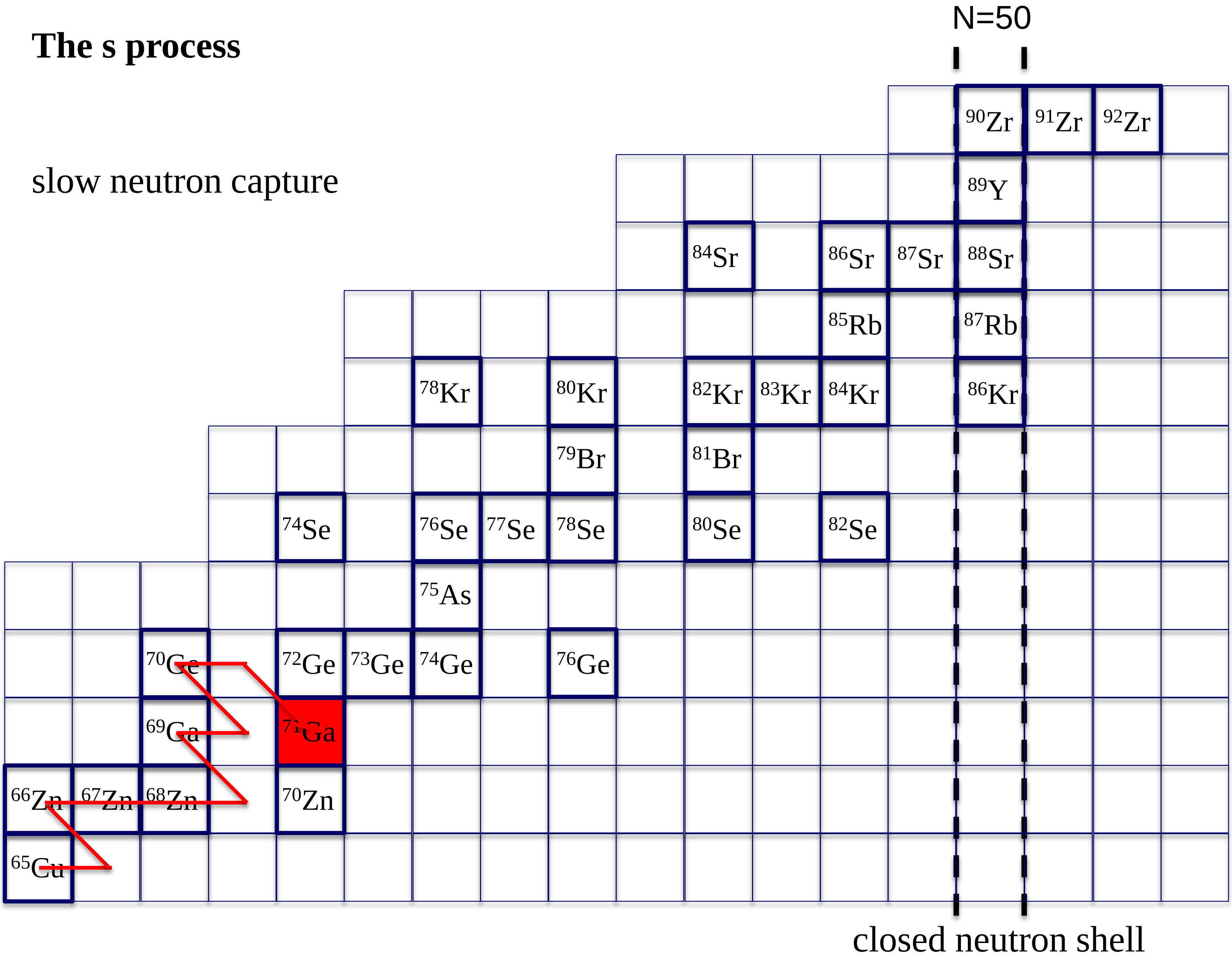

The s process

slow neutron capture

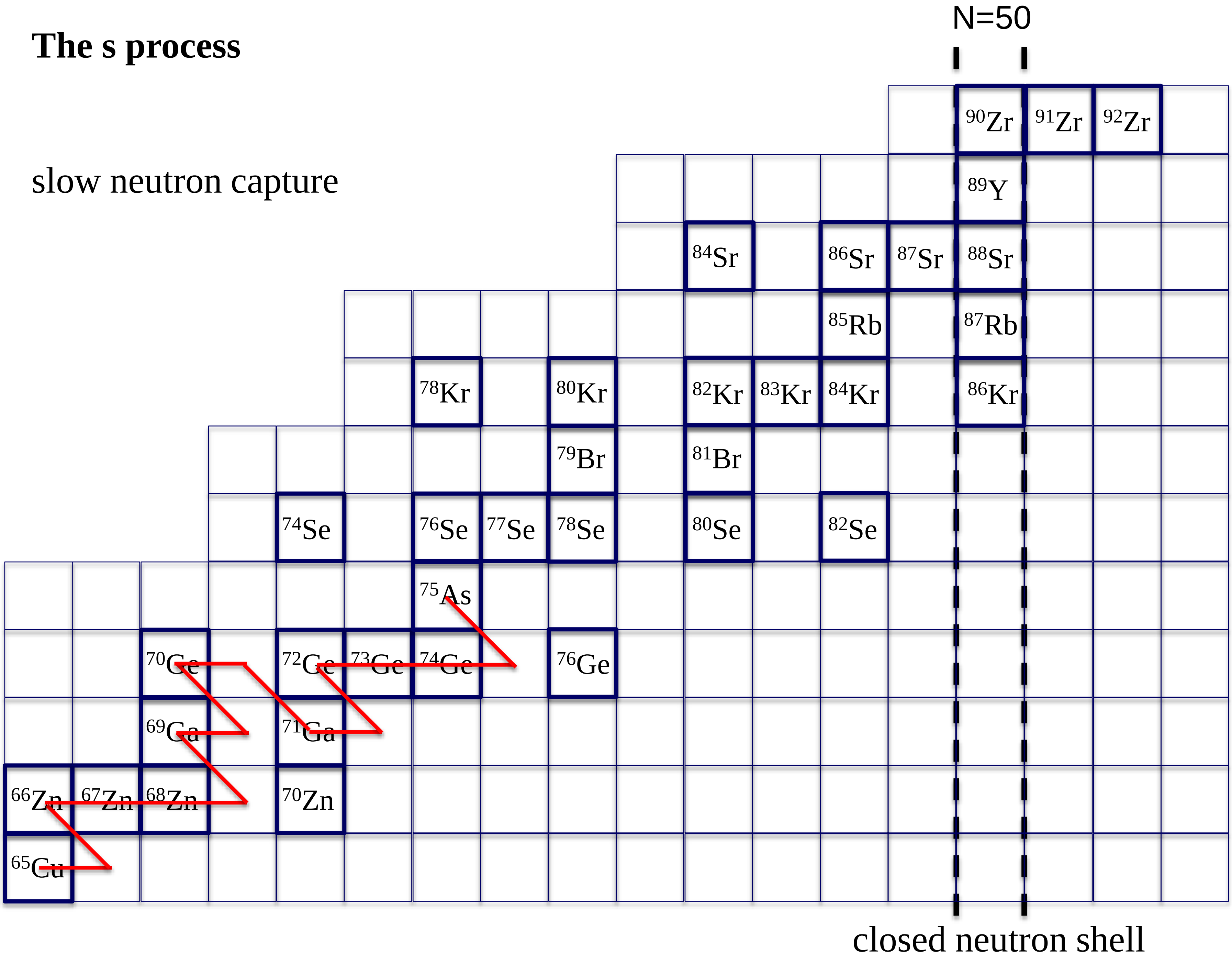

The s process

slow neutron capture

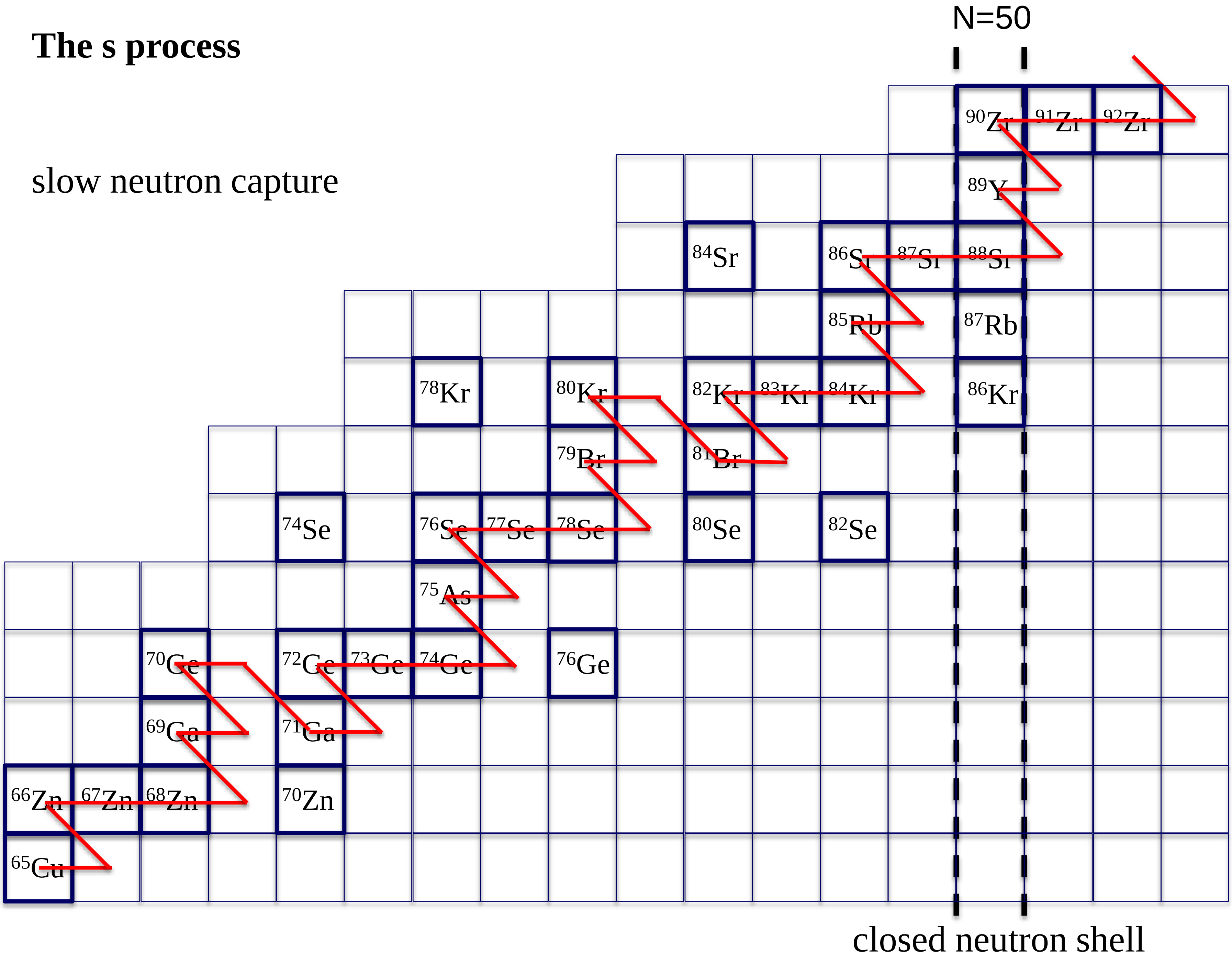

The s process

slow neutron capture

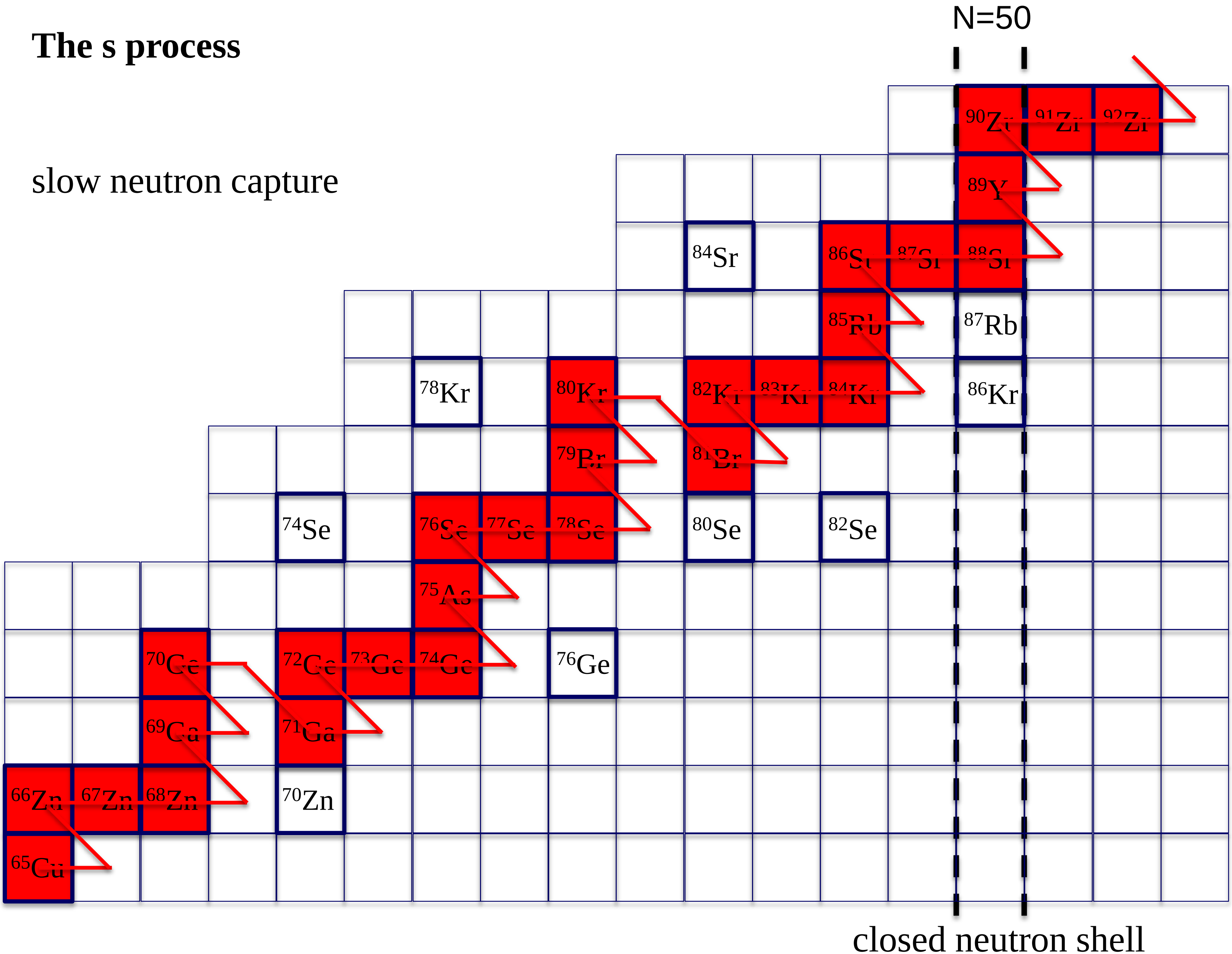

The r process

rapid neutron capture

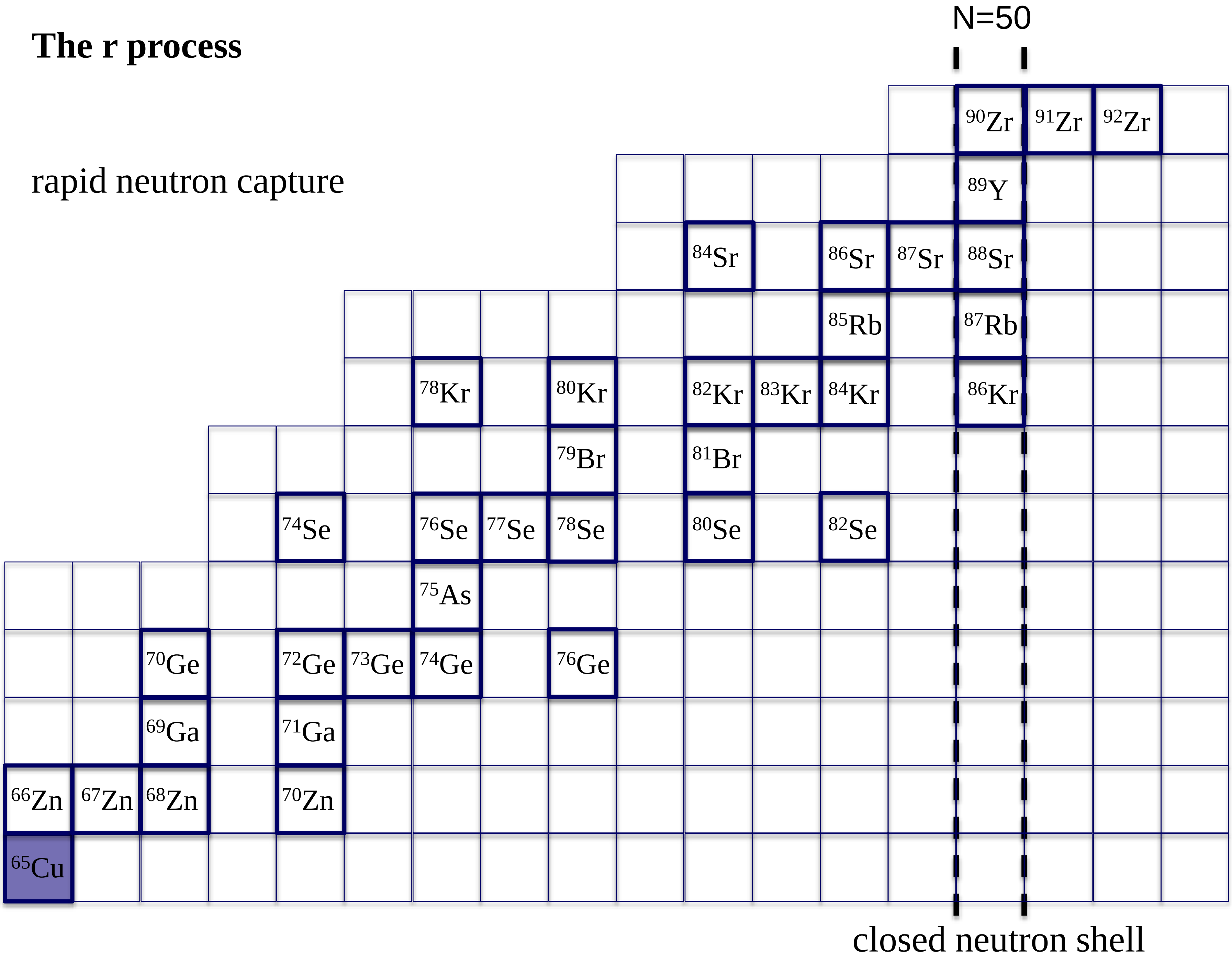

The r process

rapid neutron capture

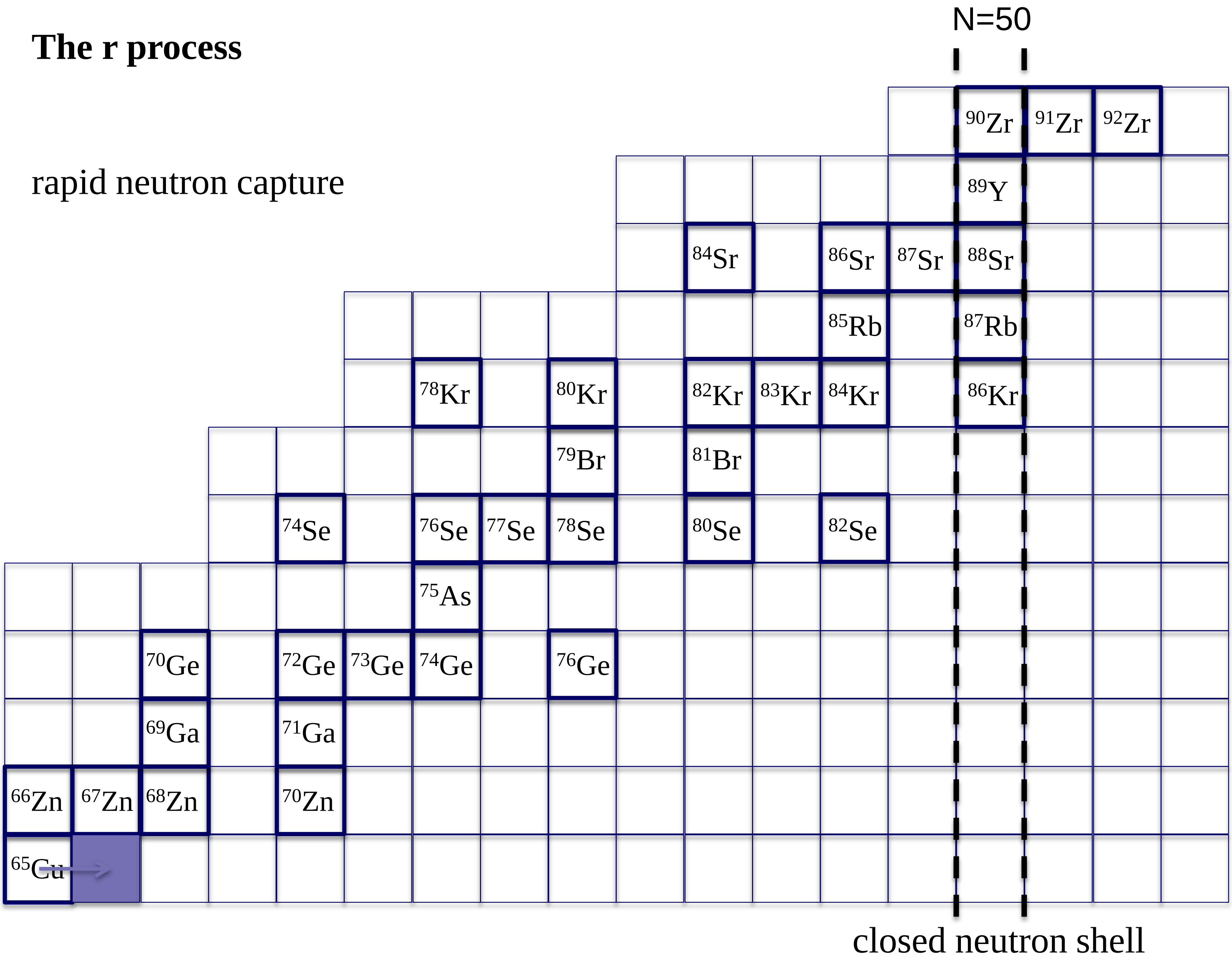

The r process

rapid neutron capture

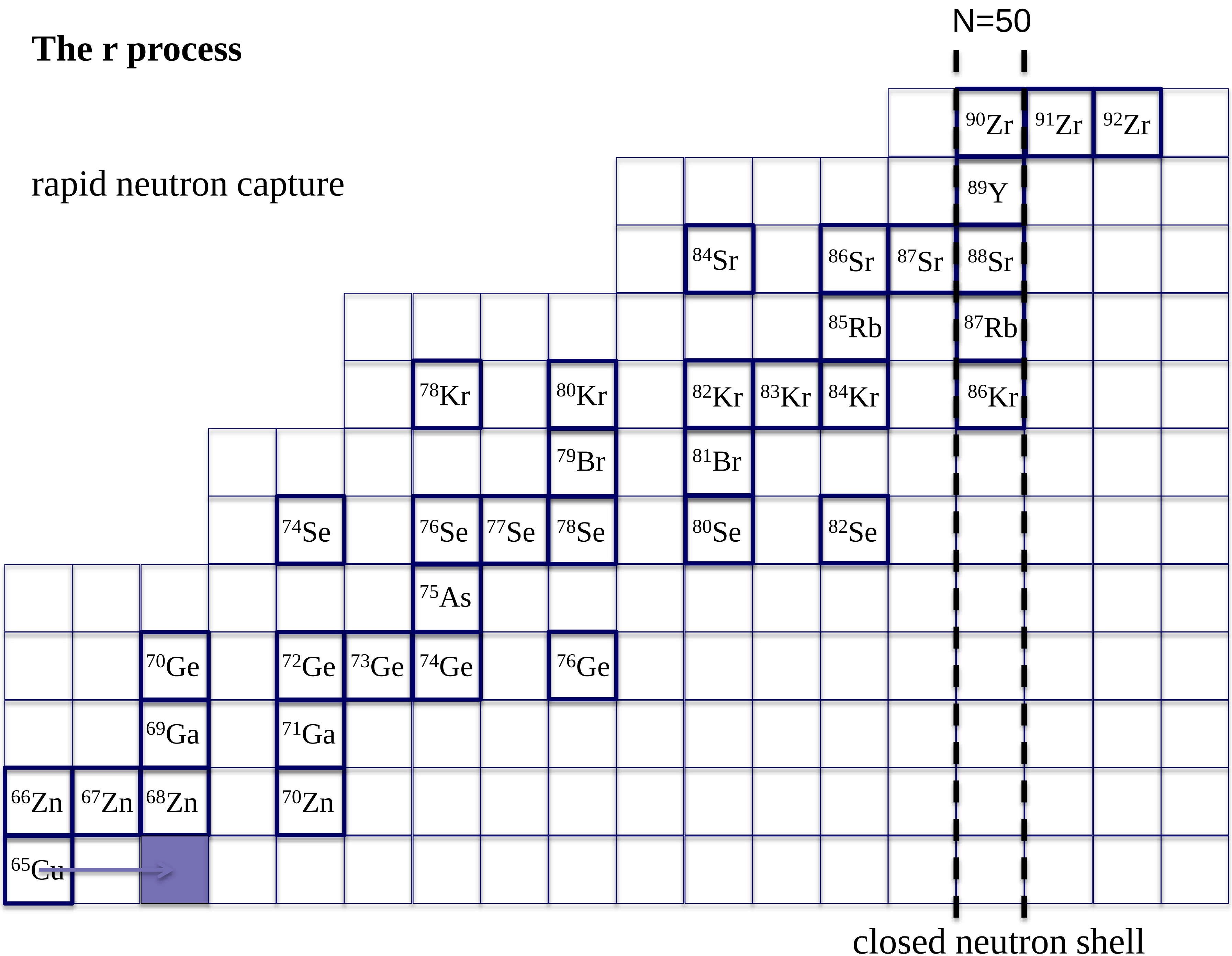

The r process

rapid neutron capture

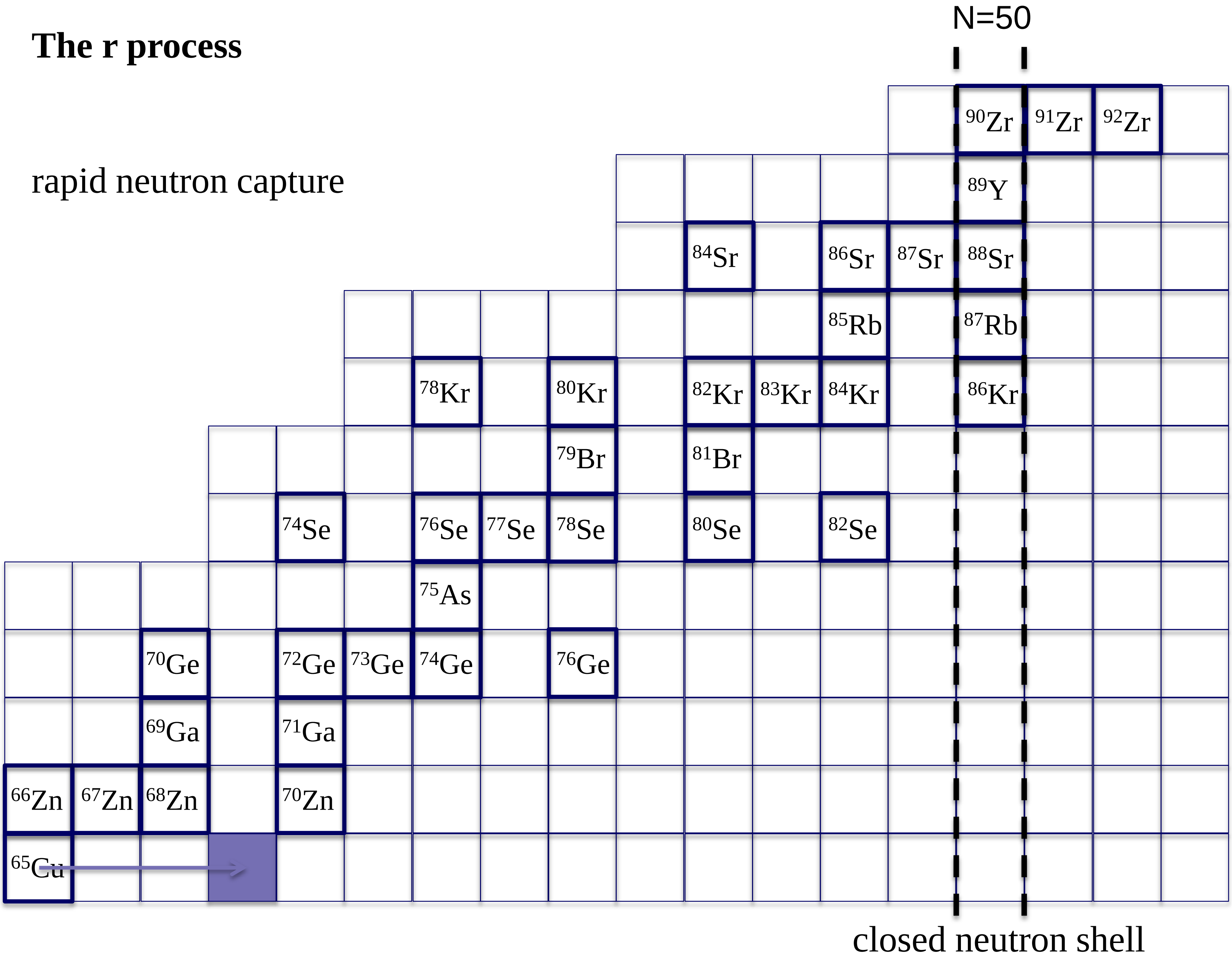

The r process

rapid neutron capture

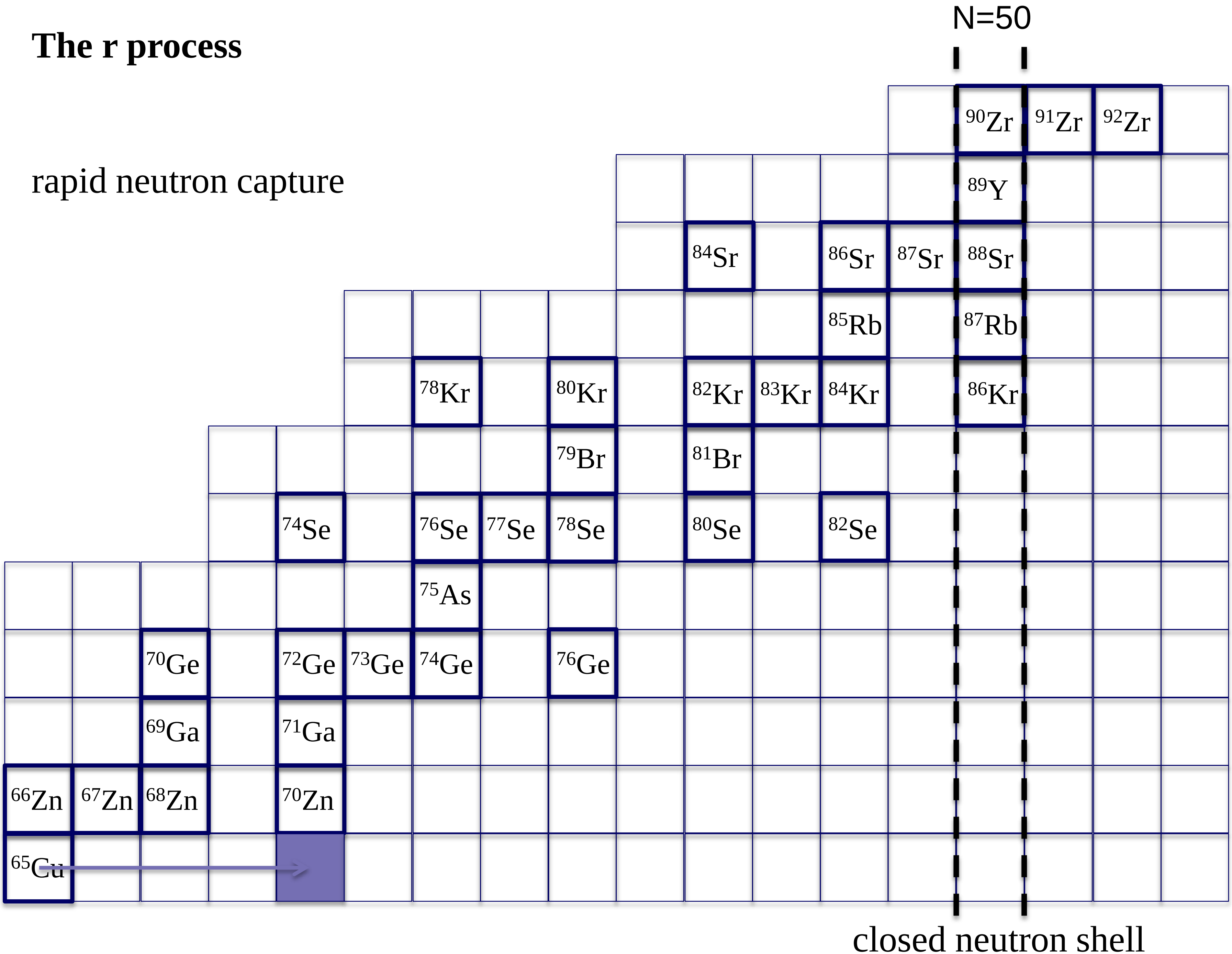

The r process

rapid neutron capture

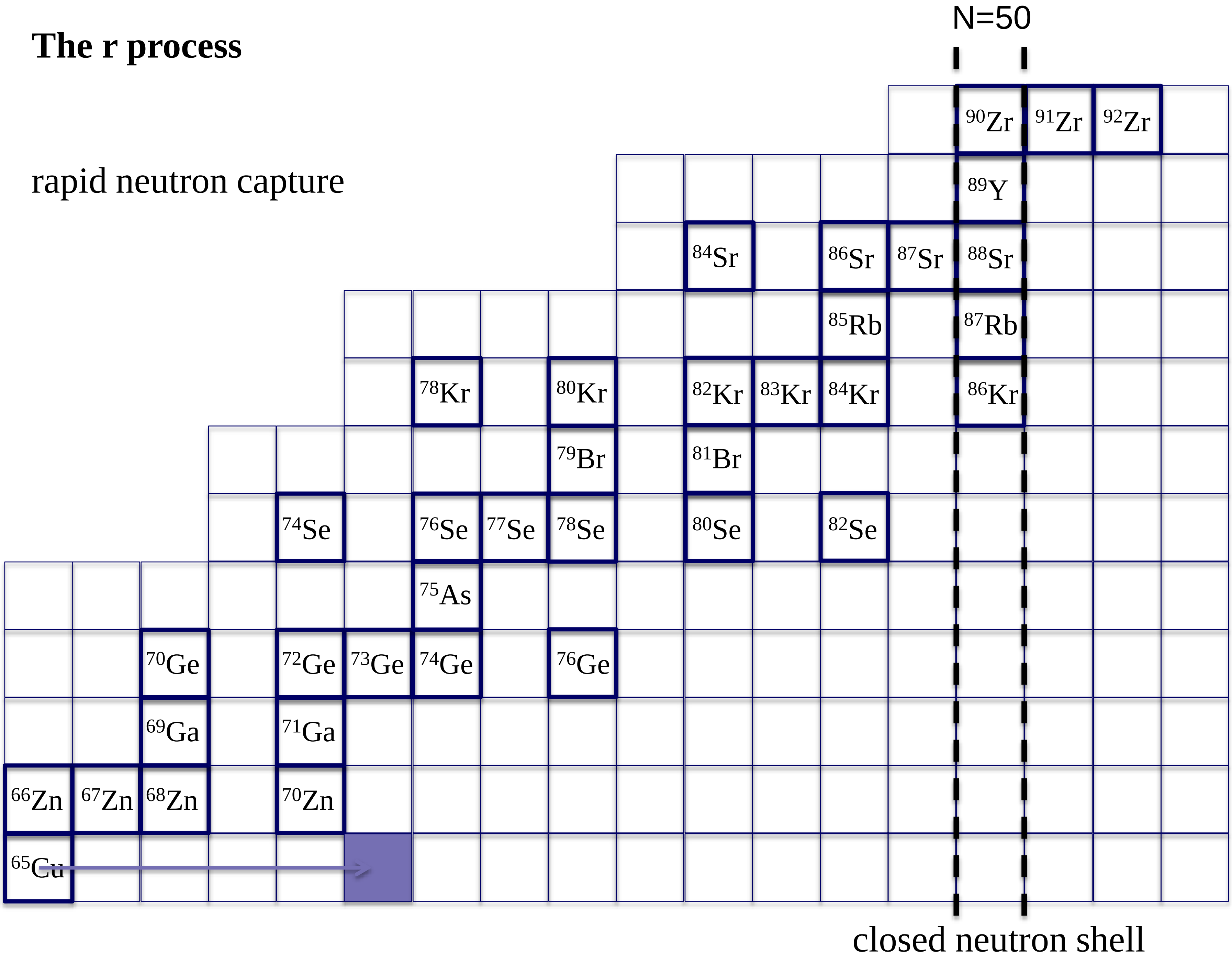

The r process

rapid neutron capture

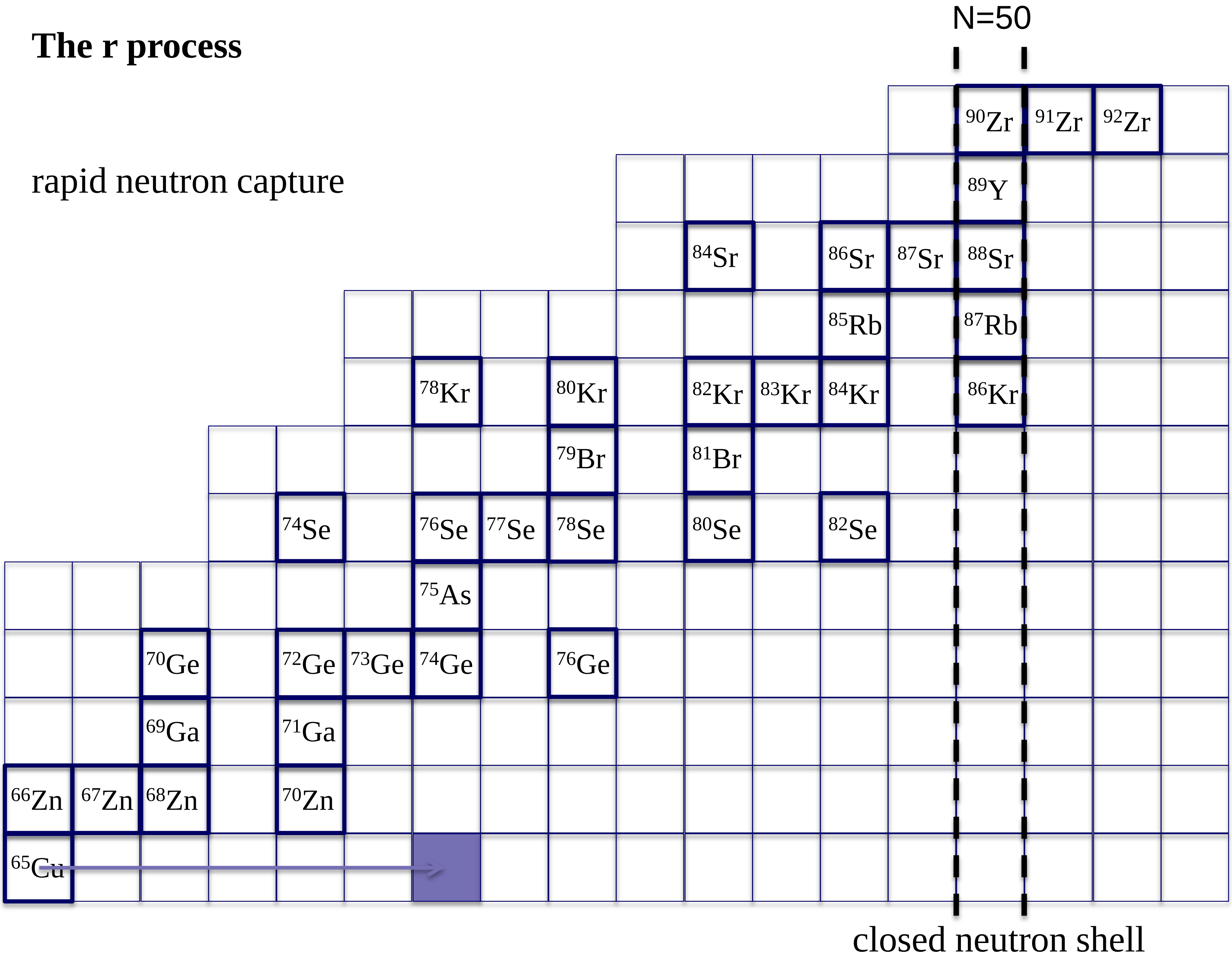

The r process

rapid neutron capture

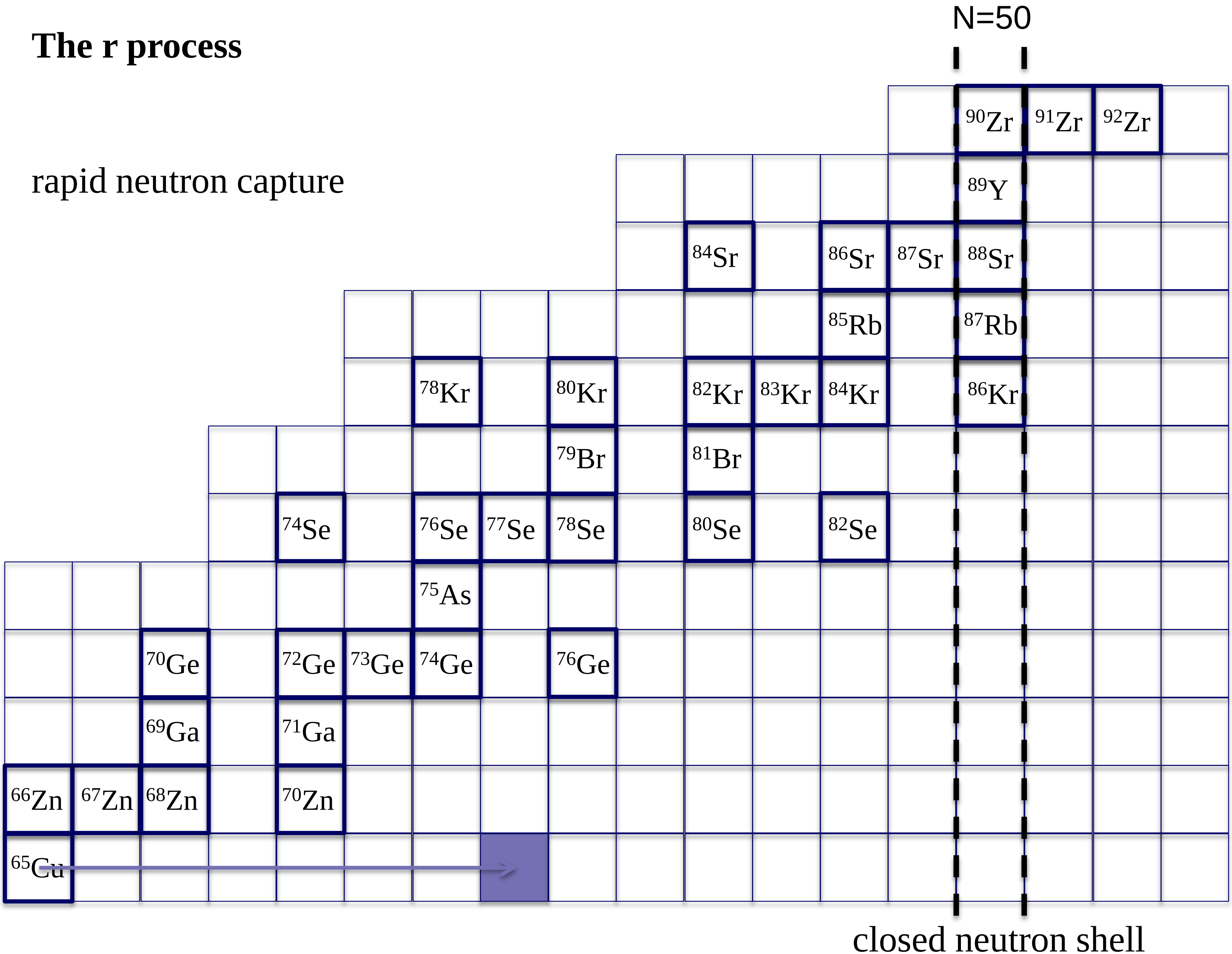

The r process

rapid neutron capture

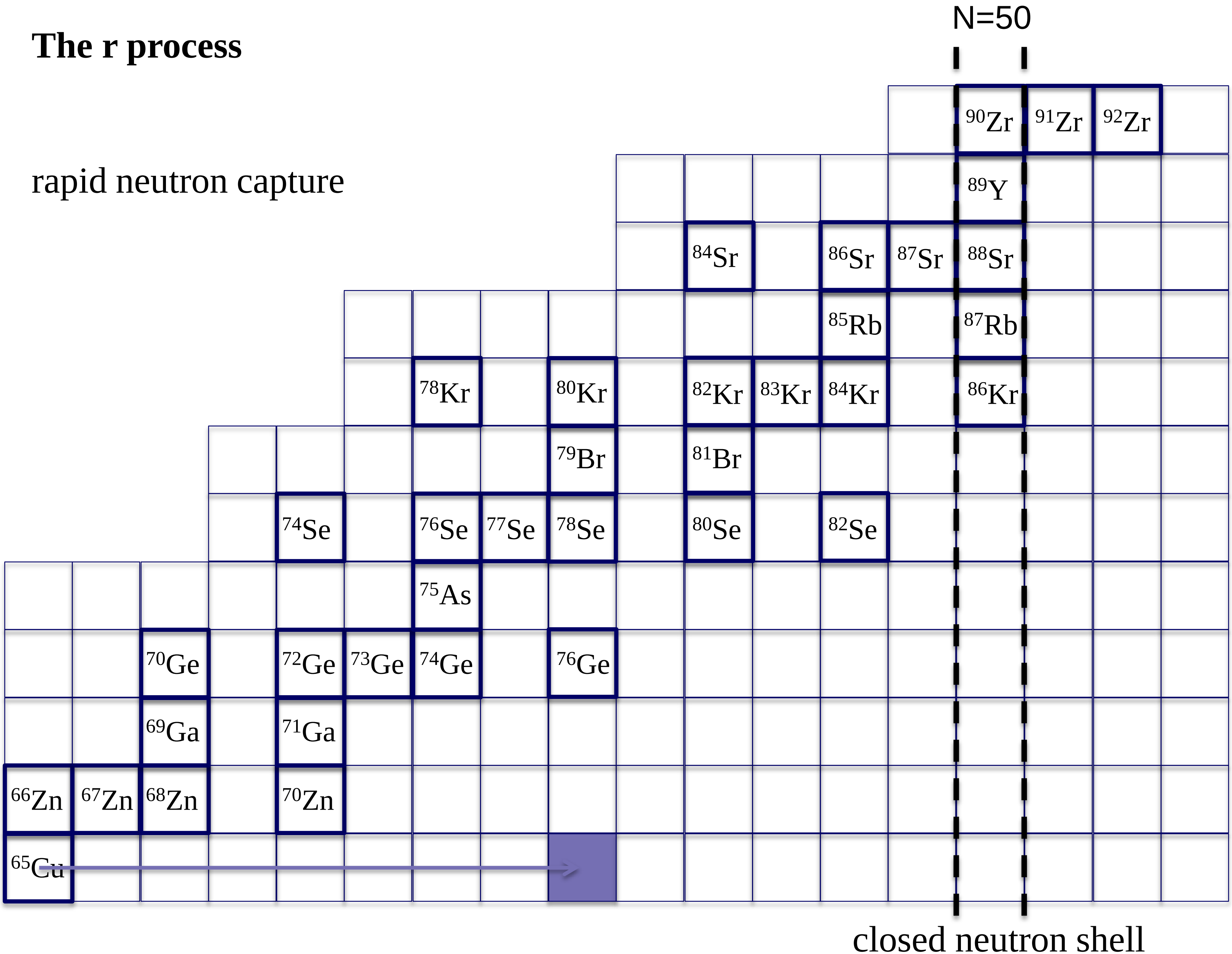

The r process

rapid neutron capture

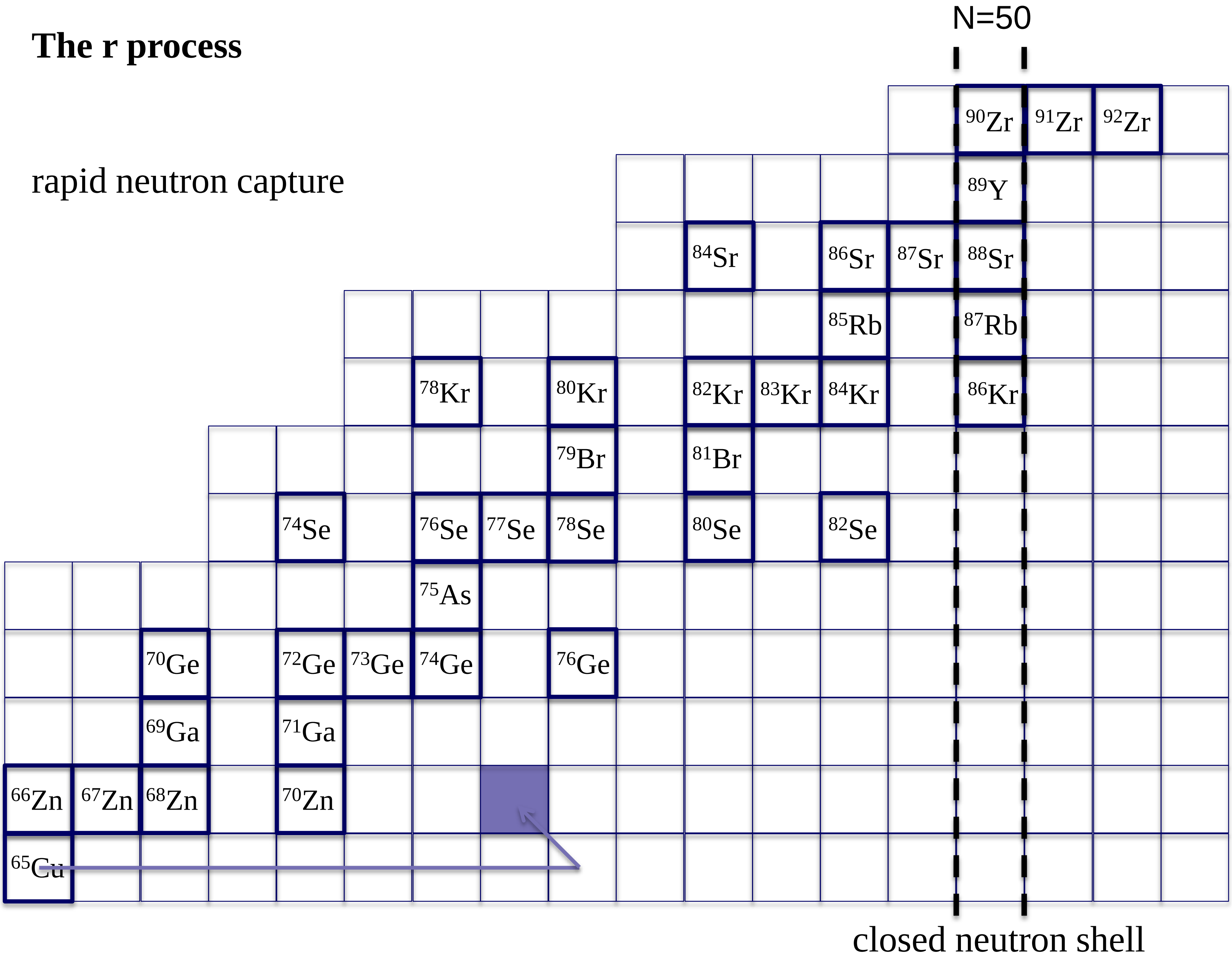

The r process

rapid neutron capture

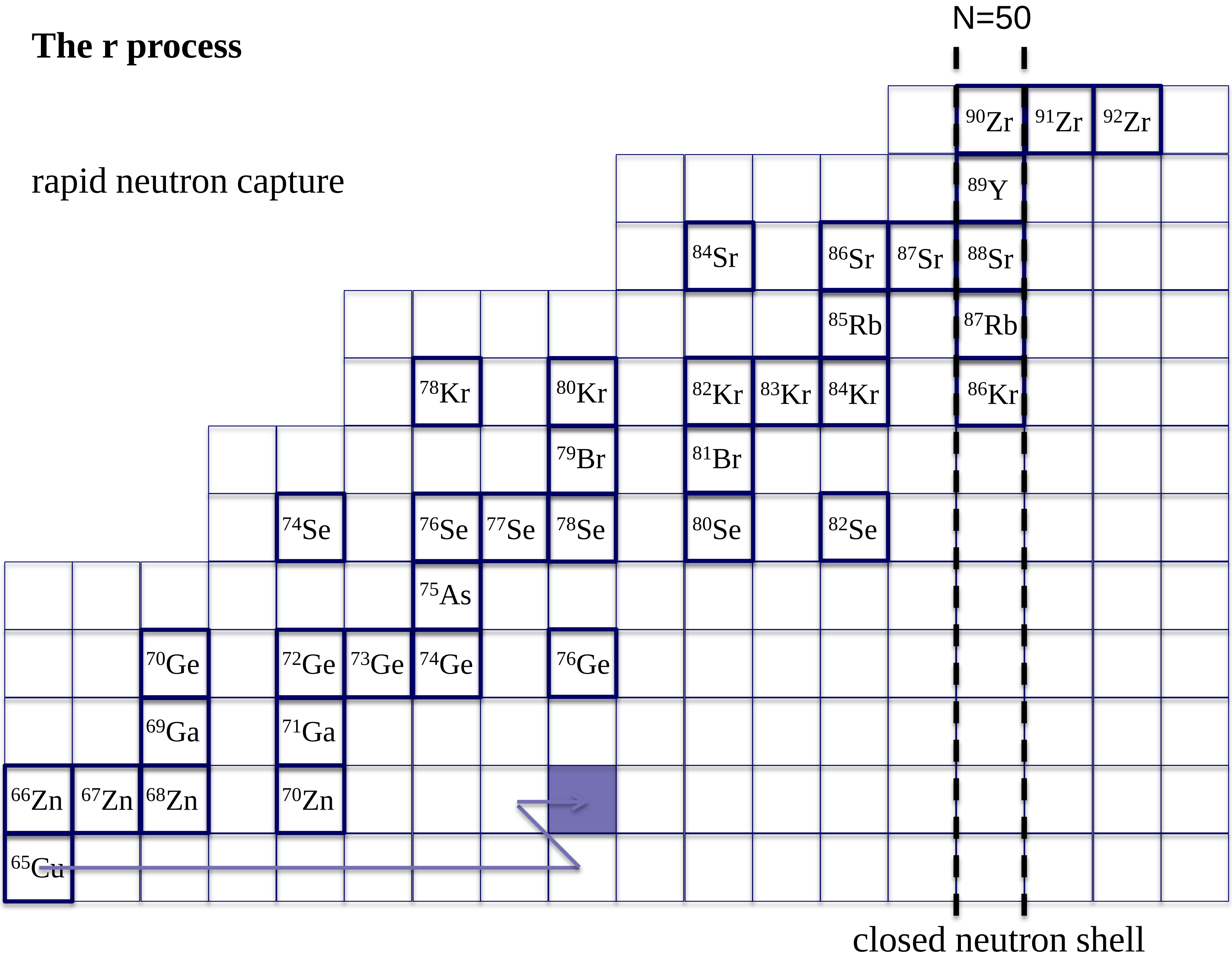

The r process

rapid neutron capture

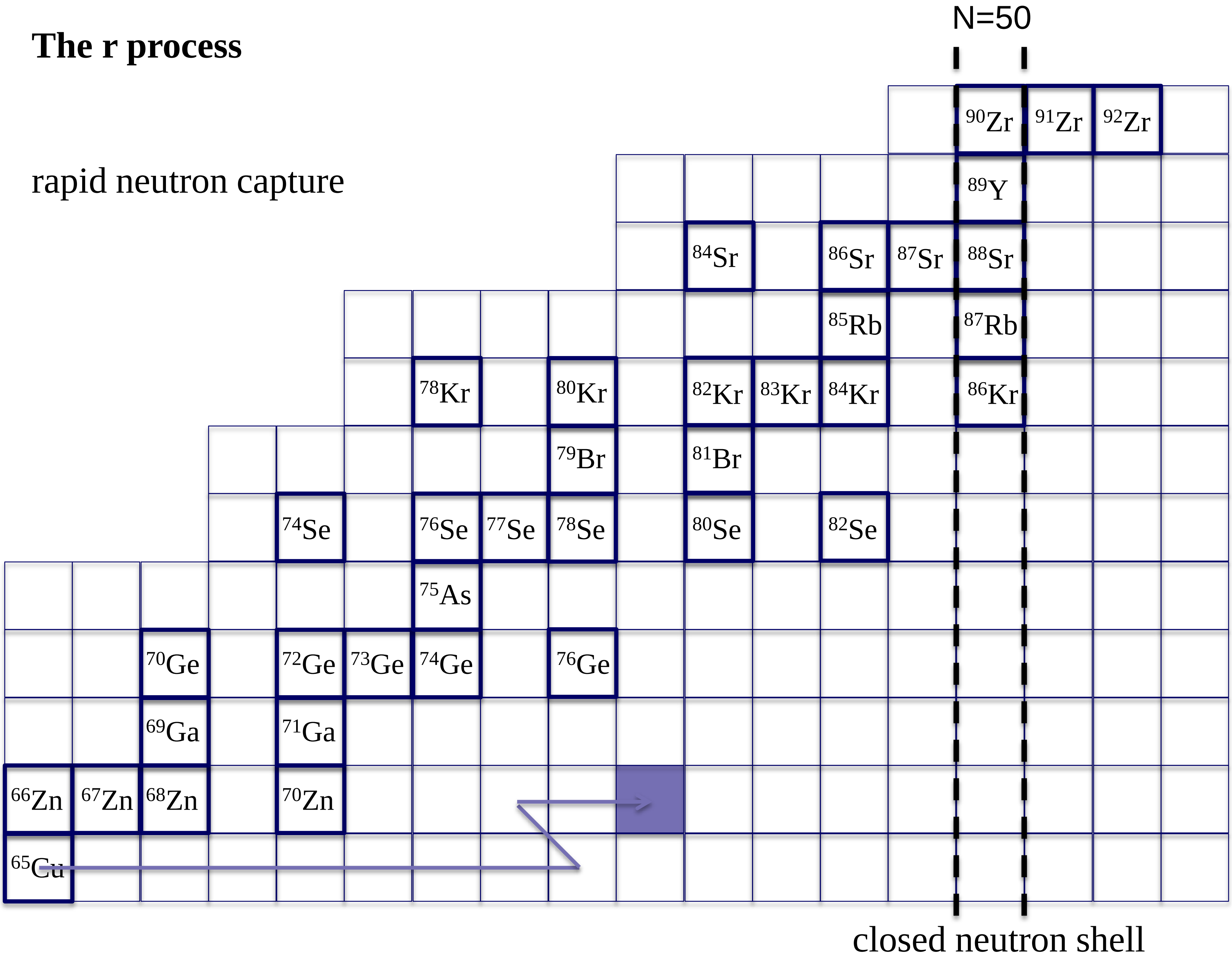

The r process

rapid neutron capture

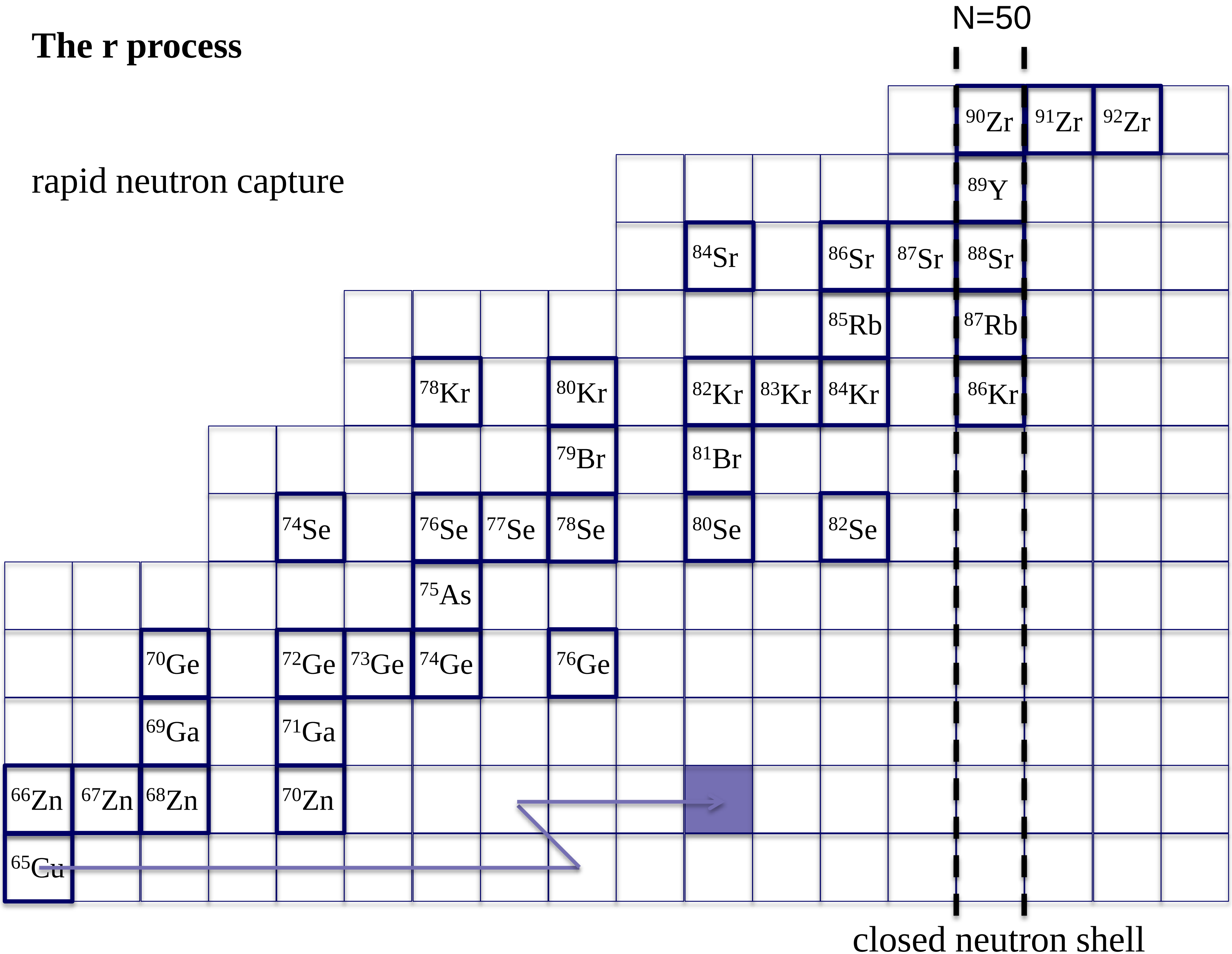

The r process

rapid neutron capture

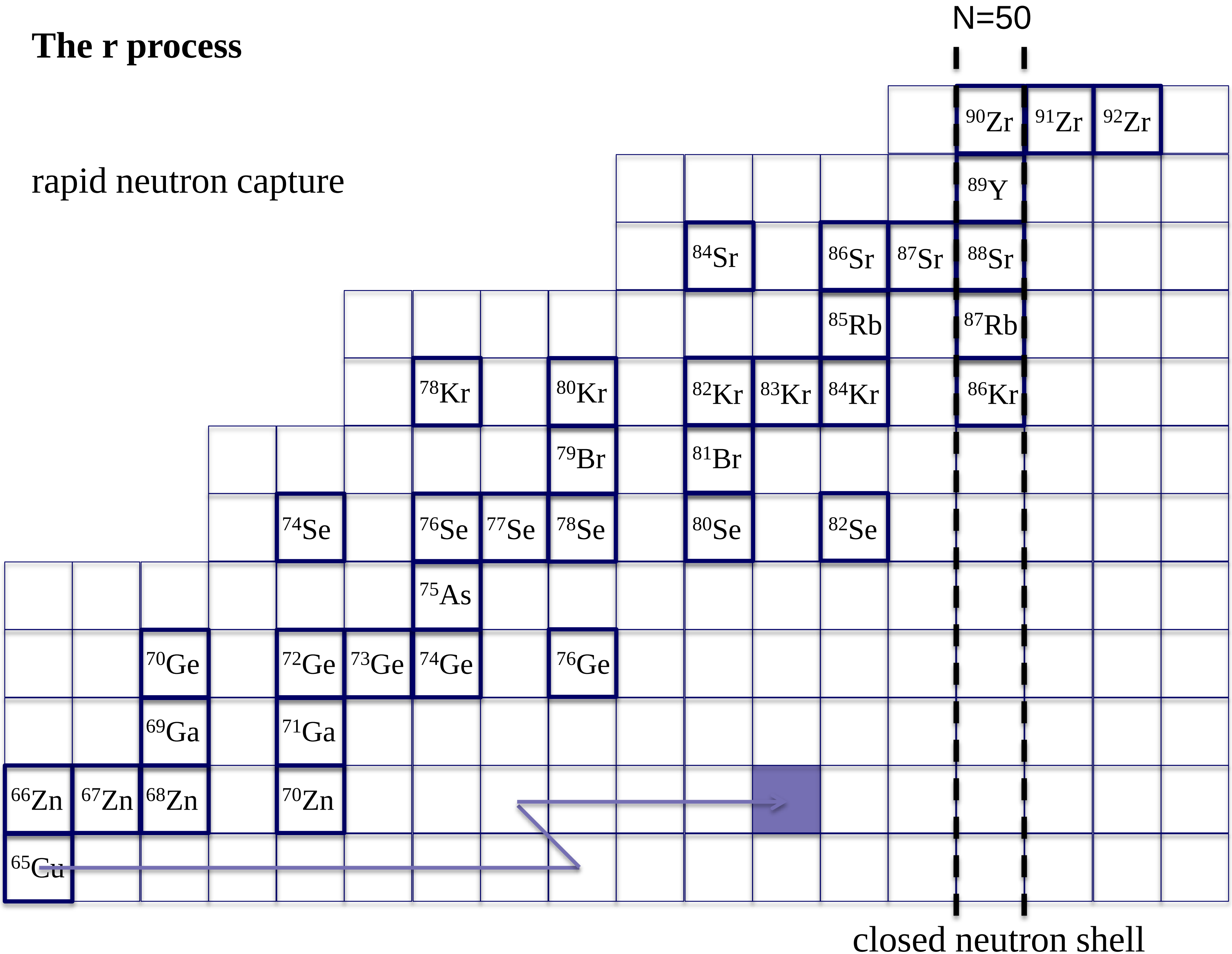

The r process

rapid neutron capture

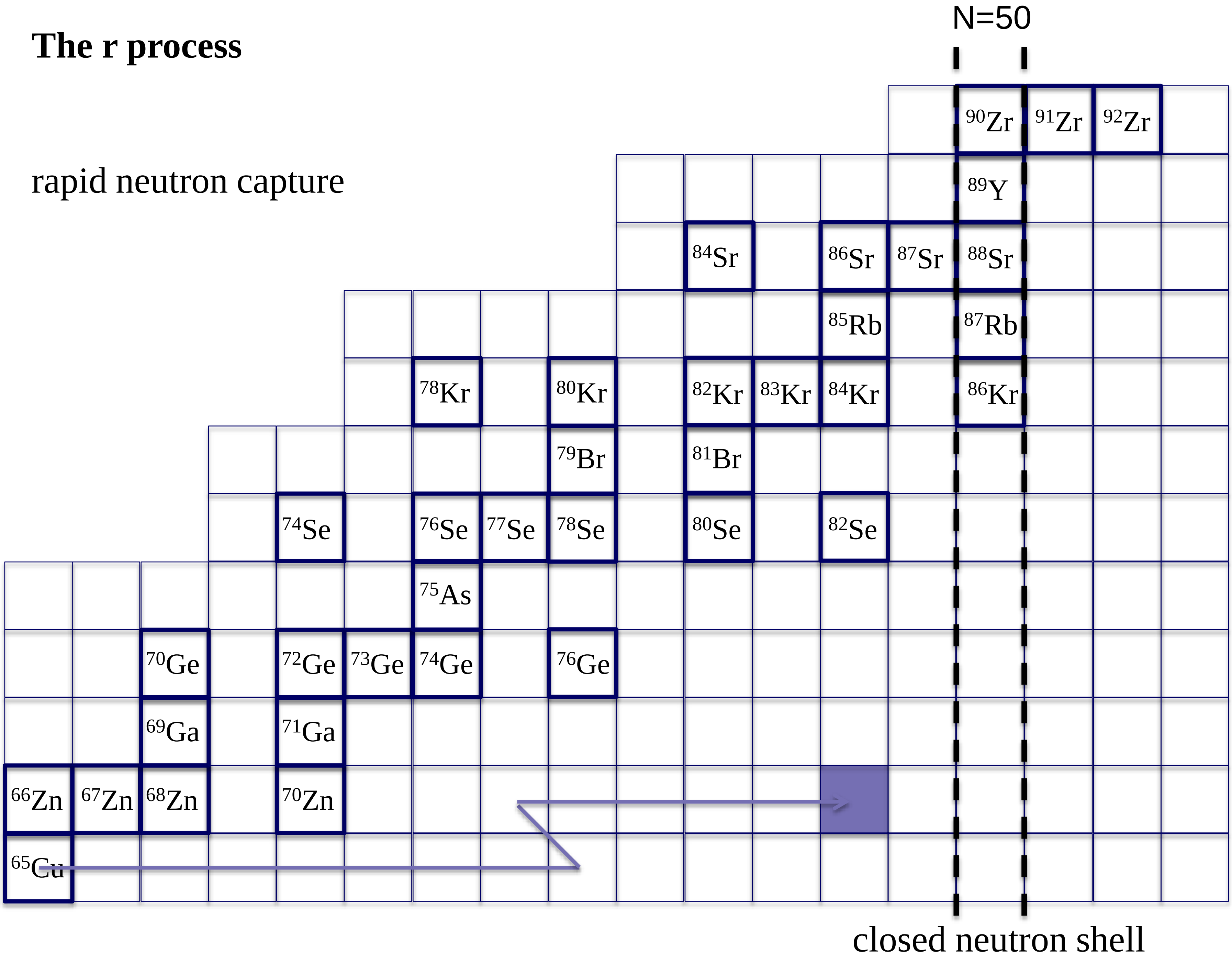

The r process

rapid neutron capture

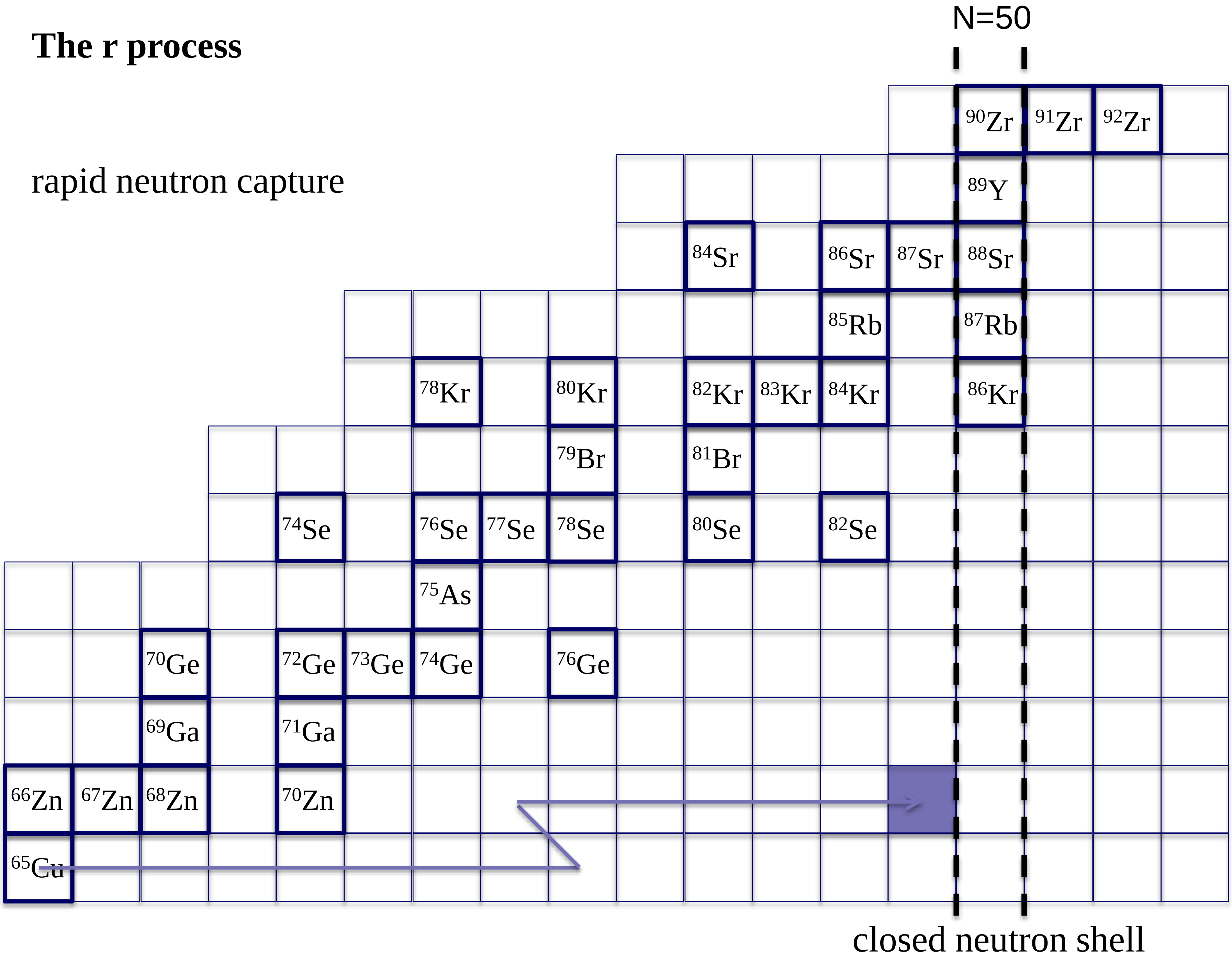

The r process

rapid neutron capture

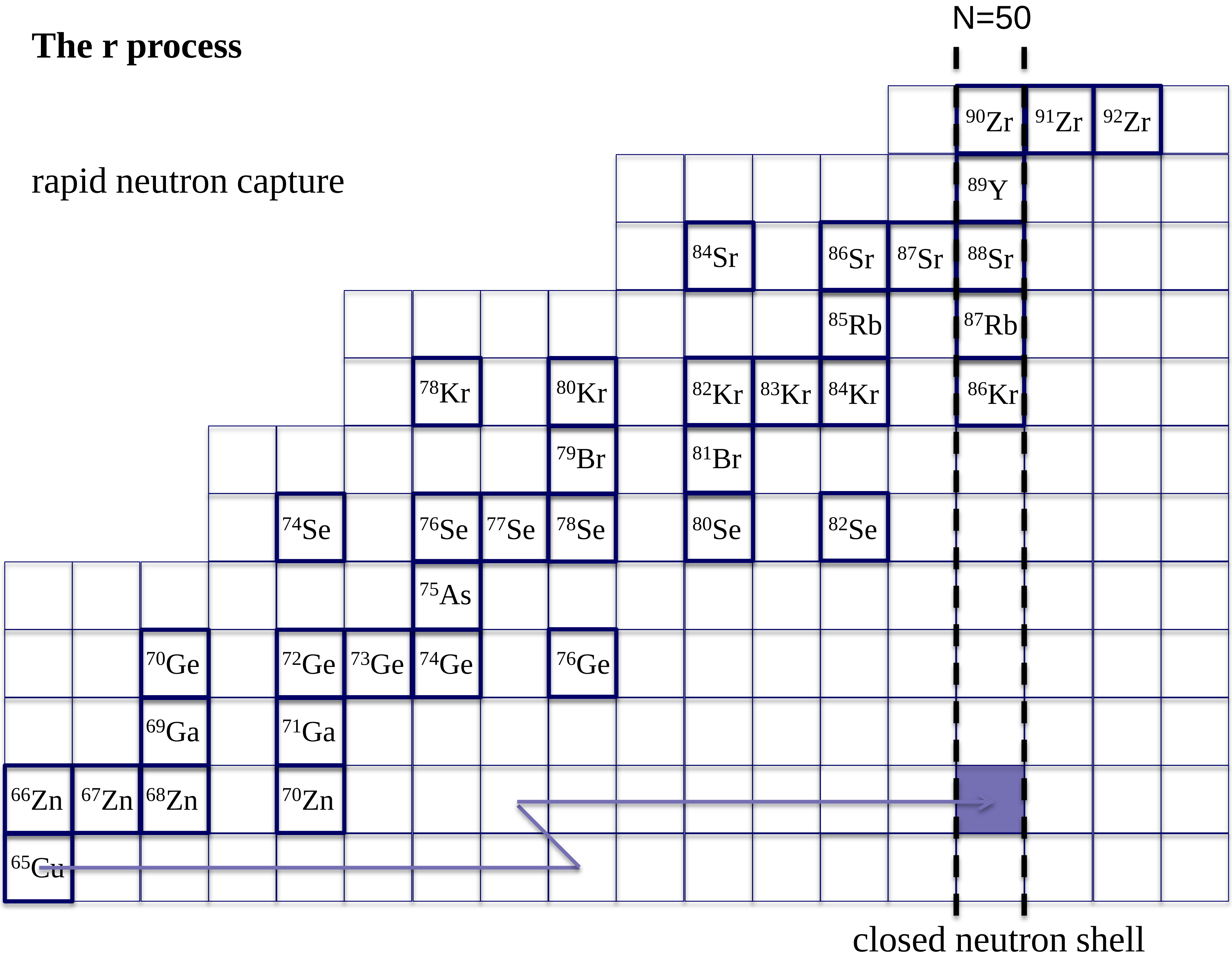

The r process

rapid neutron capture

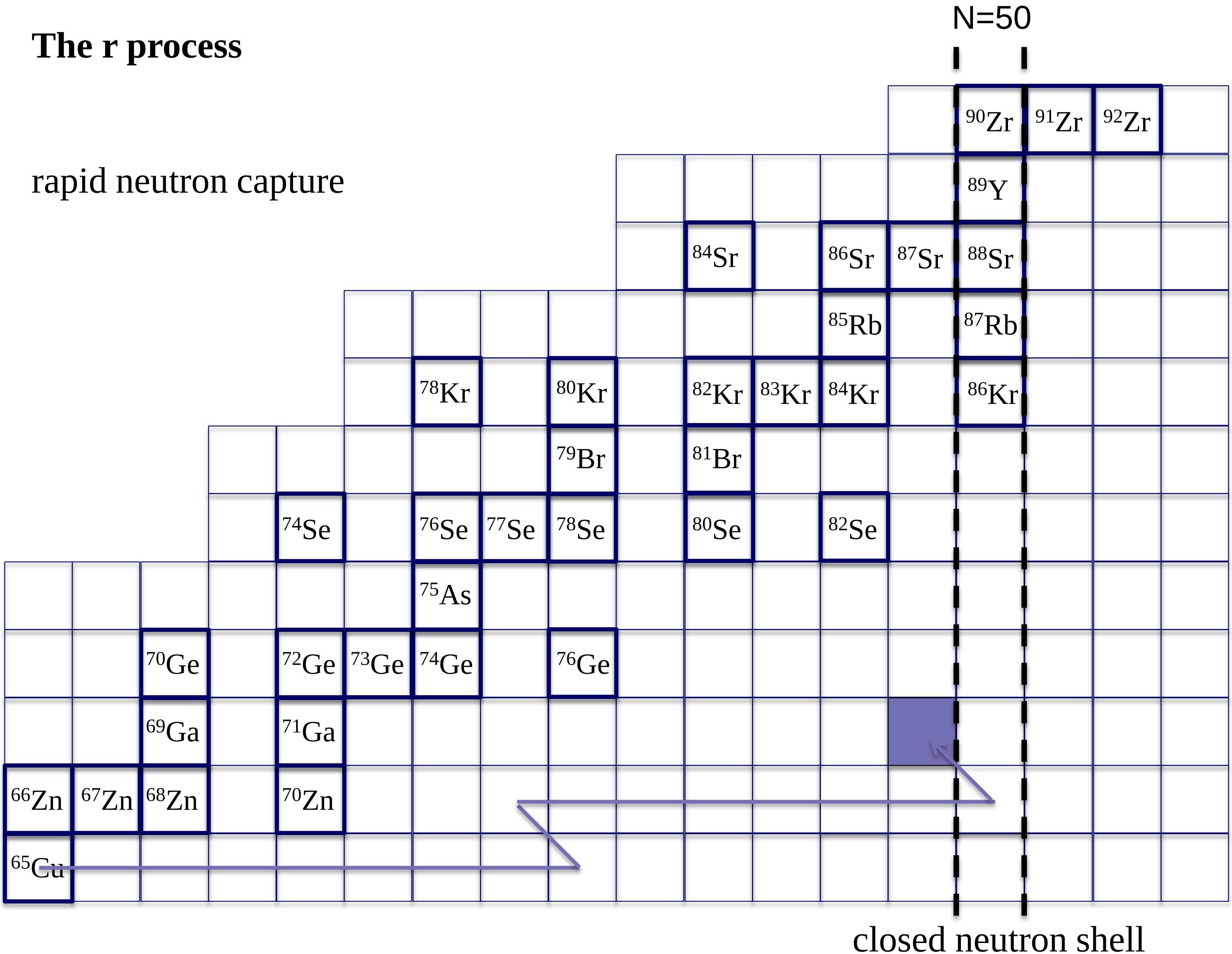

The r process

rapid neutron capture

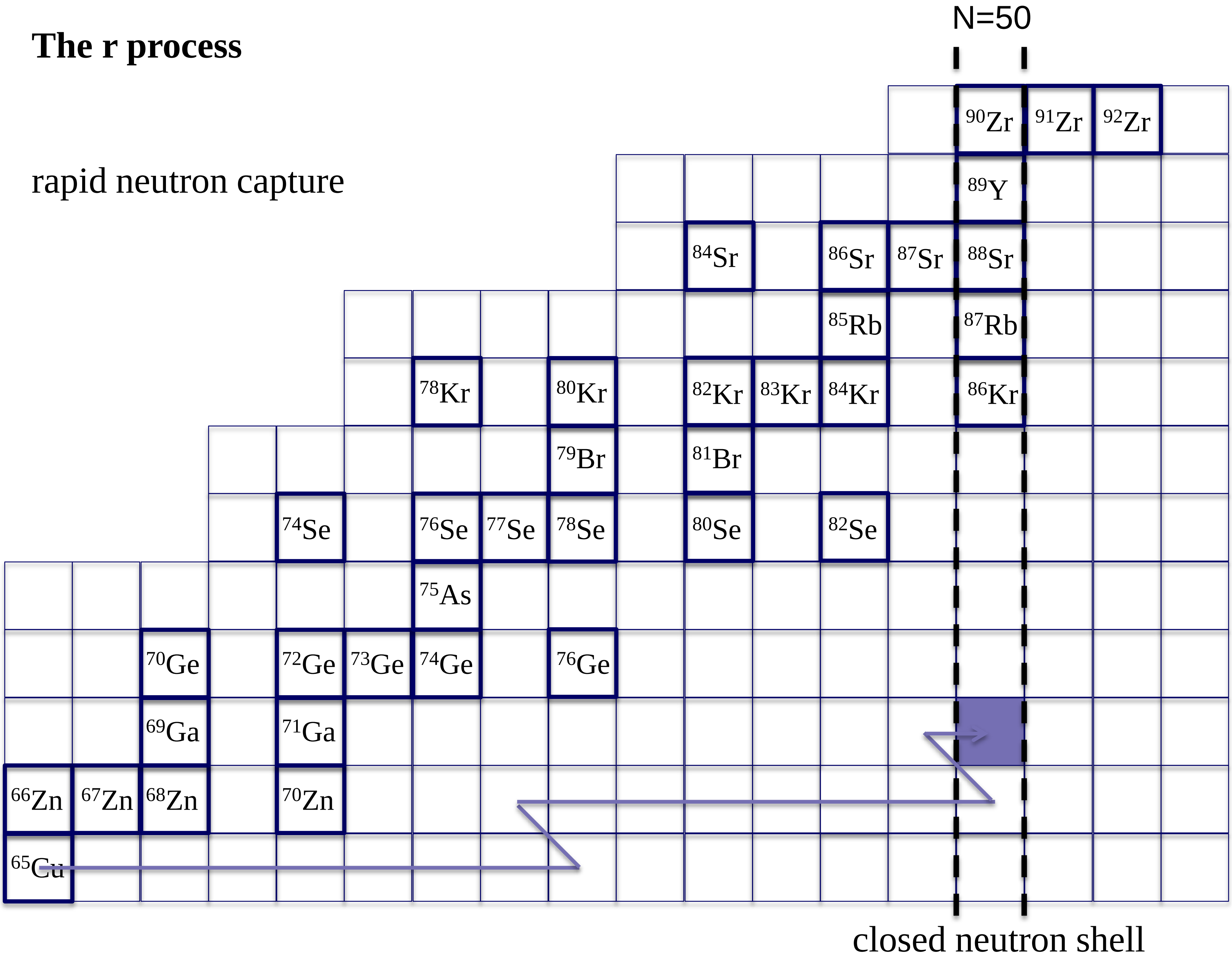

The r process

rapid neutron capture

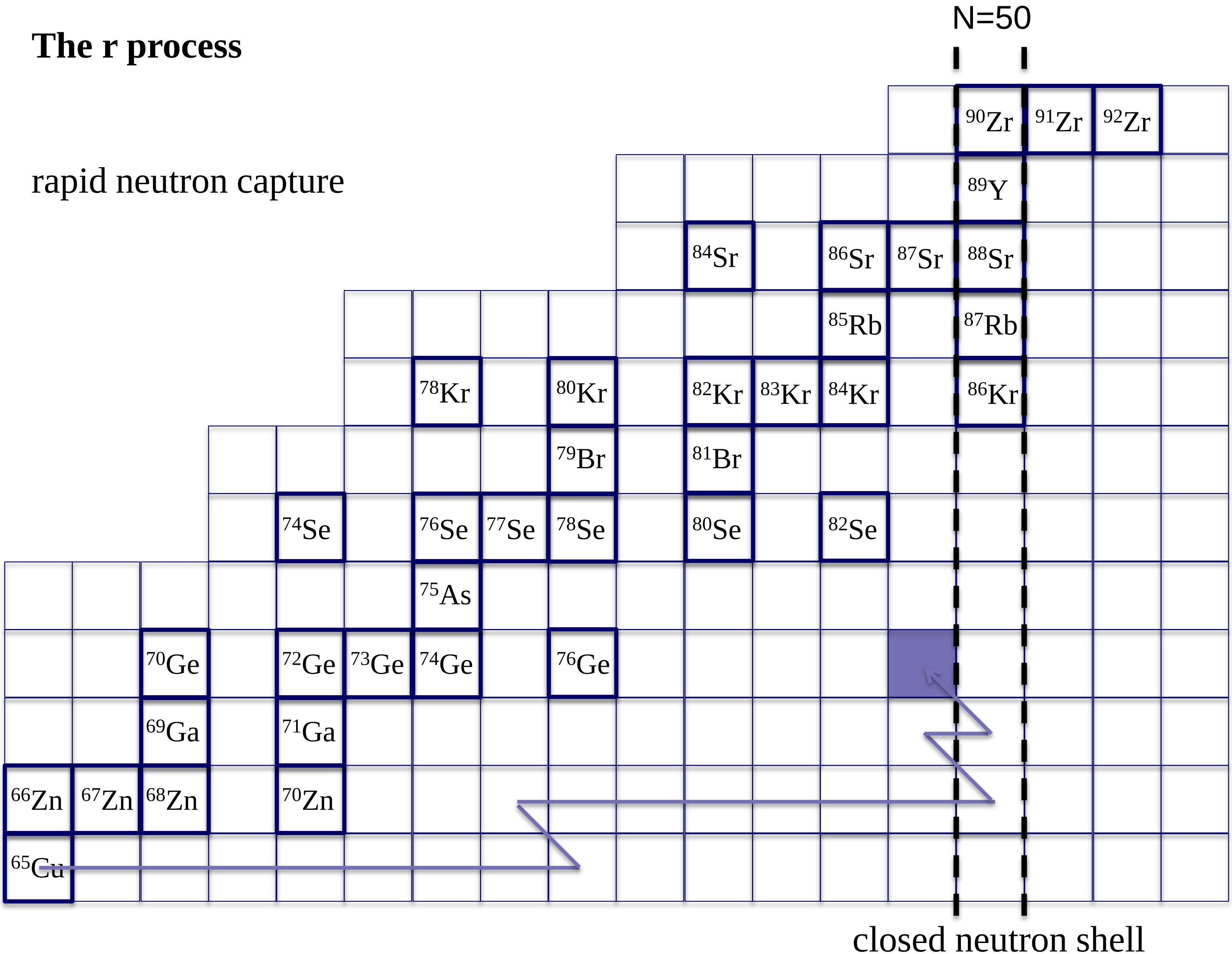

The r process

rapid neutron capture

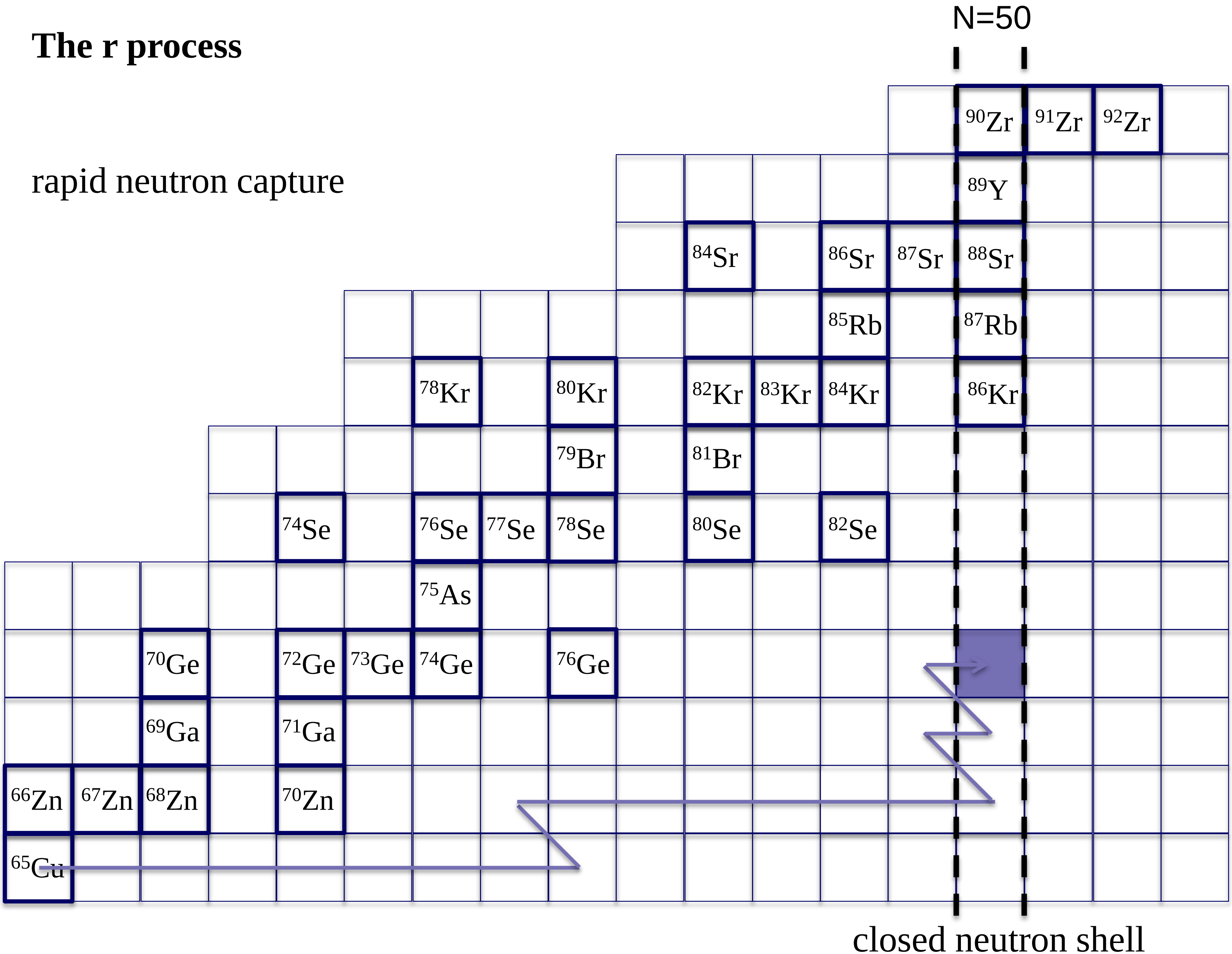

The r process

rapid neutron capture

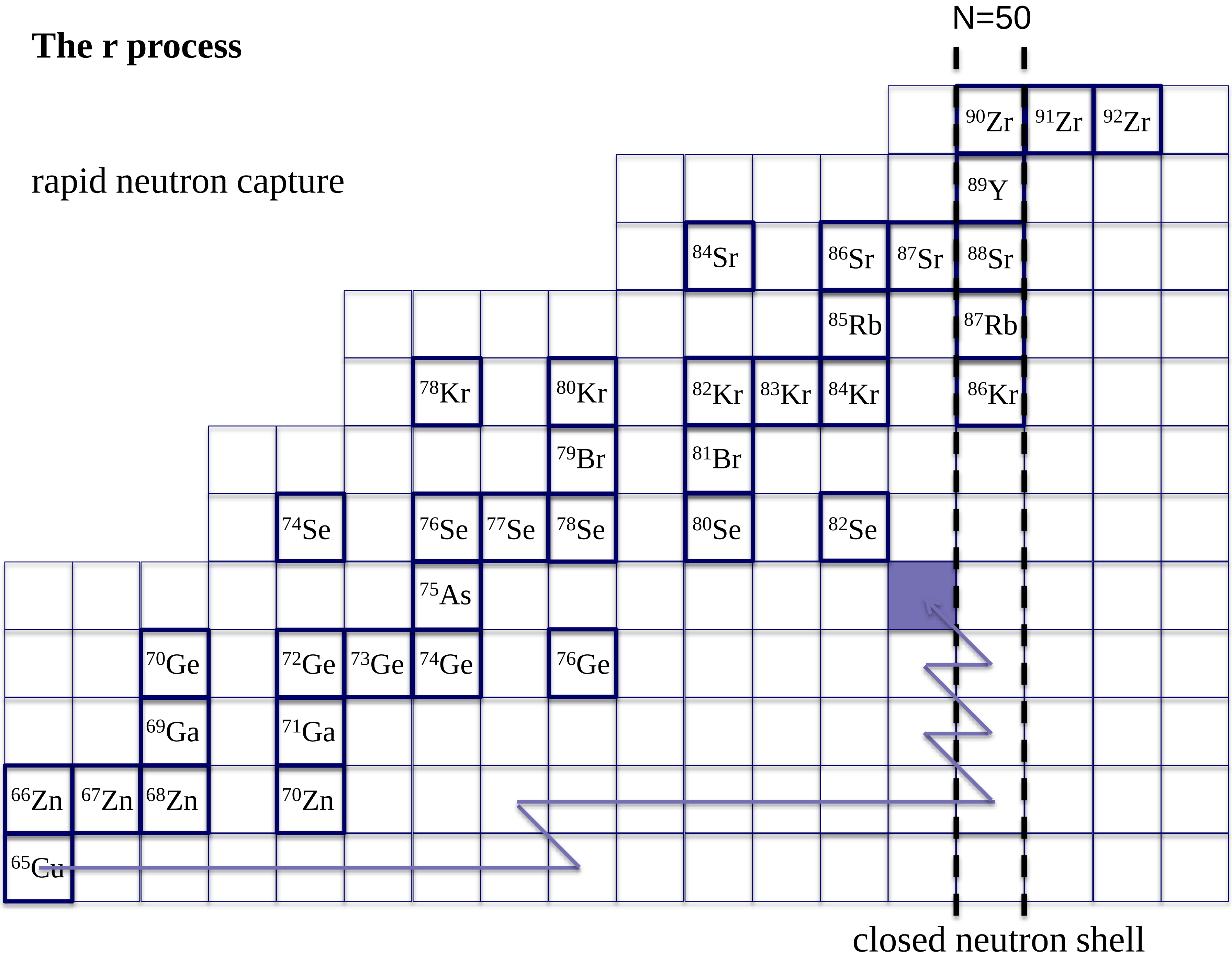

The r process

rapid neutron capture

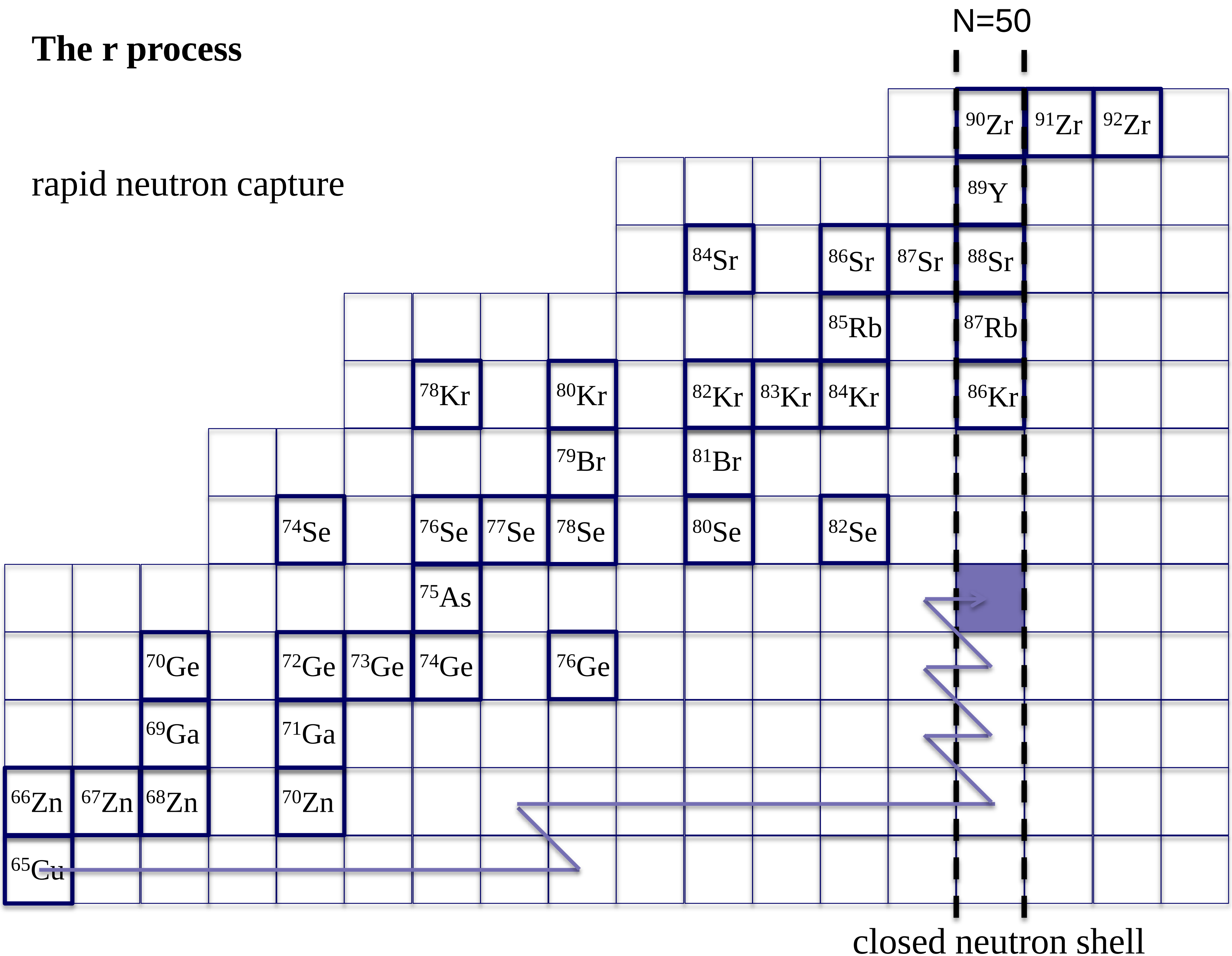

The r process

rapid neutron capture

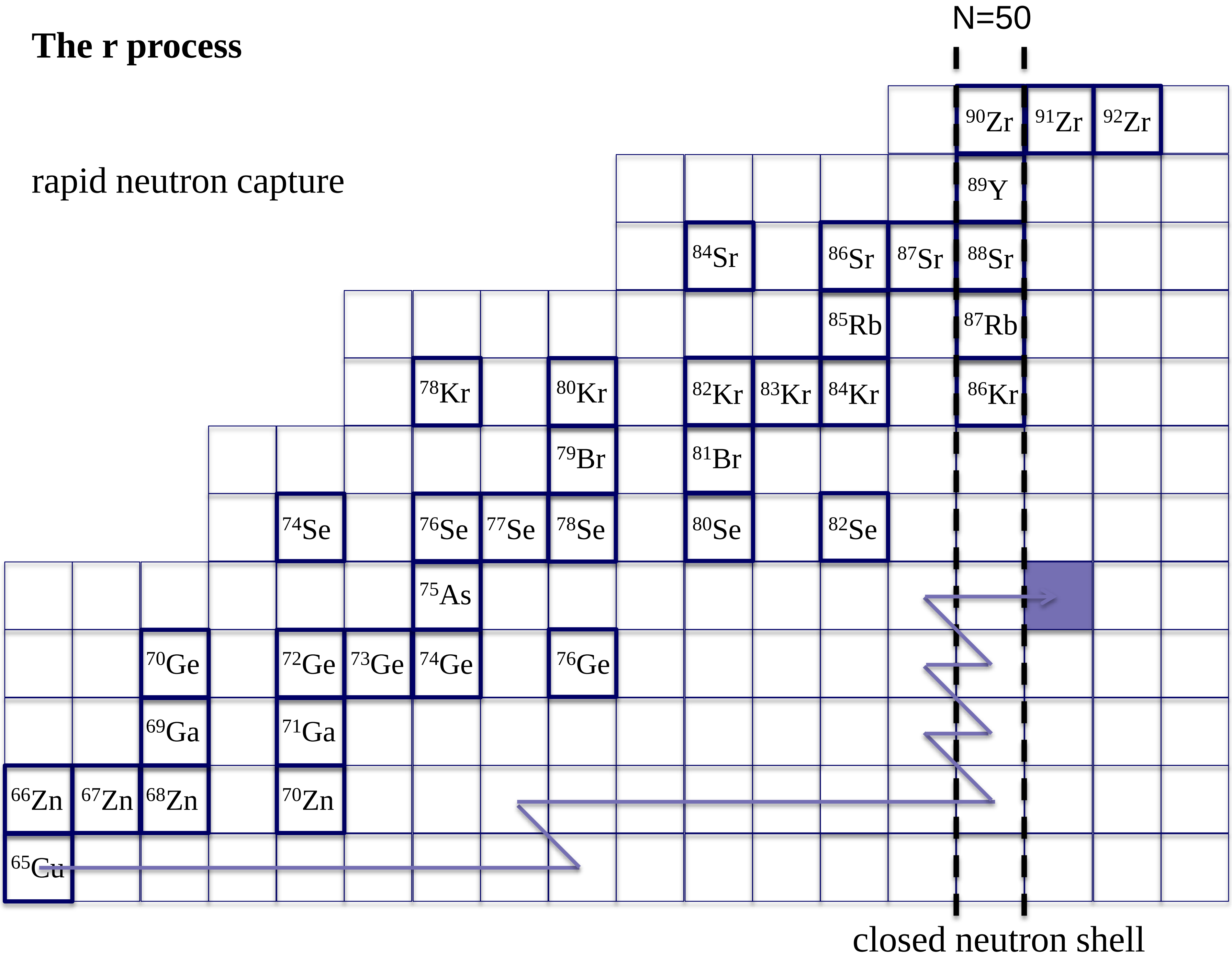

The r process

rapid neutron capture

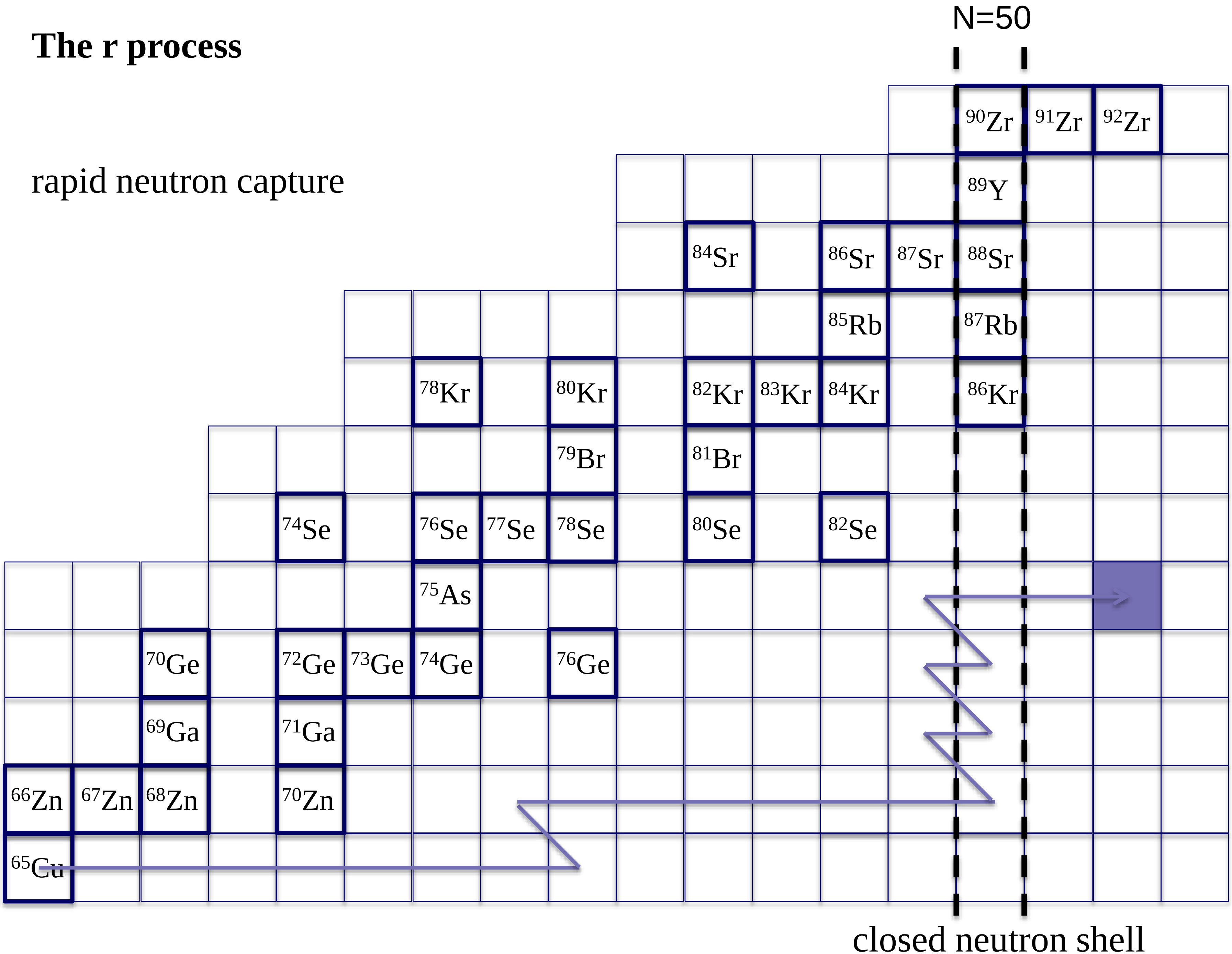

The r process

rapid neutron capture

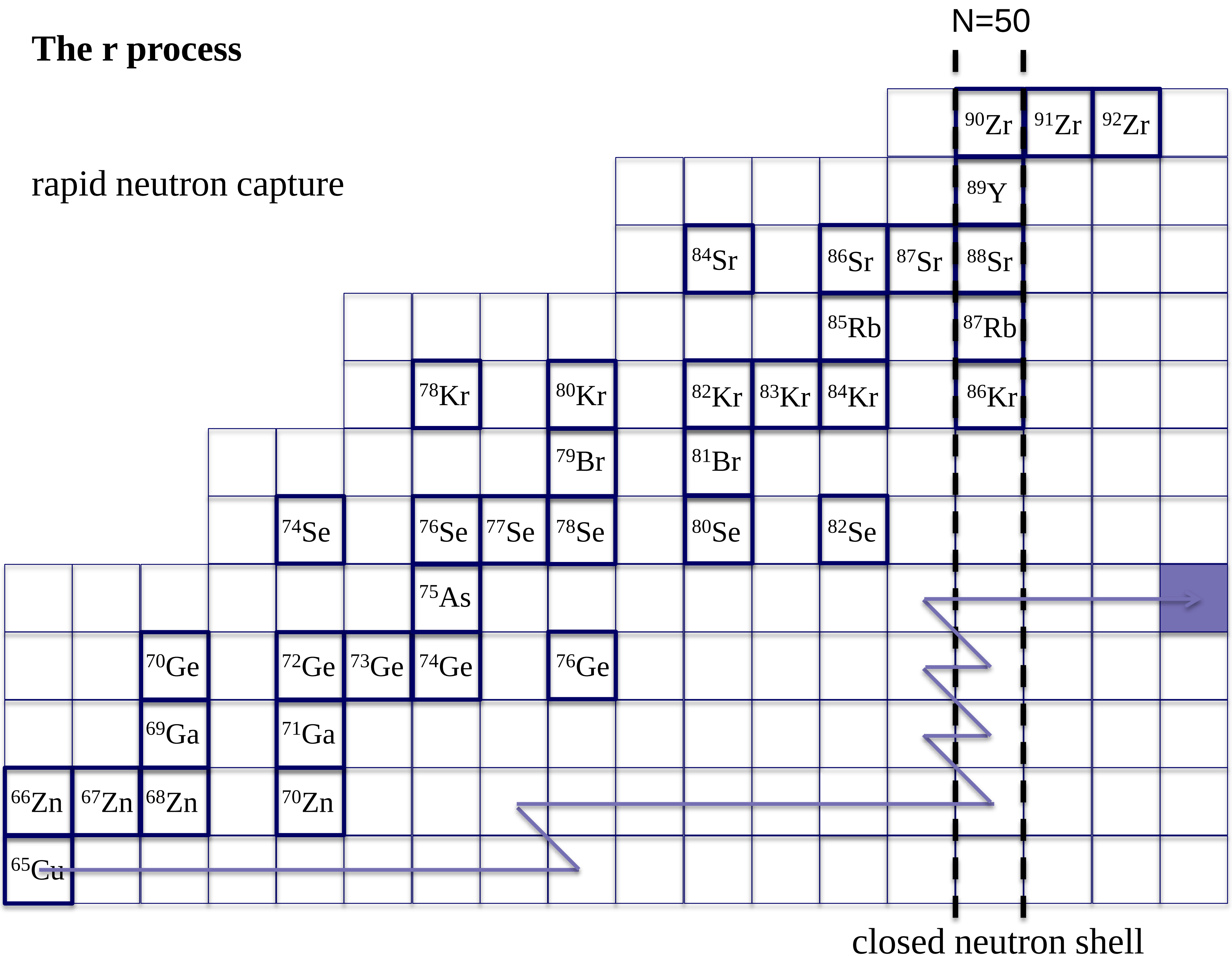

The r process

rapid neutron capture

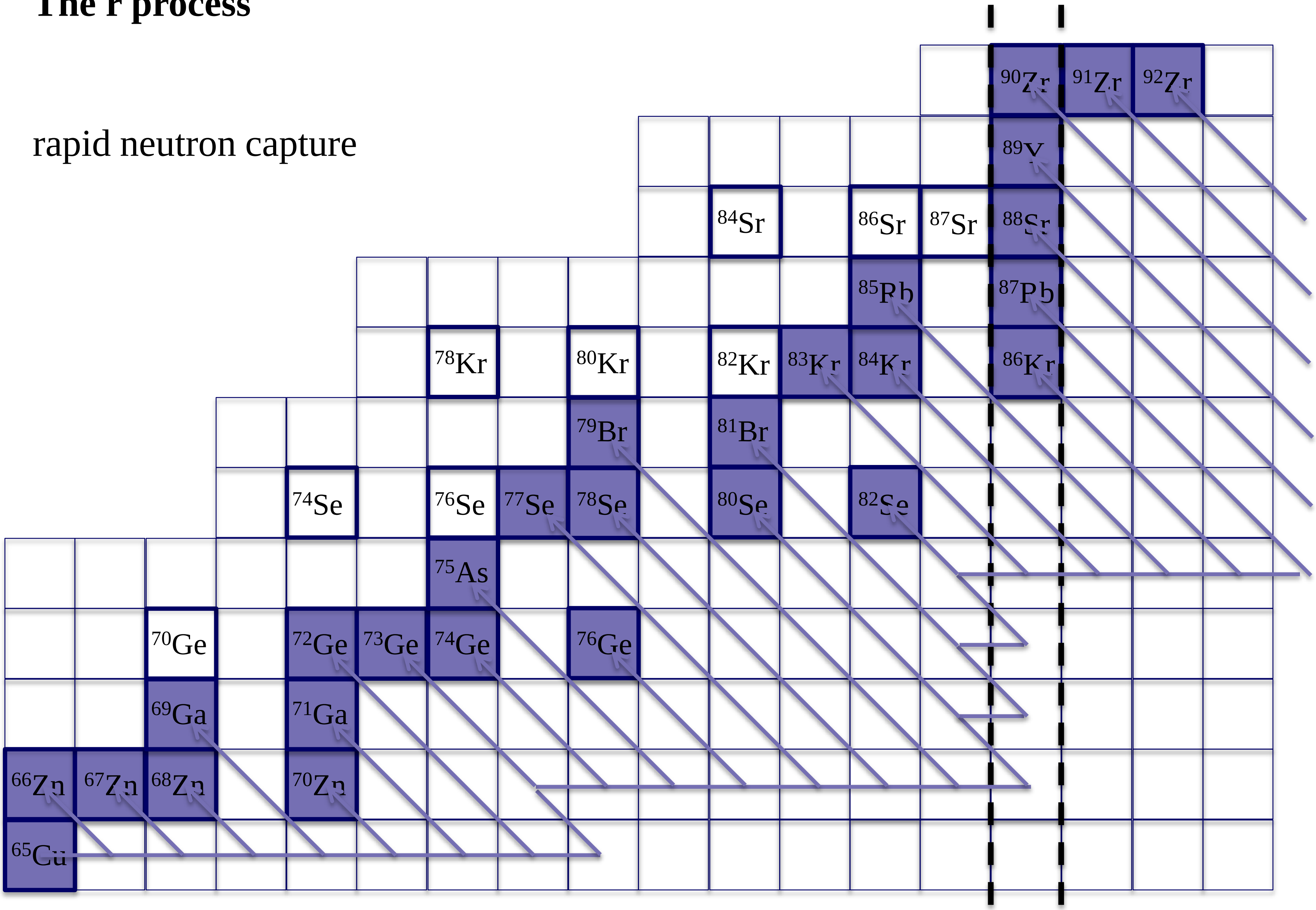

closed neutron shell

Nucleosynthesis processes

Maximum abundances related to neutron magic numbers

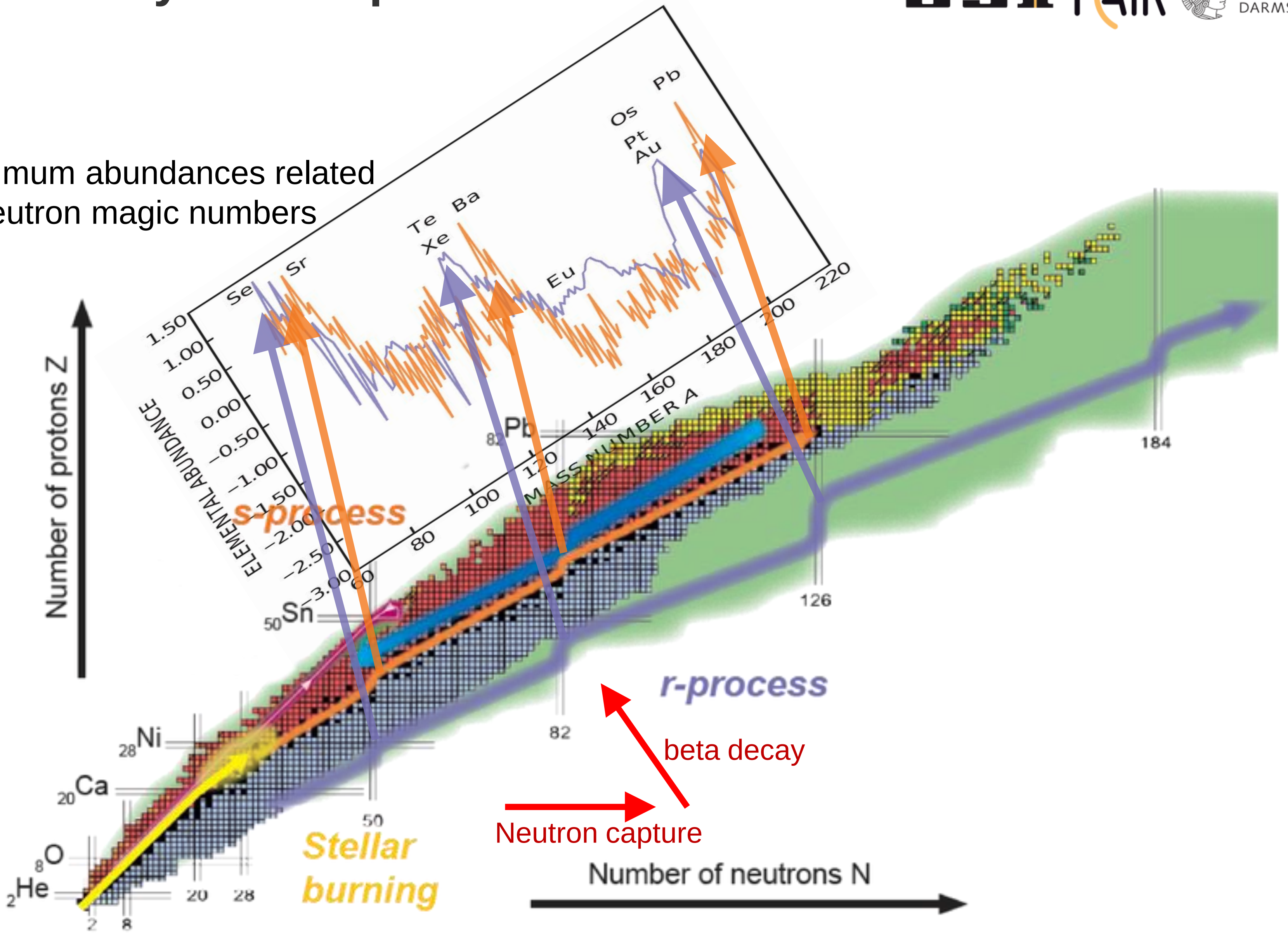

Signatures of nucleosynthesis

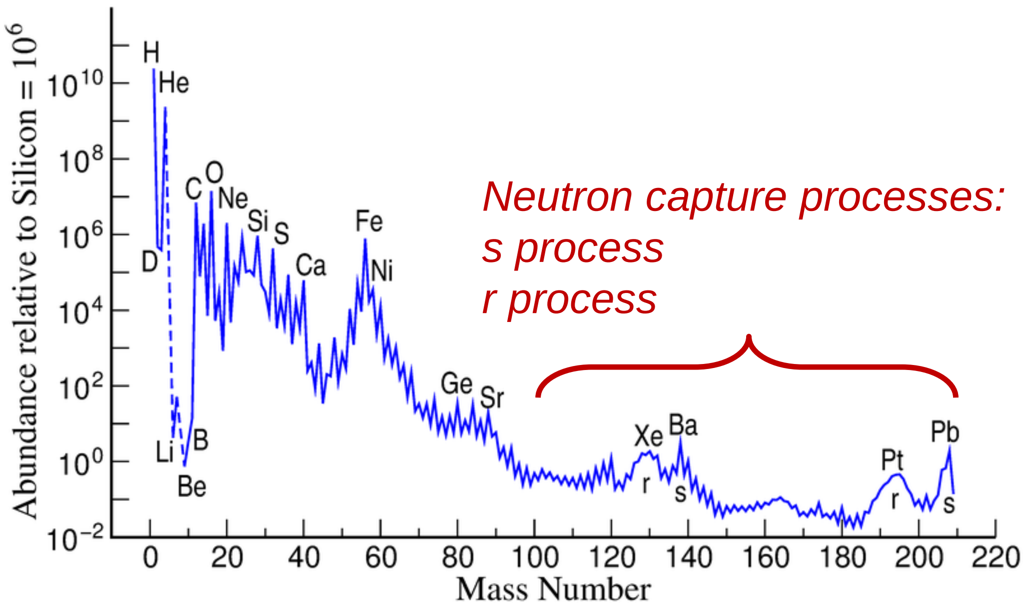

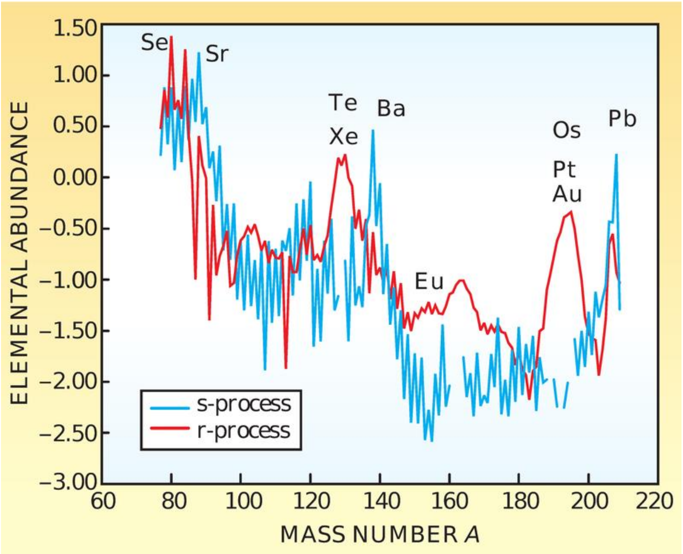

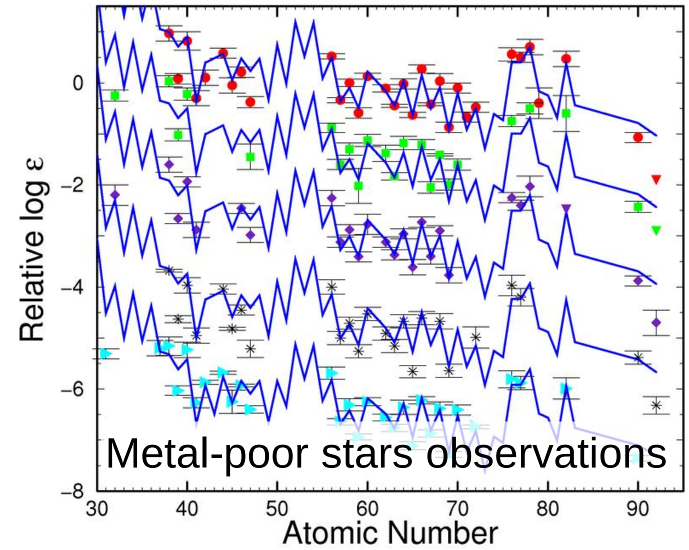

- Old metal-poor stars are enriched in r-process elements with similar relative abundances to our Sun
- r process operates at early Galactic history in rare events.

Implications from observations

Individual stars, Milky Way Halo
Sneden, Cowan & Gallino, 2008

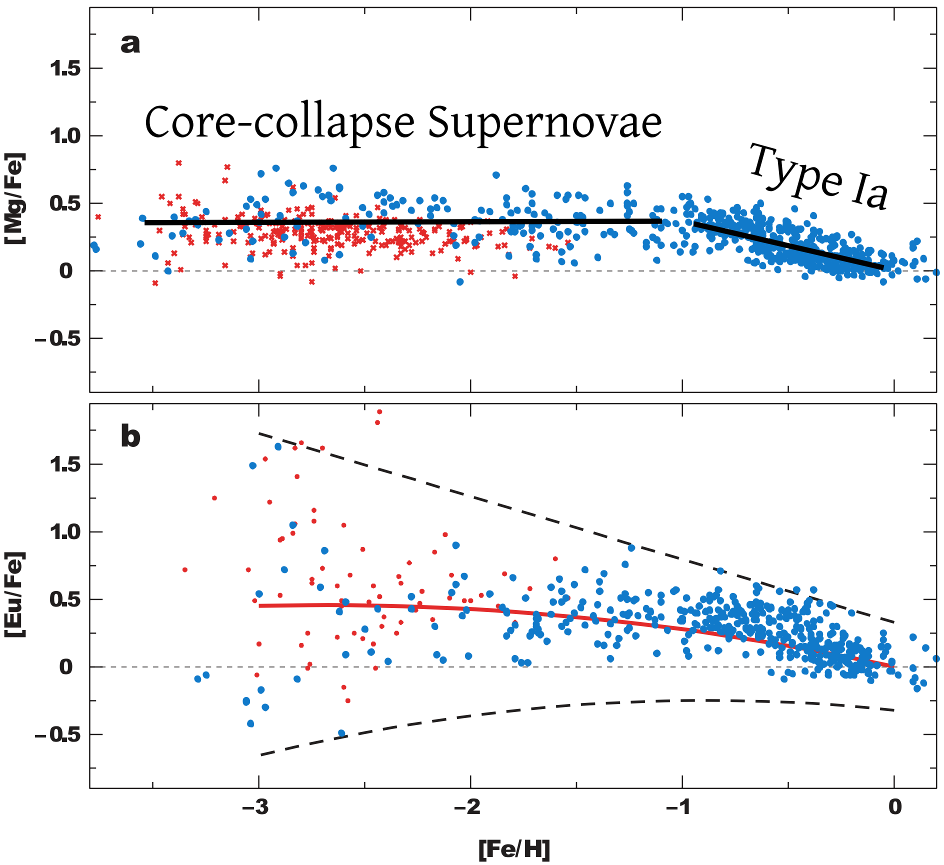

Ji et al 2016 found that only 1 of 10 ultrafaint dwarf galaxies is enriched in r-process elements

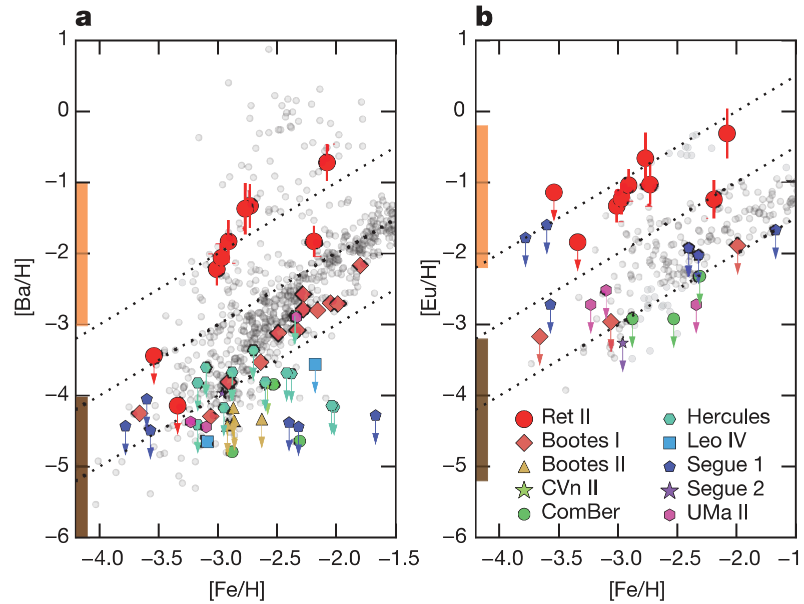

R process related to rare high yield events not correlated with Iron enrichment

Similar results obtained by ^{60}Fe and ^{244}Pu observations in deep sea sediments (Wallner et al, 2015; Hotokezaka et al, 2015)

R process nuclear needs

Astrophysical environment should provide enough neutrons per seed for the r process to operate

$$A_{\text{final}} = A_{\text{initial}} + n_{\text{seed}}$$

n_{seed} depends mainly on neutron richness ejecta

Neutron stars are an important reservoir of neutrons

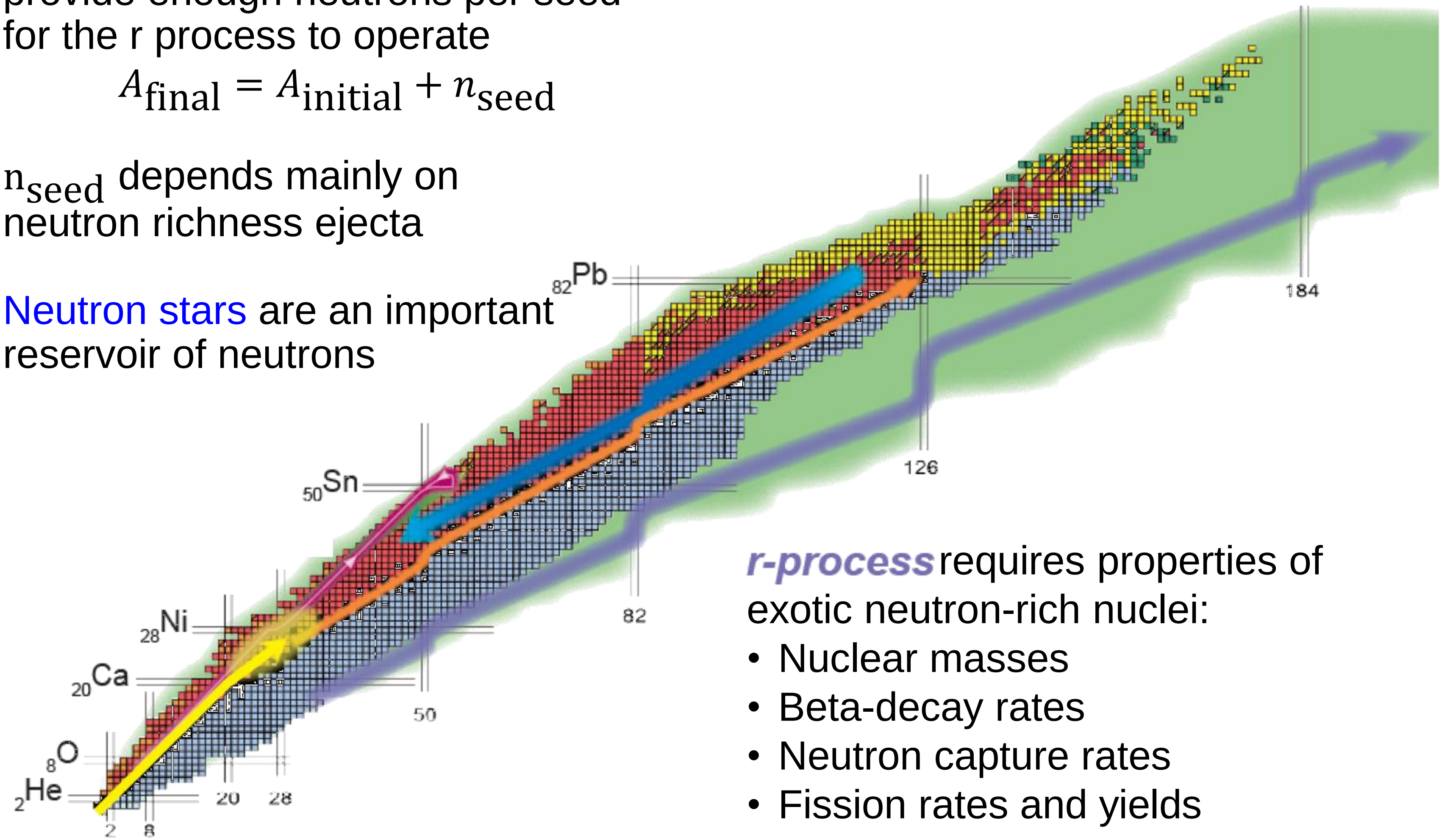

r-process requires properties of exotic neutron-rich nuclei:

- Nuclear masses
- Beta-decay rates
- Neutron capture rates
- Fission rates and yields

Stellar evolution

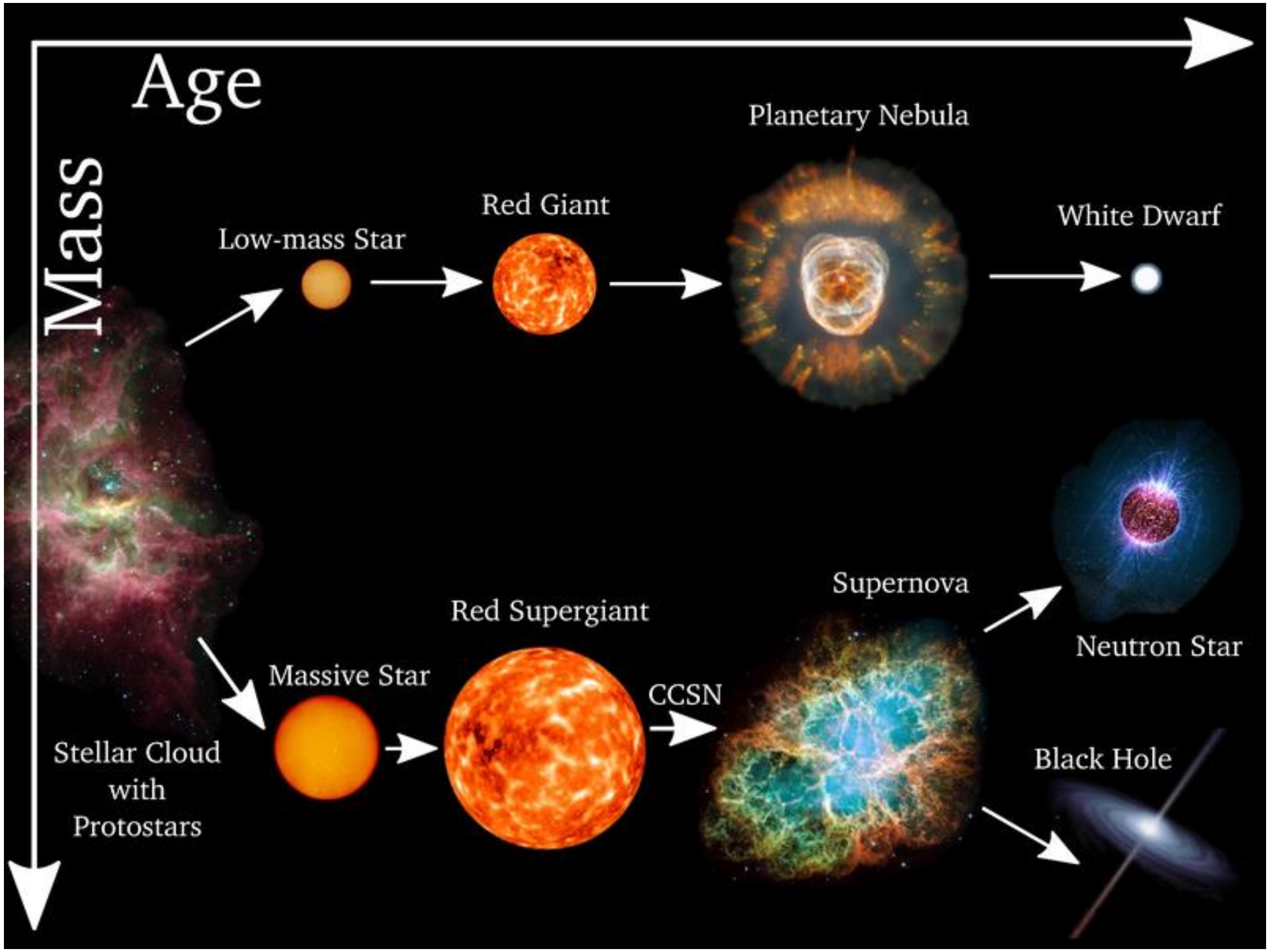

Stars with masses below 8 solar masses burn hydrogen and helium and end their lives as white dwarfs

Stars with masses above 8 solar masses follow all burning phases producing an iron core. The collapse of the iron core produces a neutron star and ejects the stellar mantle. Main products: Carbon, Oxygen, Iron

Supernova light curve:
signature of nucleosynthesis

Supernova light curves follow the beta decay of ^{56}Ni ($t_{1/2} = 6$ d) and later ^{56}Co ($t_{1/2} = 77$ d)

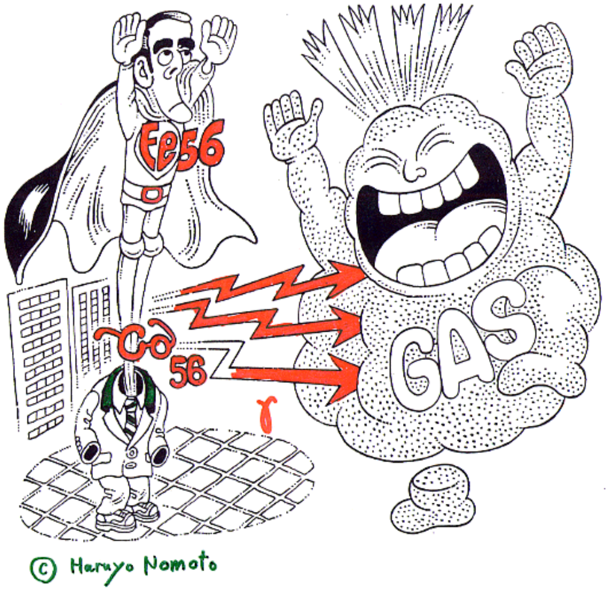

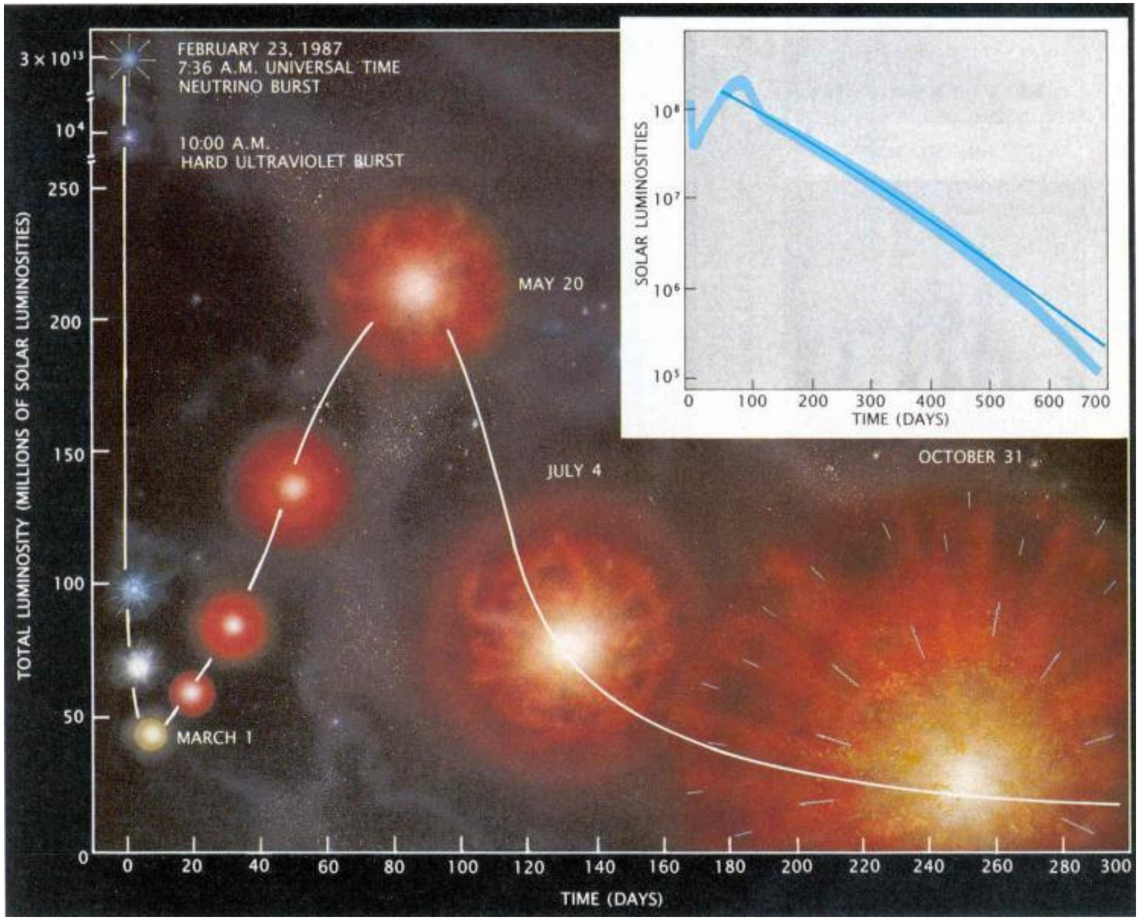

Woosley & Weaver, Scientific American 261, 1989

Supernova light curve:
signature of nucleosynthesis

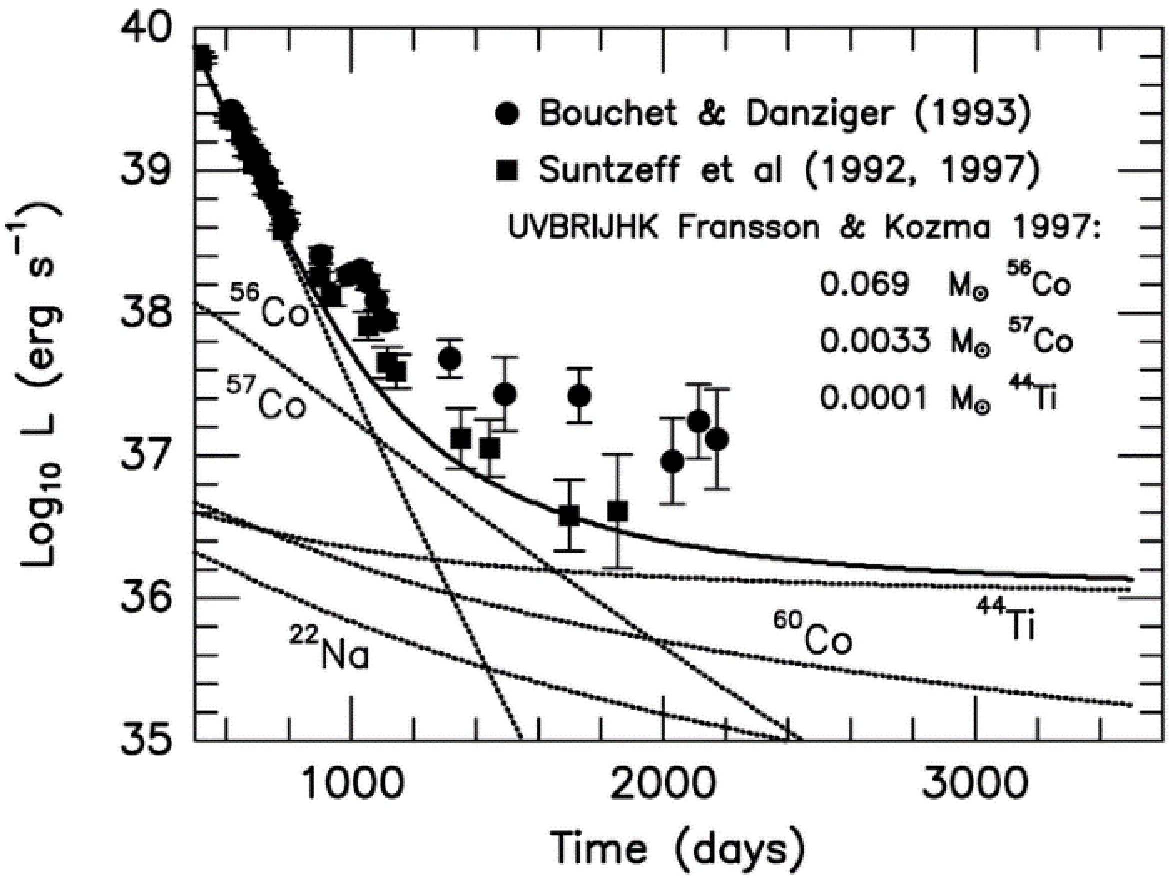

Diehl & Timmes, PASP 110, 637 (1998)

Heavy elements in supernova?

Heavy elements produced in neutrino winds from protoneutron star cooling. Neutrino interactions determine proton-to-nucleon ratio, Y_e

$$\nu_e + n \rightleftarrows p + e^-$$
$$\bar{\nu}_e + p \rightleftarrows n + e^+$$

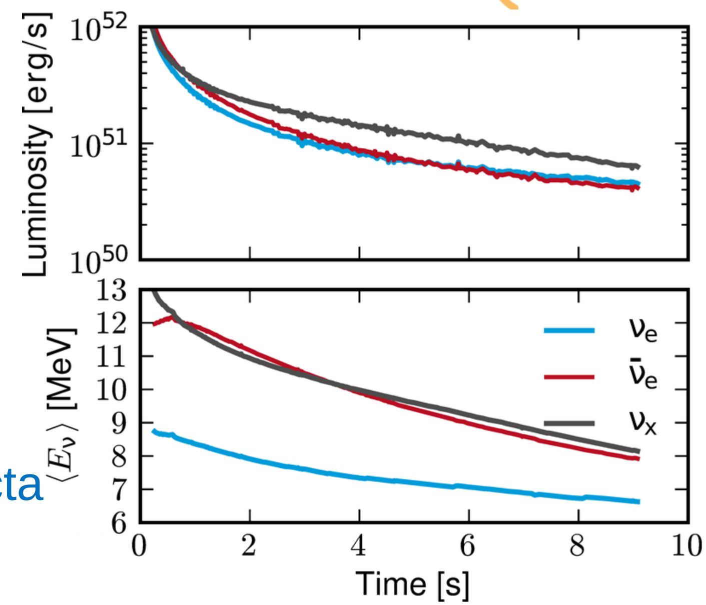

Very similar spectra ν_e and $\bar{\nu}_e$ → proton rich ejecta

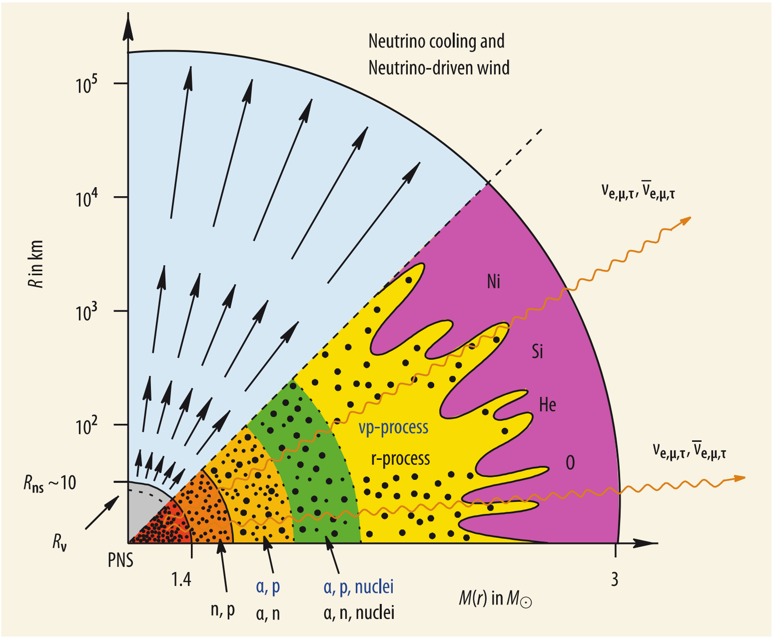

Supernova produce only medium mass nuclei

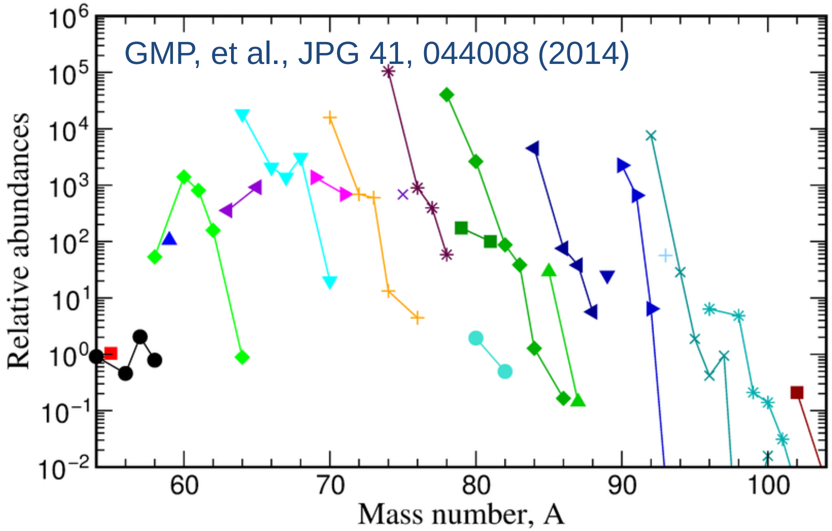

Pulsars and binary neutron star system

- Neutron stars have large magnetic fields producing a beam of radiation in the direction of the magnetic poles.
- We observe regular pulses of radiation whenever the beam point to us
- Pulsars were discovered in 1967 by Jocelyn Bell and Anthony Hewish. Anthony Hewish won the 1974 Nobel Prize in Physics.

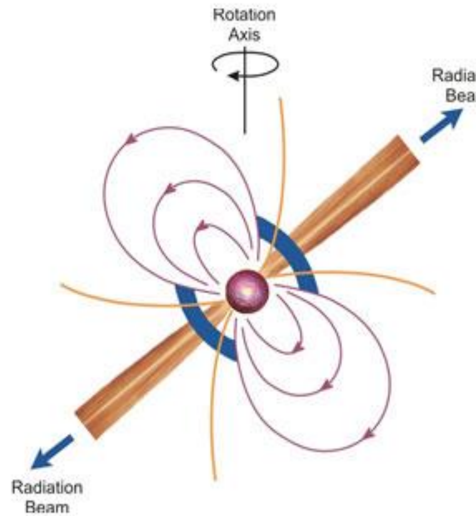

The National Radio Astronomy Observatory, AUI, NSF

John Rowe Animation/Australia Telescope National Facility, CSIRO

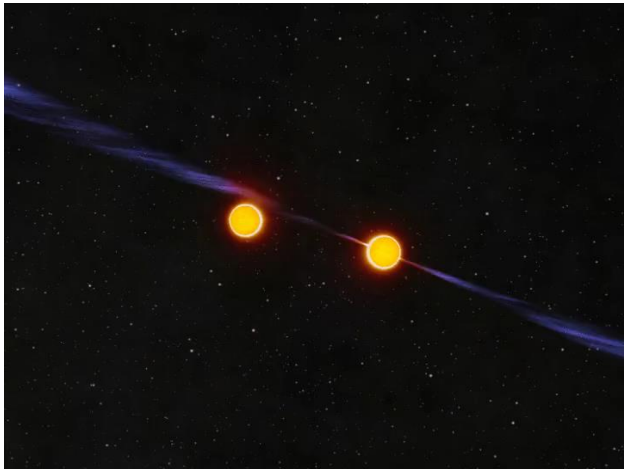

- The first binary system consisting of two neutron stars was discovered by Russel Hulse and Joseph Taylor in 1974
- Unique test laboratory for General Relativity. Emission gravitational waves leads to merger in ~ billion of years
- What is the maximum mass of a neutron star? Determines transition from neutron stars to black holes

Astrophysical sites

Core-collapse supernova

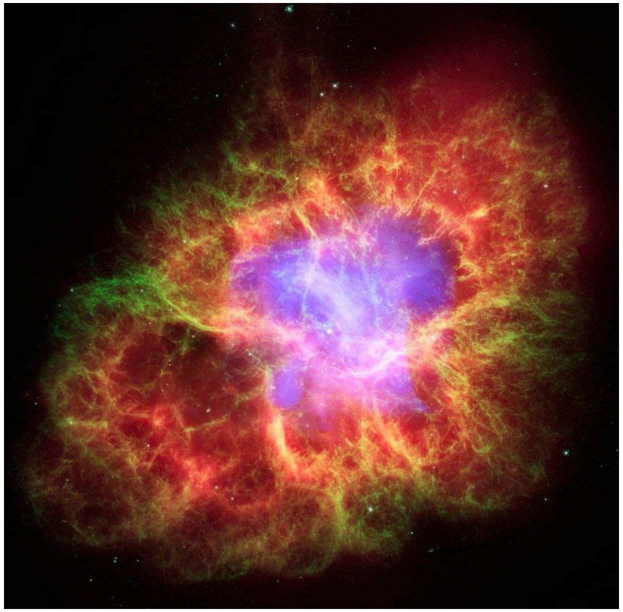

Compact binary mergers

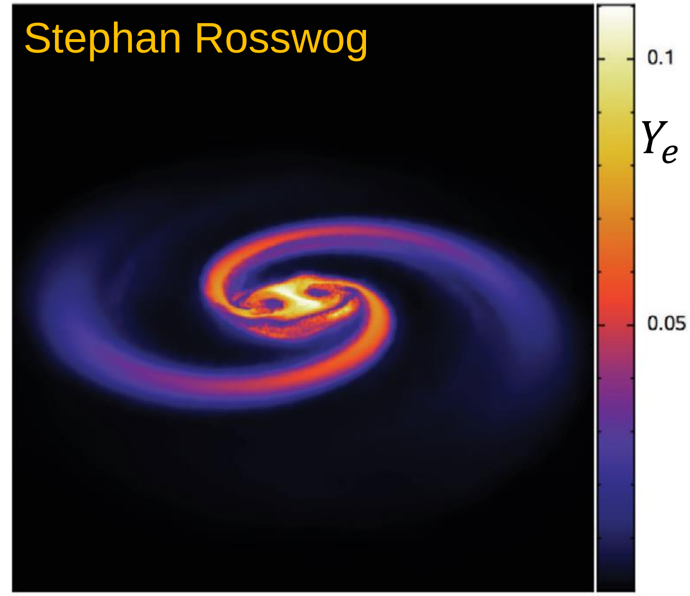

	Supernova	Mergers
Optimal conditions	☹	☺
Yield / Frequency	😐	☺
Direct signature	☹	☺

Mass ejection neutron star merger

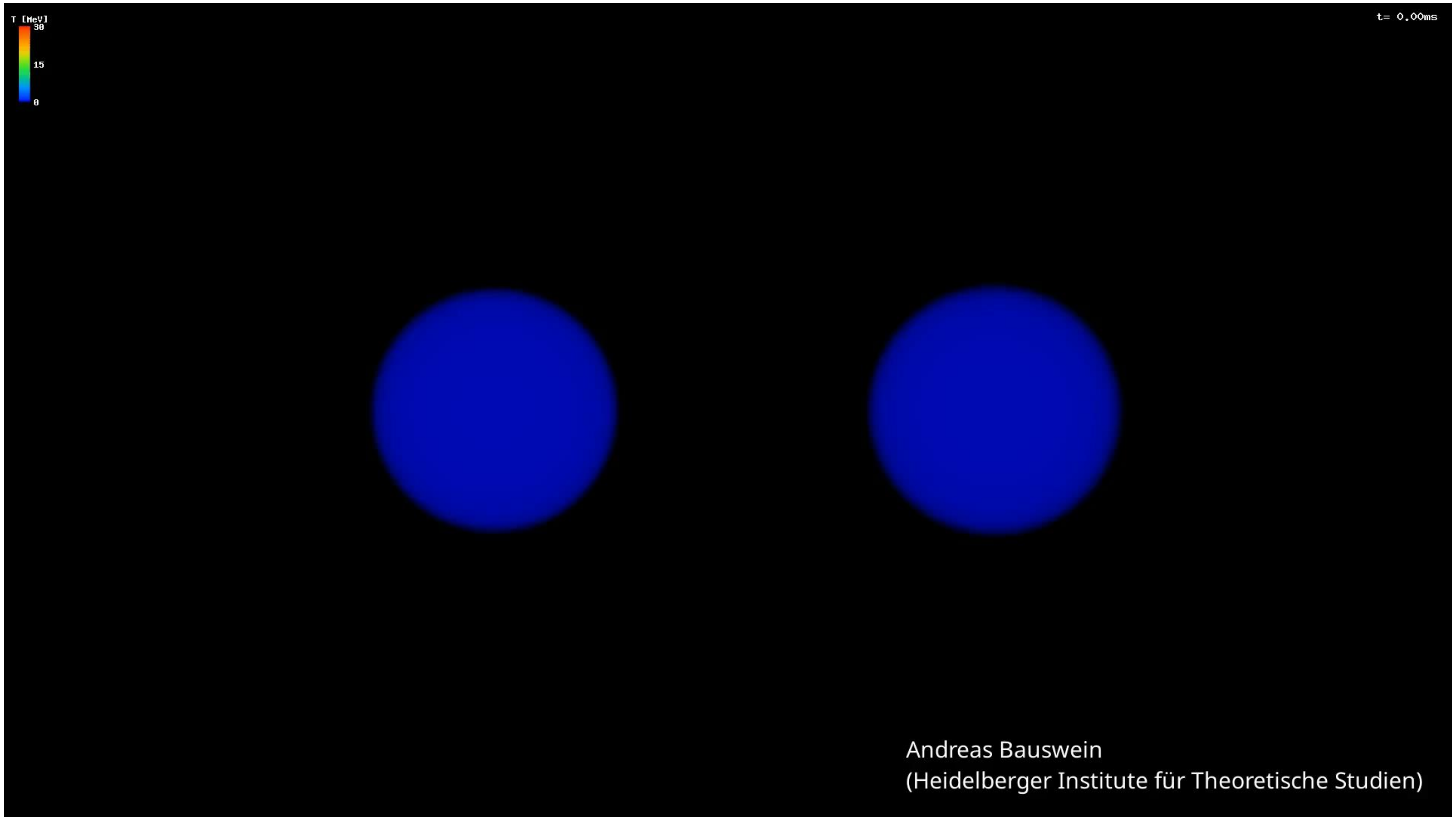

Two sources of ejecta:

- Dynamical during the early phases of the merger
- Accretion disc on longer timescales

Ejecta properties depend on central remnant (neutron star or black hole). Determines the strength of neutrino emission

R process in merger ejecta

Heavy elements produced in merger ejecta. Radioactive decay liberates energy

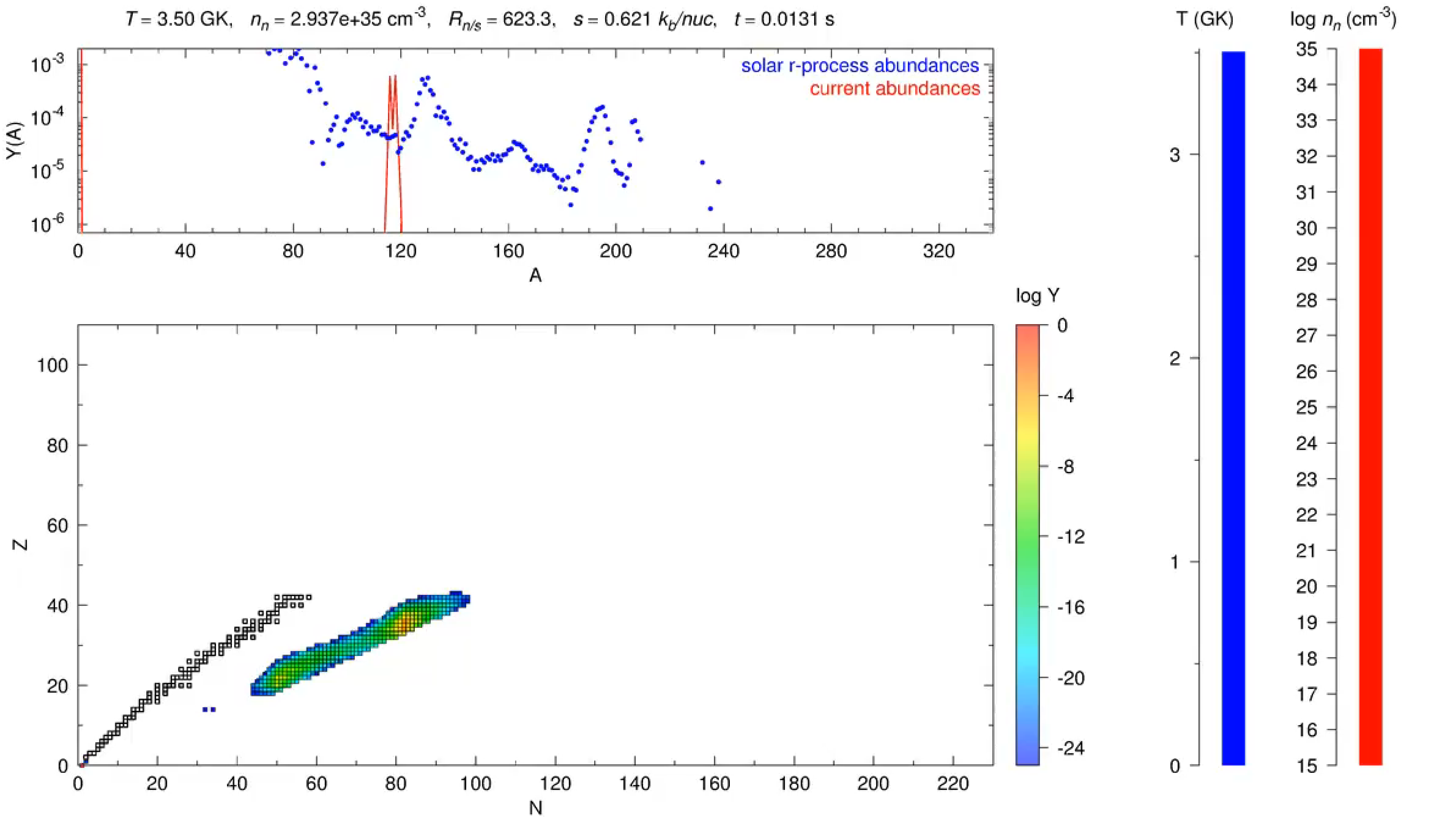

Nucleosynthesis dependence on Y_e

Nucleosynthesis mainly sensitive to proton-to-nucleon ratio, $Y_e = n_n/(n_n + n_p)$

$$\nu_e + n \rightleftarrows p + e^- \quad \text{vs} \quad \bar{\nu}_e + p \rightleftarrows n + e^+$$

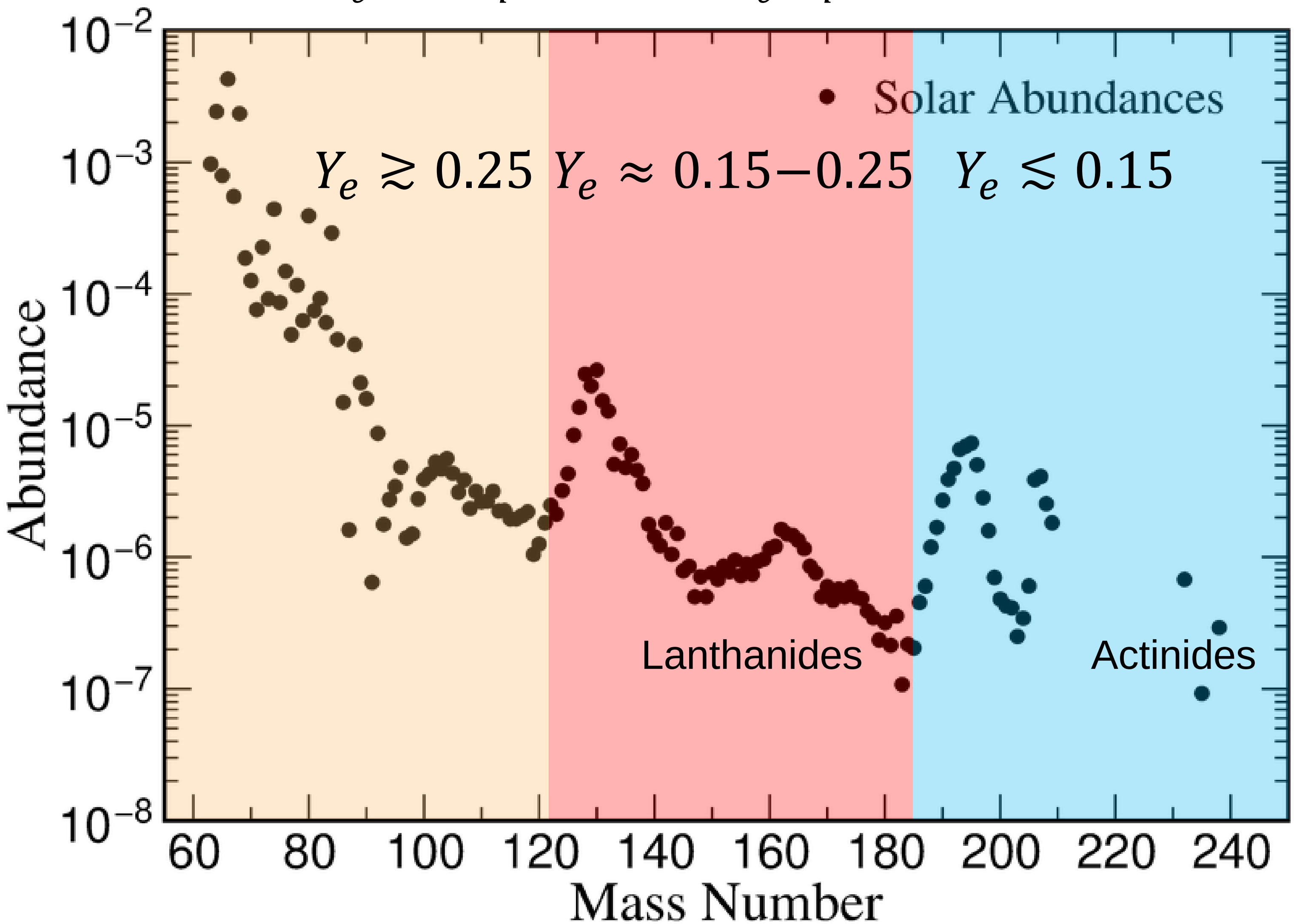

Dependence on nuclear masses

Mendoza-Temis, et al, PRC 92, 055805 (2015)

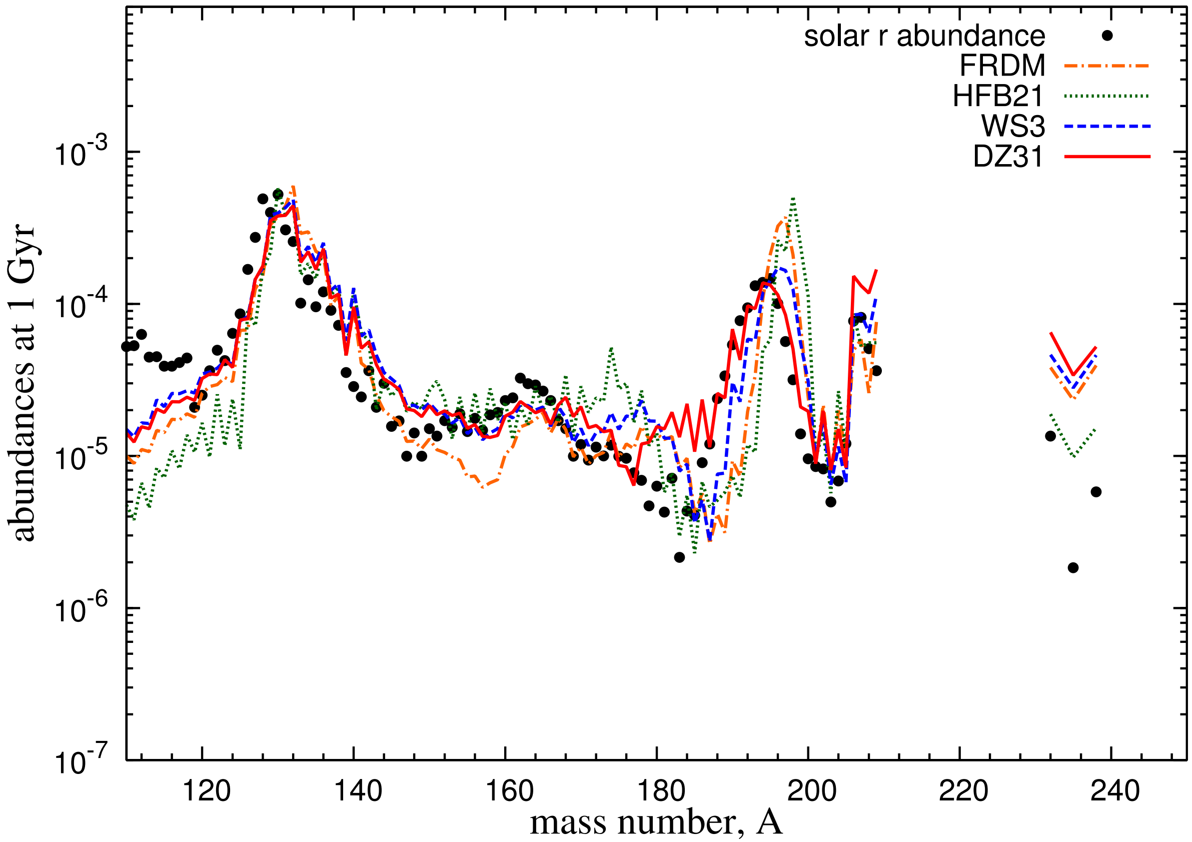

- Robustness astrophysical conditions, sensitive nuclear physics
- Second peak (A ~ 120) sensitive to fission yields (Goriely, 2015)
- Third peak (A ~ 195) sensitive to masses and half-lives
- Elements lighter than A ~ 120 are not produced

Impact beta-decay half-lives

- Beta-decay half-lives determine the speed at which heavy elements are build starting from light ones
- Theoretical advances allow for fully microscopic calculations

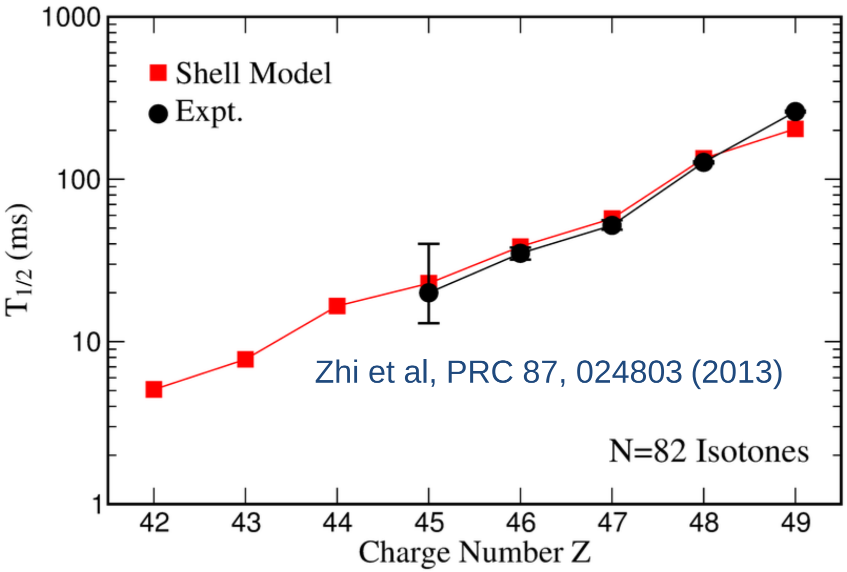

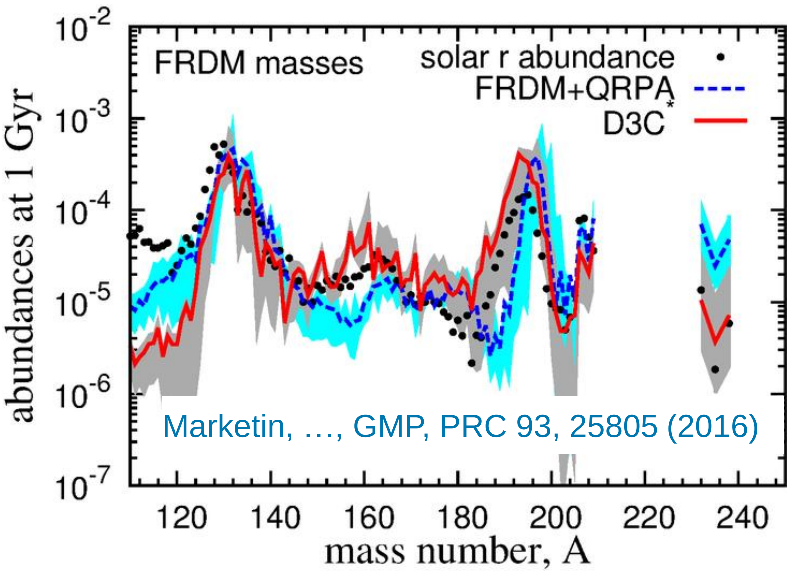

- Microscopic calculations reproduce available data
- Predict shorter half-lives for nuclei $Z > 80$ having a strong impact on the position of the A ~ 195 peak [Eichler et al, ApJ 808, 30 (2015)]

Impact of the merger remnant

After the merger an hyper massive neutron star is formed that is stable before collapsing to a black hole

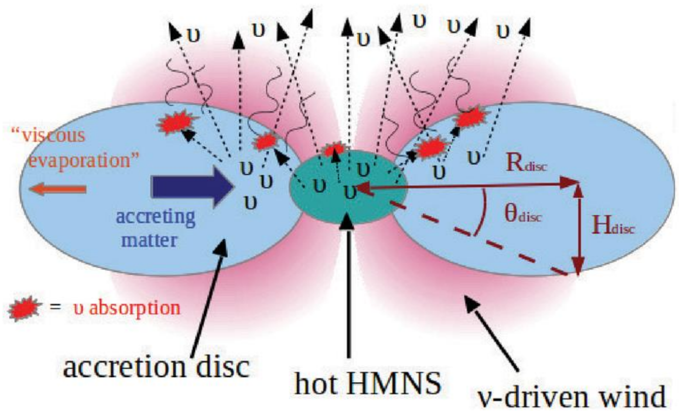

Large neutrino fluxes mainly in polar region decrease neutron-to-proton ratio by reactions

$$\nu_e + n \rightarrow p + e^-$$
$$\bar{\nu}_e + p \rightarrow n + e^+$$

Martin, et al, ApJ 813, 2 (2015)

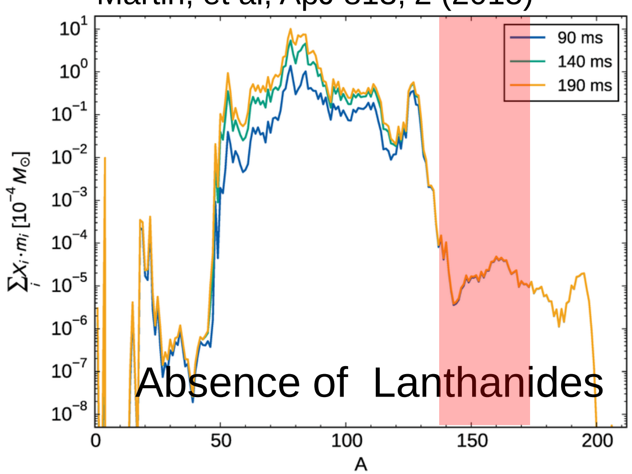

Once neutron star collapses to a black hole neutrinos emission ceases. Larger neutron-to-proton ratio

Wu et al, MNRAS 463, 2323 (2016)

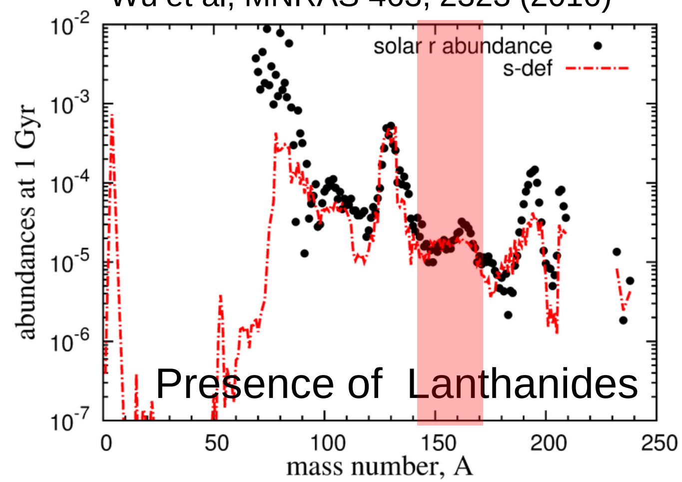

Energy production from r process ejecta

At early times (days), the decay of r process products produces energy following a power law $\dot{\varepsilon} \sim t^{-1.3}$. Many nuclei decaying at the same time heating up the ejecta

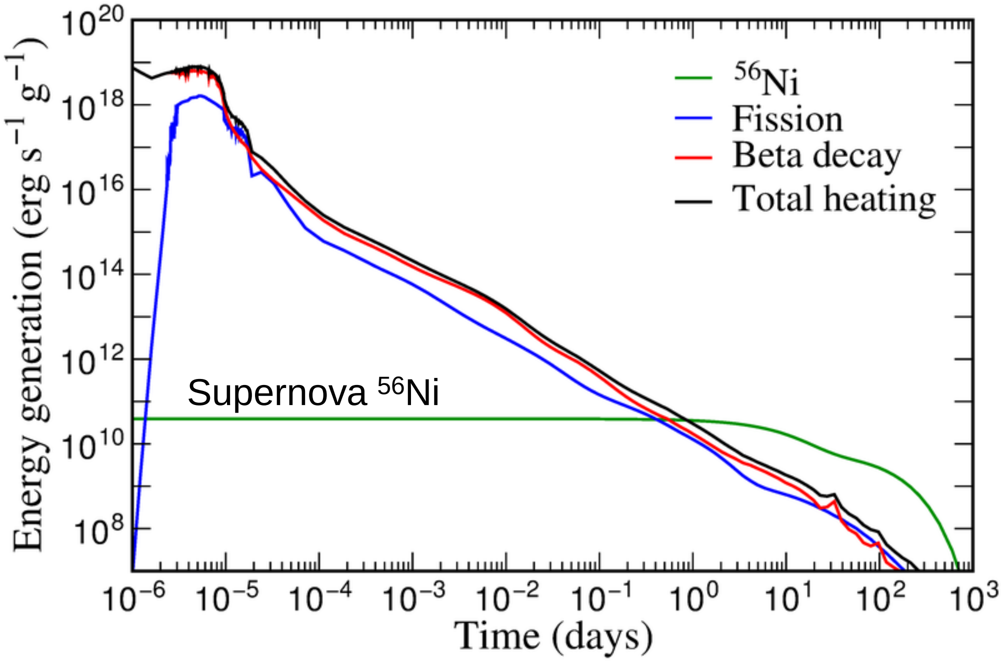

We expect an electromagnetic transient with properties depending:

- Energy production rate
- Efficiency energy is absorbed by the gas (thermalization efficiency)
- Opacity of the gas (depends on composition, presence of Lanthanides/Actinides)

Impact of opacity

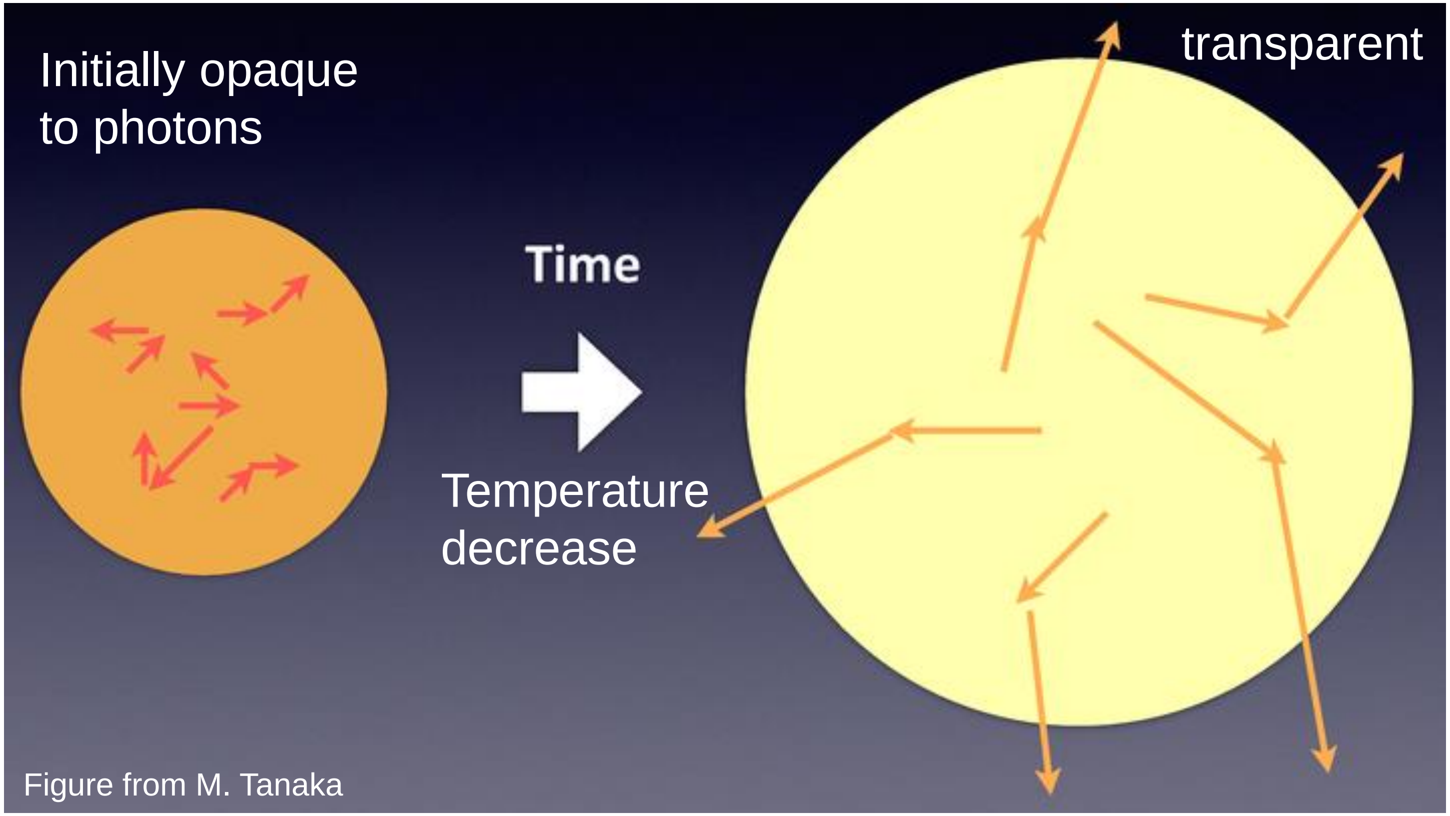

Figure from M. Tanaka

The transition from an opaque to transparent regime depends on the interaction probability of the photons (opacity). Depends on the structure of the atoms.

Low opacity: early emission from hot material at short wavelengths (blue)

High opacity: late emission from colder material at longer wavelengths (red)

Impact Lanthanides

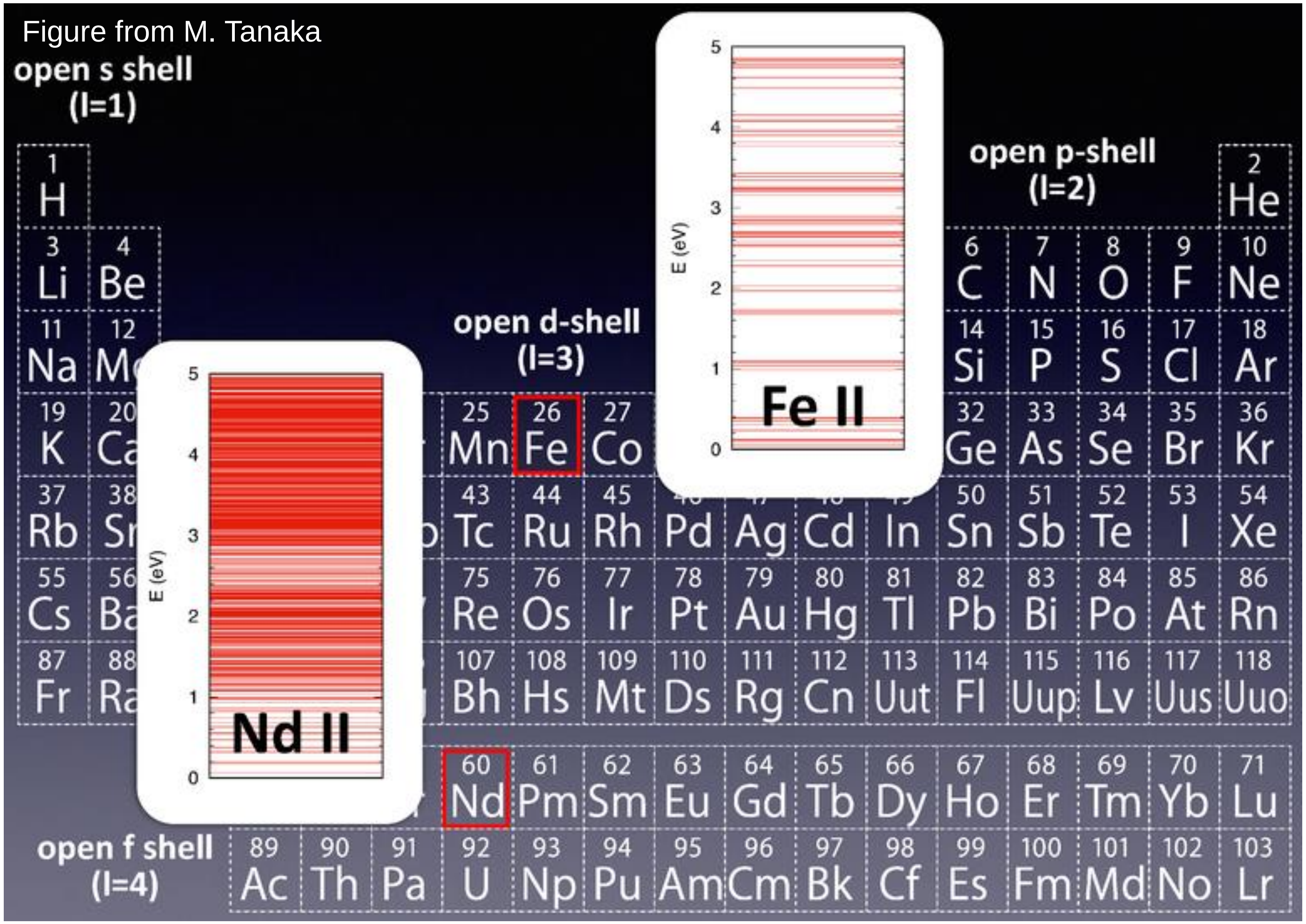

Large number of states of Lanthanides/Actinides leads to a high opacity

Barnes & D. Kasen, Astrophys. J. 775, 18 (2013);Tanaka & Hotokezaka, Astrophys. J. 775, 113 (2013).

Kilonova: Electromagnetic signature of the r process

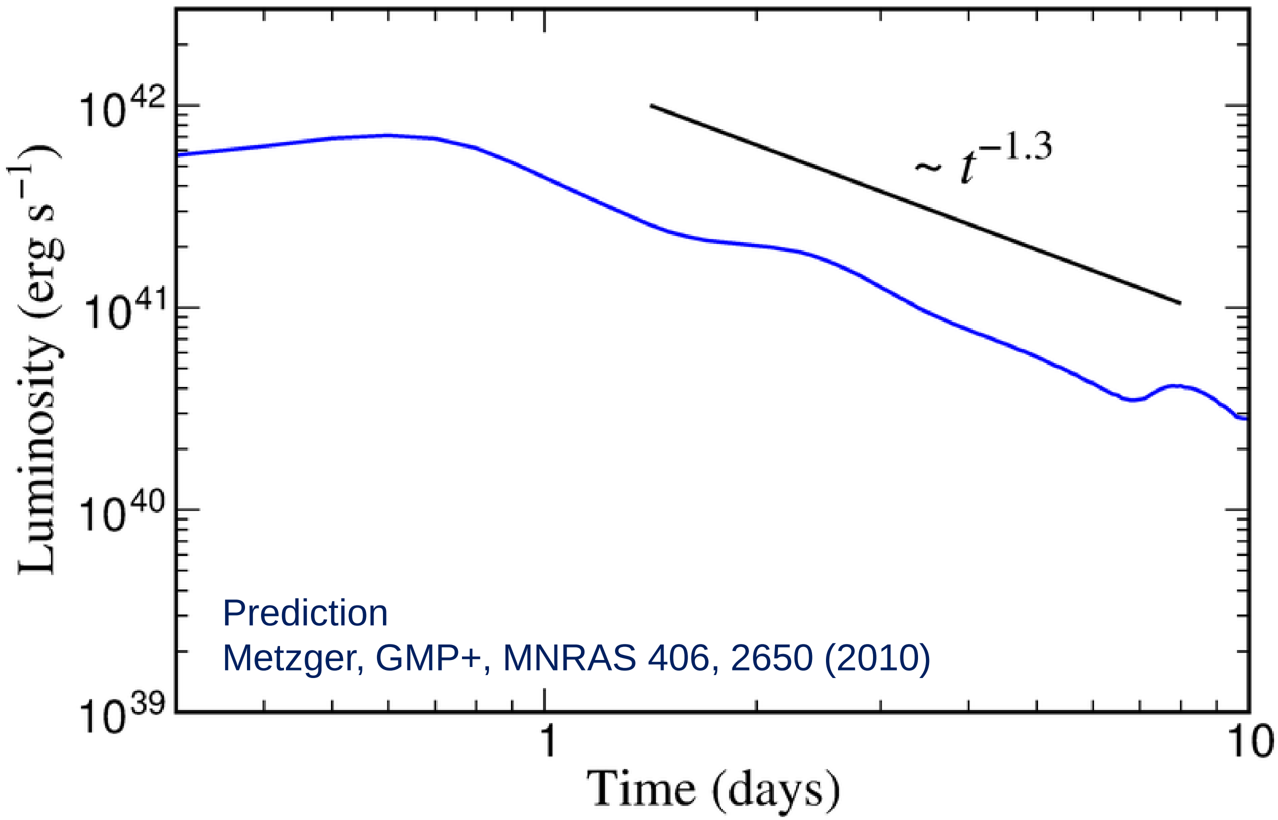

Luminosity equivalent to 1000 novas (kilonova) in timescales of days.
Depends on amount of ejected material, velocity and composition.

Simple Kilonova model

Light curve is expected to peak when photon diffusion time is comparable to elapsed time (Metzger et al 2010, Kasen et al 2017)

$$t_{\text{diff}} = \frac{\rho \kappa R^2}{c}, \qquad \rho = \frac{M}{4\pi R^3/3}, \qquad R = vt$$

$$t_{\text{peak}} \approx \left(\frac{3\kappa M}{4\pi c v}\right)^{\frac{1}{2}} \approx 2.7\ \text{days} \left(\frac{M}{0.01\ M_\odot}\right)^{\frac{1}{2}} \left(\frac{v}{0.01c}\right)^{-\frac{1}{2}} \left(\frac{\kappa}{1\ \text{cm}^2\ \text{g}^{-1}}\right)^{\frac{1}{2}}$$

The Luminosity is $L(t) \approx M\,\dot{\varepsilon}(t)$, $\dot{\varepsilon}(t) \approx 10^{10} \left(\frac{t}{1\ \text{day}}\right)^{-\alpha}\ \text{erg s}^{-1}\ \text{g}^{-1}$

$$L_{\text{peak}} \approx 5 \times 10^{40} \text{erg s}^{-1} \left(\frac{M}{0.01\ M_\odot}\right)^{1-\frac{\alpha}{2}} \left(\frac{v}{0.01c}\right)^{\frac{\alpha}{2}} \left(\frac{\kappa}{1\ \text{cm}^2\ \text{g}^{-1}}\right)^{-\frac{\alpha}{2}}$$

Very sensitive to atomic opacity

$\kappa \approx 1\ \text{cm}^2\ \text{g}^{-1}$, light r process material (blue emission)

$\kappa \approx 10\ \text{cm}^2\ \text{g}^{-1}$, heavy (lanthanide/actinide rich) r process (red emis.)

GW170817: First detection gravitational waves from a NS merger

On August 17, 12:41:04 UTC advanced LIGO and Virgo detect the first GW signal from a binary neutron star inspiral

Abbott, et al, PRL 119, 161101 (2017).

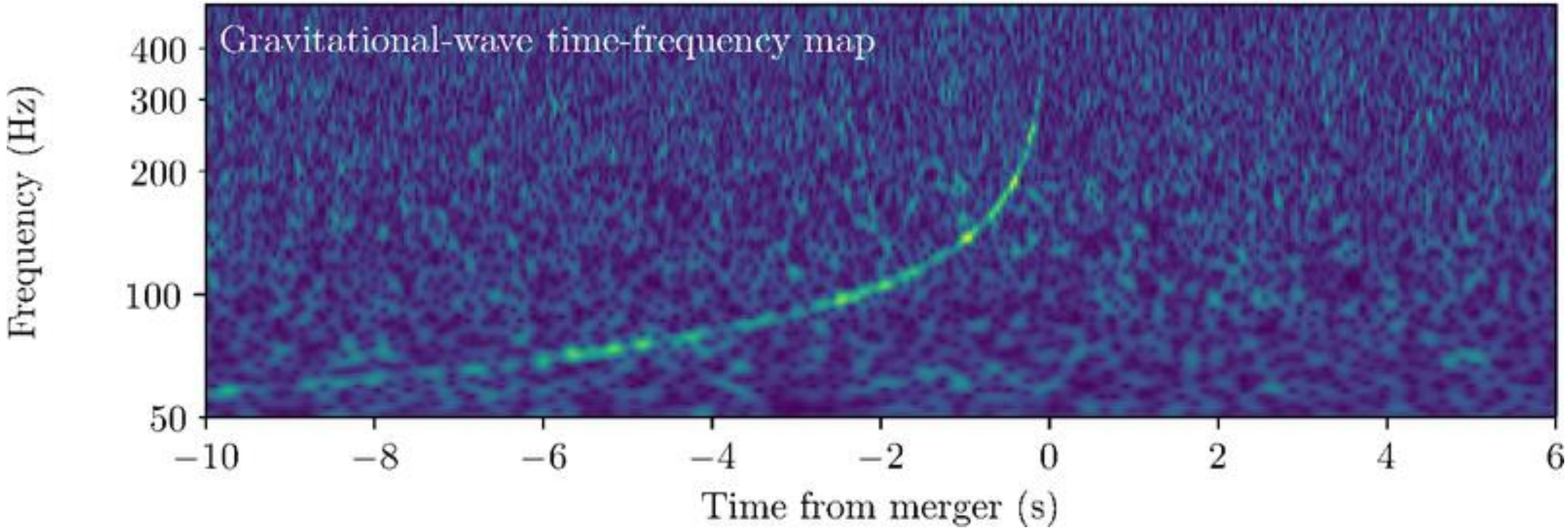

Frequency growth determined by chirp mass $\mathcal{M} = \frac{(m_1 m_2)^{3/5}}{(m_1+m_2)^{1/5}} = 1.188^{+0.004}_{-0.002}\ \mathrm{M}_\odot$

Total mass: $M = 2.74^{+0.04}_{-0.01}\ \mathrm{M}_\odot$
Primary mass: $m_1 \in (1.36-1.60)\ \mathrm{M}_\odot$
Secondary mass: $m_2 \in (1.17-1.36)\ \mathrm{M}_\odot$
Distance: 40^{+8}_{-14} Mpc (130 million light years)

GRB170817A: detection of gamma rays

- 1.7 s later Fermi and INTEGRAL detected the short GRB 170817 A
- Closest SGRB yet it is 2-6 orders of magnitude weaker than typical SGRBs.
- Explained assuming jet forms ~ $30°$ with line of view.
- Combined analysis favors formation BH on timescales $\lesssim 100$ ms.

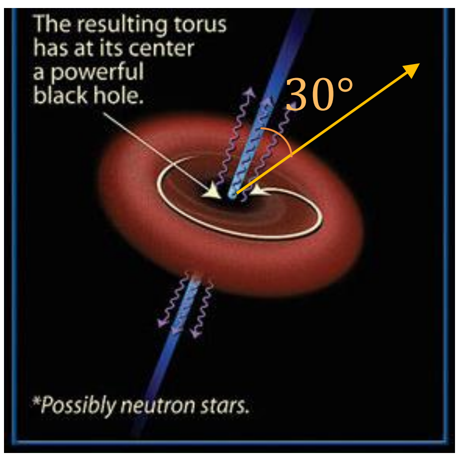

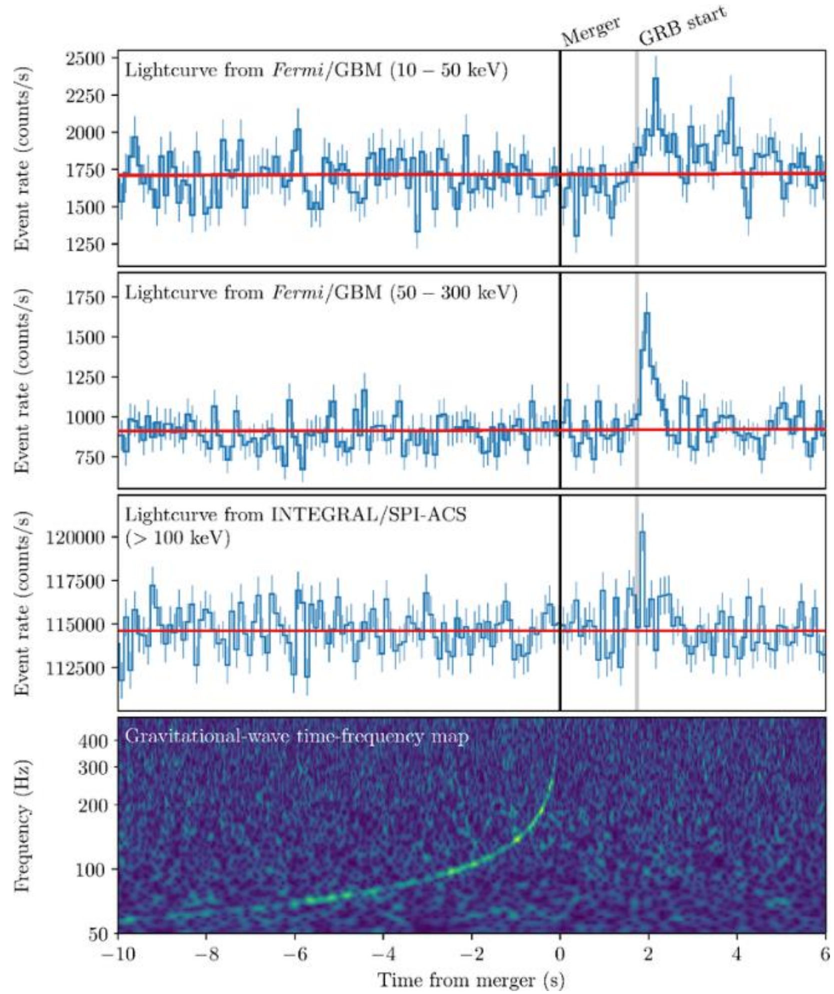

B. P. Abbott, et al, Astrophys. J. 848, L13 (2017).

Optical transient identified

Kilonova identified 10.9 hours after the merger in the Galaxy NGC 4993 near the constellation of Hydra (Southern hemisphere). Denoted AT 2017 gfo

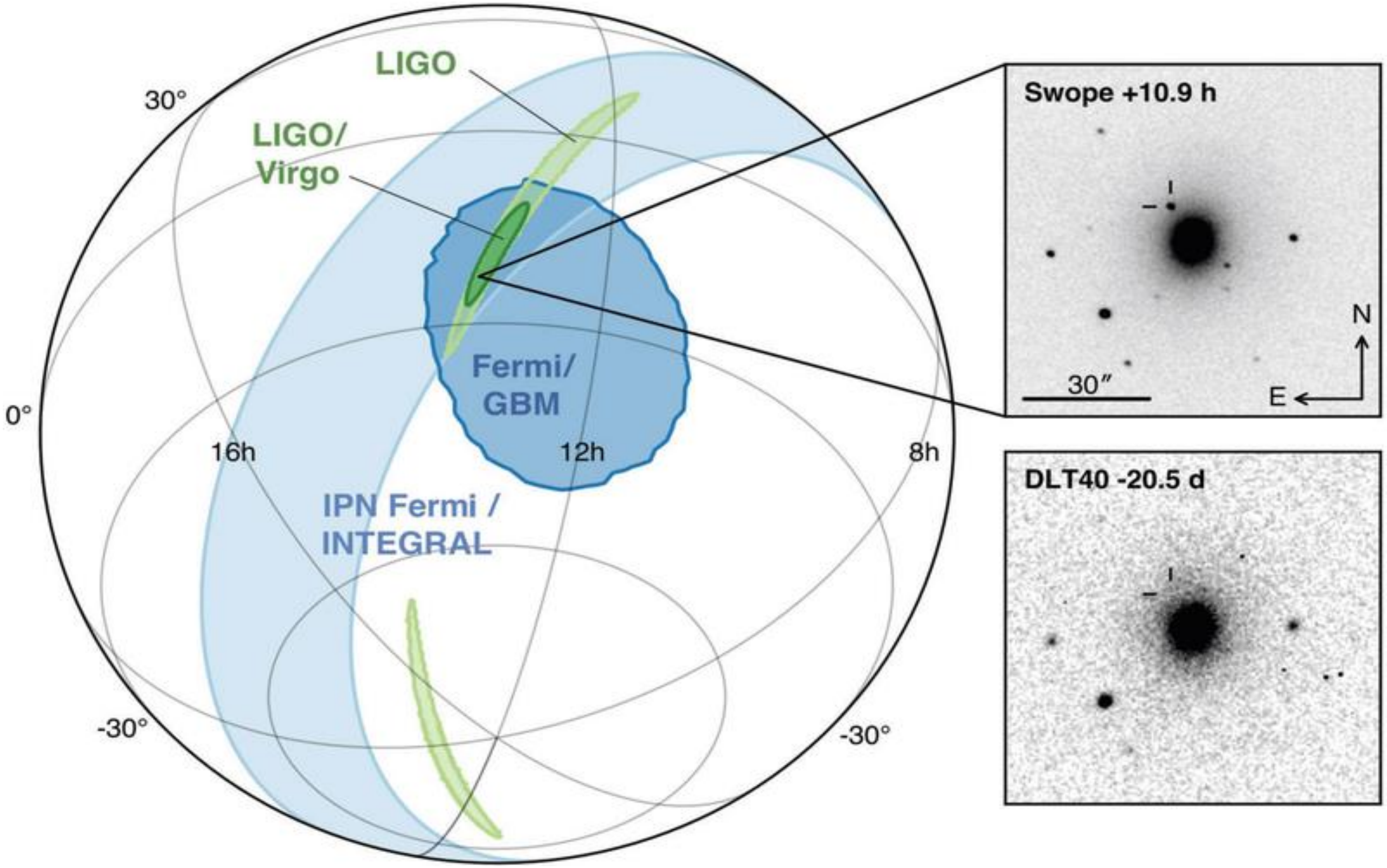

Light curve and spectra evolution

https://youtu.be/kZiCKULA2cE

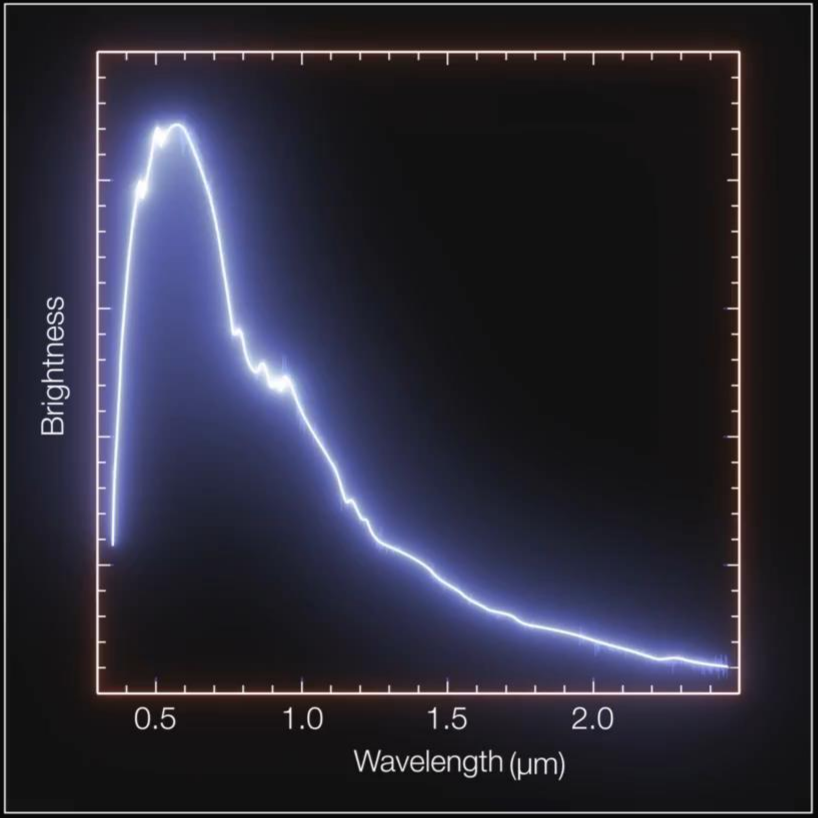

Time: +1.5 days

ESO/E. Pian/S. Smartt & ePESSTO/N. Tanvir/VIN-ROUGE, Pian et al, Nature 551, 67, 2017

Kilonova: Electromagnetic transient powered by decay of r-process nuclei

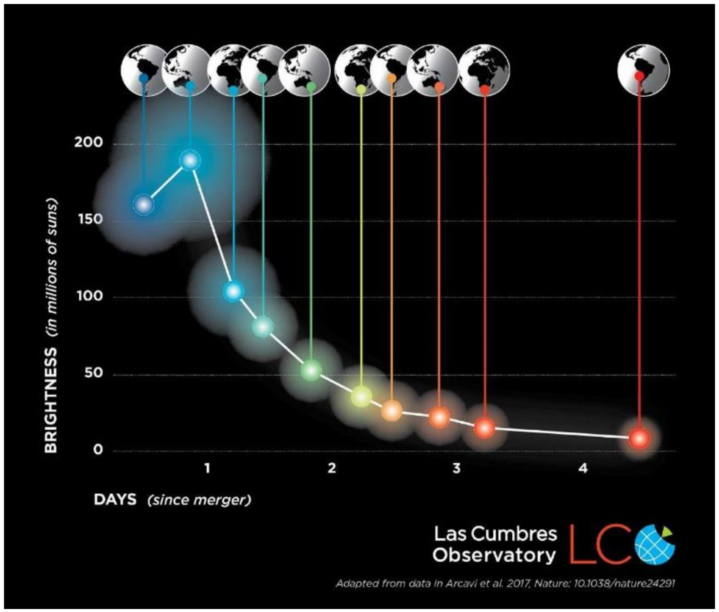

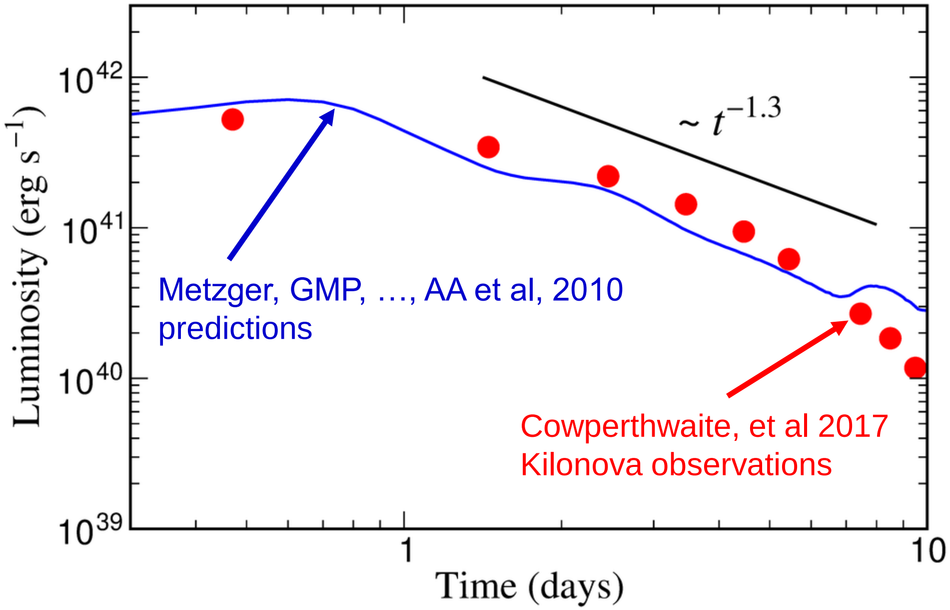

- Time evolution determined by the radioactive decay of r-process nuclei
- Two components:
  - blue dominated by light elements ($Z < 50$)
  - Red due to presence of lanthanides ($Z = 57$-71) and/or Actinides ($Z = 89$-103)
- Likely source of heavy elements including Gold, Platinum and Uranium

Two components model

Kasen et al, Nature 551, 80 (2017)

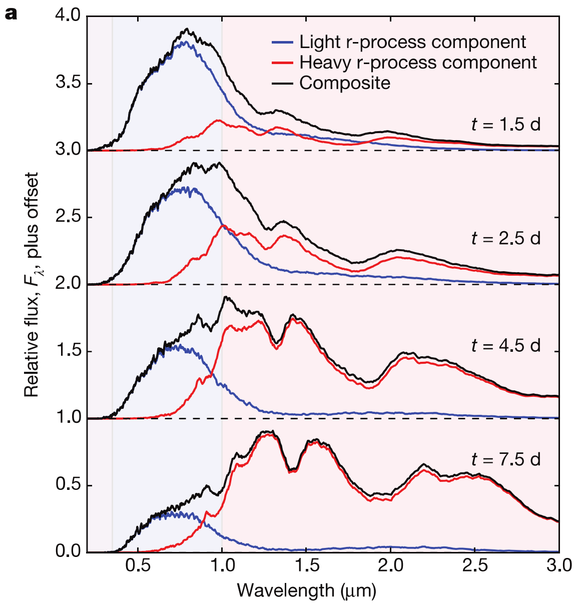

- Blue component from polar ejecta subject to strong neutrino fluxes (light r process)
  $M = 0.025\ M_{\odot}, v = 0.3c, X_{\mathrm{lan}} = 10^{-4}$
- Red component disk ejecta after NS collapse to a black hole (light and heavy r process)
  $M = 0.04\ M_{\odot}, v = 0.15c, X_{\mathrm{lan}} = 10^{-1.5}$

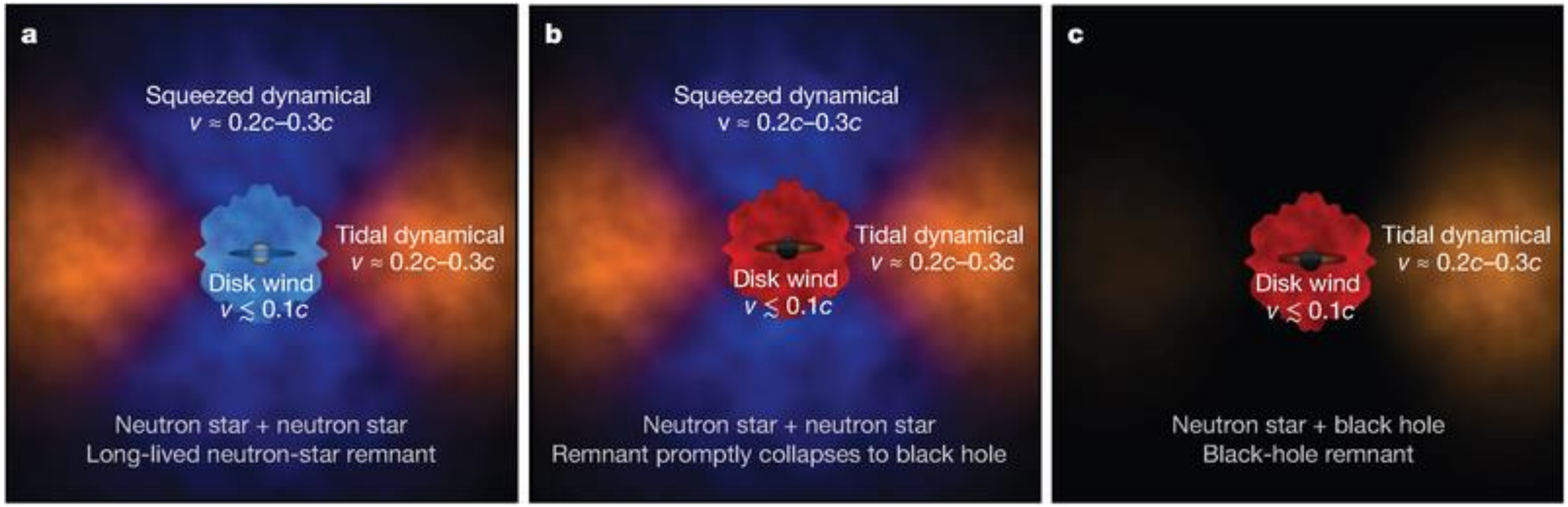

Summary GW170817 observations

Al Cameron

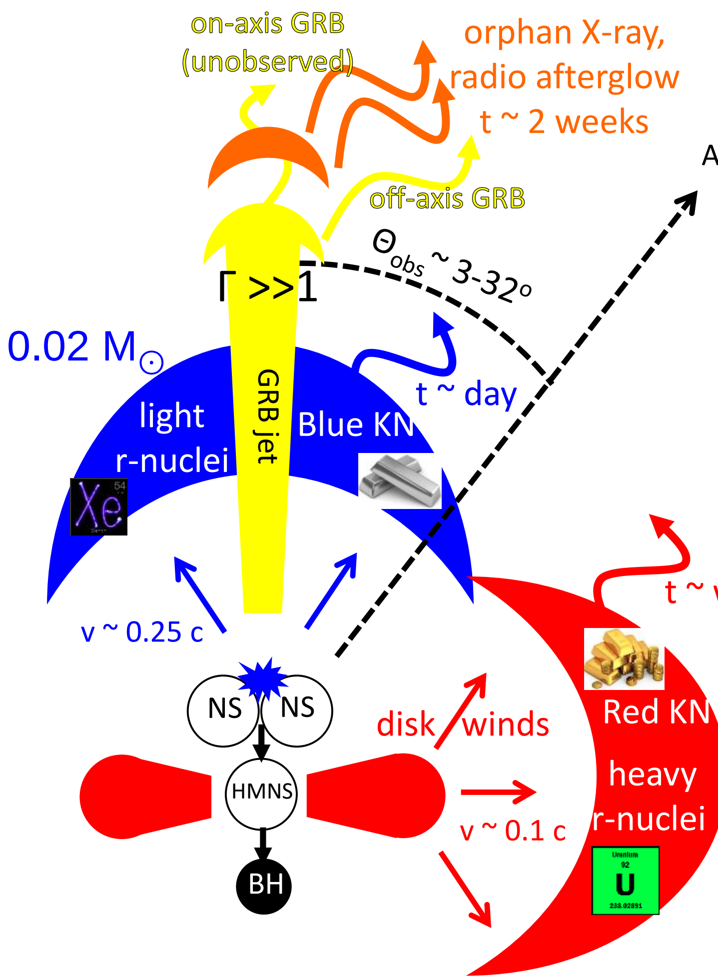

Sketch from B. Metzger

- Emission gravitational waves before merger
- Ejected material is the polar region subject to large neutrino fluxes from the neutron star. Production of light r-process nuclei and blue emission.
- Neutron star collapses to a black hole after a few 100 ms. Maximum mass NS around 2.2 solar masses.
- Neutrino emission ceases. Production heavy r-process nuclei and red emission.
- Around 0.06 solar masses of material ejected including (assuming solar proportions):
  10 Earth masses Gold
  50 Earth masses Platinum
  5 Earth masses Uranium

Nuclear fingerprints light curve

Can we identify particular nuclear signatures in the light curve?

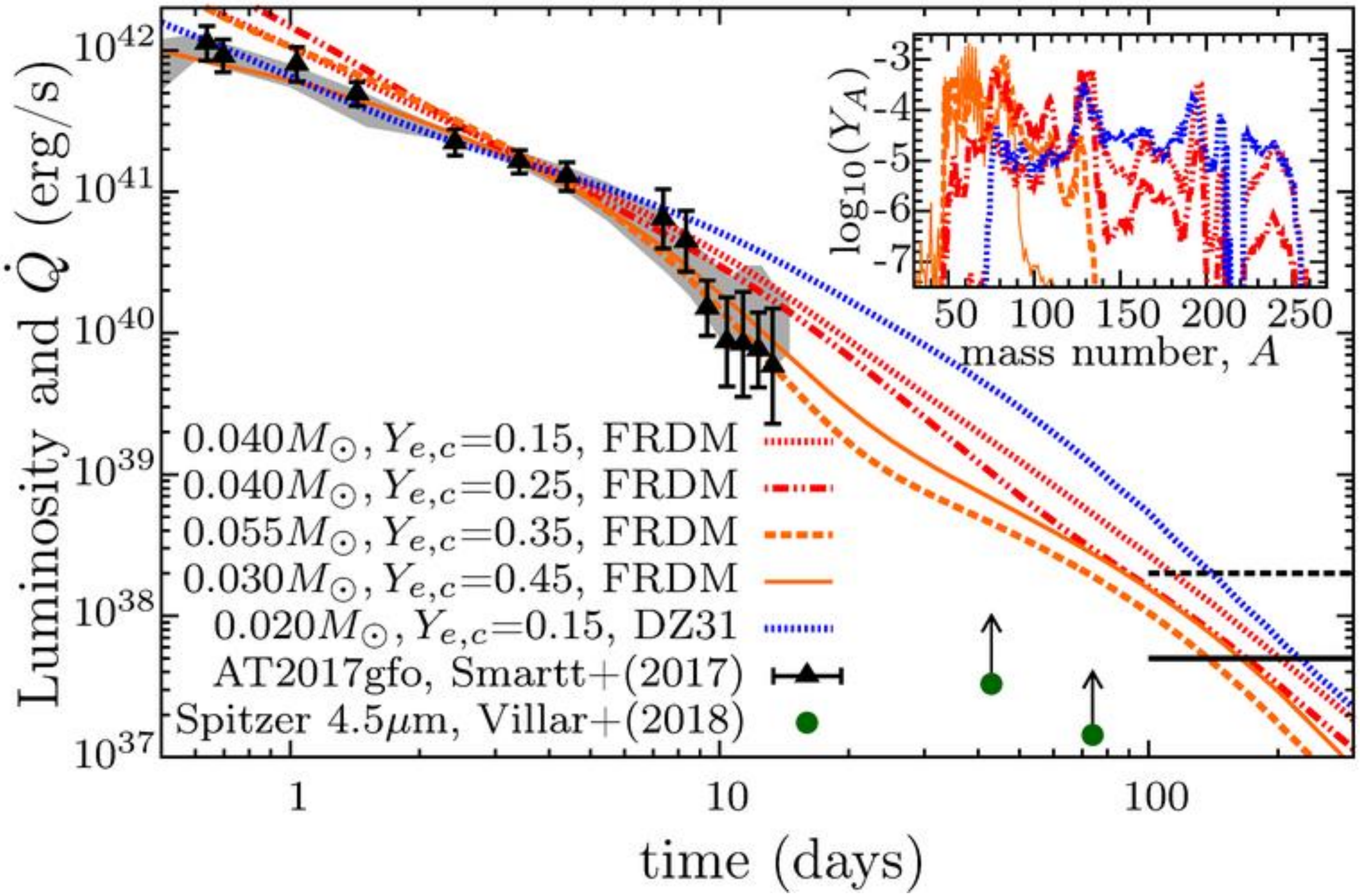

Wu, Barnes, GMP, Metzger, arXiv:1808.10459

Observations between 10 and 100 days are sensitive to composition.
Light curve becomes dominated by individual decays

Dominating decay chains

TABLE I. The decay property of r-process nuclei with half-lives $t_{1/2} = 10 - 100$ days plus selected decays discussed in the main paper (from [1]). Nuclei that are blocked by long-lived ($t_{1/2} \gg 100$ days) preceding isotopes are excluded. Q is the total energy released per decay (chain). E_α, E_e, E_γ are the total kinetic energy per decay (chain) carried by the α, $e^\pm$ and photons, respectively. For the spontaneous fission of ^{254}Cf, the kinetic energy $E_{\rm Kinetic}$ carried by the fission fragments is taken from Ref. [2]. No data is available for the neutron and photon effective energies but they are expected to be much smaller.

Isotope	Decay channel	$t_{1/2}$ (d)	Q (MeV)	E_α (MeV)	E_e (MeV)	E_γ (MeV)
^{56}Ni	EC	6.075(10)	2.133	-	-	1.721
^{56}Co	EC,β^+	77.236(26)	4.567	-	0.121	3.607
^{66}Ni	β^- to ^{66}Zn	2.2750(125)	2.893	-	1.1396	0.098
^{72}Zn	β^-	1.937(4)	0.443	-	0.080	0.152
^{72}Ga	β^-	0.587(4)	3.998	-	0.468	2.767
^{224}Ra	$\alpha\beta^-$ to ^{208}Pb	3.6319(23)	30.875	26.542	0.891	1.474
^{222}Rn	$\alpha\beta^-$ to ^{210}Pb	3.8215(2)	23.826	19.177	0.949	1.715
^{225}Ra	β^-	14.9(2)	0.356	-	0.097	0.012
^{225}Ac	$\alpha\beta^-$ to ^{209}Bi	10.0(1)	30.196	27.469	0.632	0.046
^{246}Pu	β^- to ^{246}Cm	10.84(2)	2.778	-	0.504	1.123
^{147}Nd	β^-	10.98(1)	0.895	-	0.232	0.144
^{223}Ra	$\alpha\beta^-$ to ^{207}Pb	11.43(5)	29.986	26.354	0.937	0.304
^{140}Ba	β^- to ^{140}Ce	12.7527(23)	4.807	-	0.809	2.490
^{143}Pr	β^-	13.57(2)	0.934	-	0.215	-
^{156}Eu	β^-	15.19(8)	2.452	-	0.430	1.235
^{191}Os	β^-	15.4(1)	0.314	-	0.125	0.074
^{253}Cf	β^-	17.81(8)	0.291	-	0.074	-
^{253}Es	α	20.47(3)	6.739	6.587	-	-
^{234}Th	β^- to ^{234}U	24.10(3)	2.468	-	0.860	0.016
^{233}Pa	β^-	26.975(13)	0.570	-	0.065	0.218
^{141}Ce	β^-	32.511(13)	0.583	-	0.145	0.077
^{103}Ru	β^-	39.247(3)	0.765	-	0.0638	0.497
^{255}Es	$\alpha\beta^-$ to ^{251}Cf	39.8(12)	7.529	6.968	0.175	0.021
^{181}Hf	β^-	42.39(6)	1.035	-	0.198	0.532
^{203}Hg	β^-	46.594(12)	0.492	-	0.095	0.238
^{89}Sr	β^-	50.563(25)	1.499	-	0.587	0.0
^{91}Y	β^-	58.51(6)	1.544	-	0.603	0.0
^{95}Zr	β^-	64.032(6)	1.126	-	0.117	0.733
^{95}Nb	β^-	34.991(6)	0.926	-	0.043	0.764
^{188}W	β^- to ^{188}Os	69.78(5)	2.469	-	0.878	0.061
^{185}W	β^-	75.1(3)	2.469	-	0.127	-
Isotope	Decay channel	$t_{1/2}$ (d)	Q (MeV)	$E_{\rm Kinetic}$ (MeV)	E_n (MeV)	E_γ (MeV)
^{254}Cf	Fission	60.5(2)	-	185(2)	-	-

Wu, Barnes, GMP, Metzger, arXiv:1808.10459

Main heating sources late times

Relevant α-decays

Plus fission of ^{254}Cf

Signature dominating decay chains

Isotope	Decay channel	$t_{1/2}$ (d)	Q (MeV)	E_α (MeV)	E_e (MeV)	E_γ (MeV)
^{224}Ra	$\alpha\beta^-$ to ^{208}Pb	3.6319(23)	30.875	26.542	0.891	1.474
^{222}Rn	$\alpha\beta^-$ to ^{210}Pb	3.8215(2)	23.826	19.177	0.949	1.715
^{225}Ra	β^-	14.9(2)	0.356	-	0.097	0.012
^{225}Ac	$\alpha\beta^-$ to ^{209}Bi	10.0(1)	30.196	27.469	0.632	0.046
^{223}Ra	$\alpha\beta^-$ to ^{207}Pb	11.43(5)	29.986	26.354	0.937	0.304

Isotope	Decay channel	$t_{1/2}$ (d)	Q (MeV)	E_{Kinetic} (MeV)	E_n (MeV)	E_γ (MeV)
^{254}Cf	Fission	60.5(2)	-	185(2)	-	-

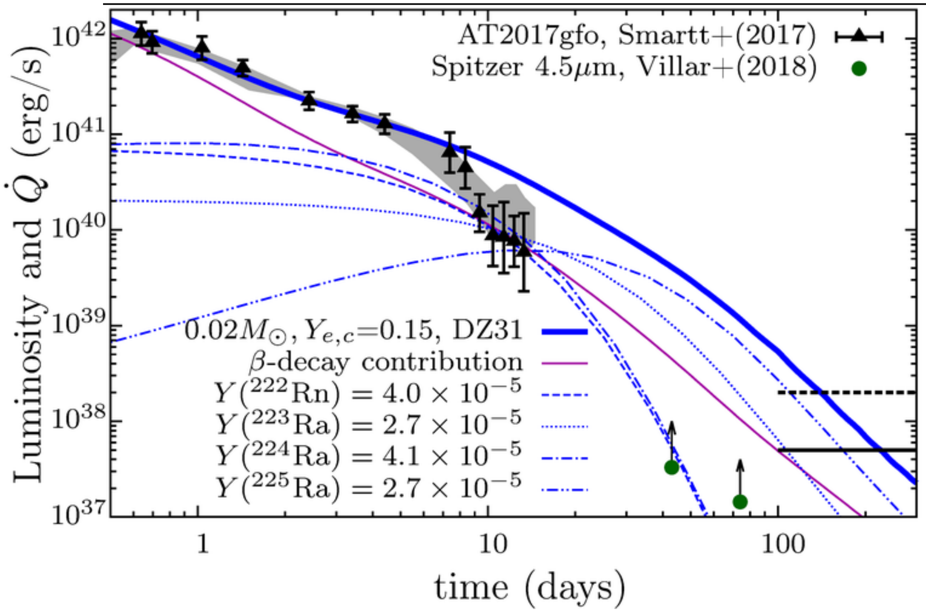

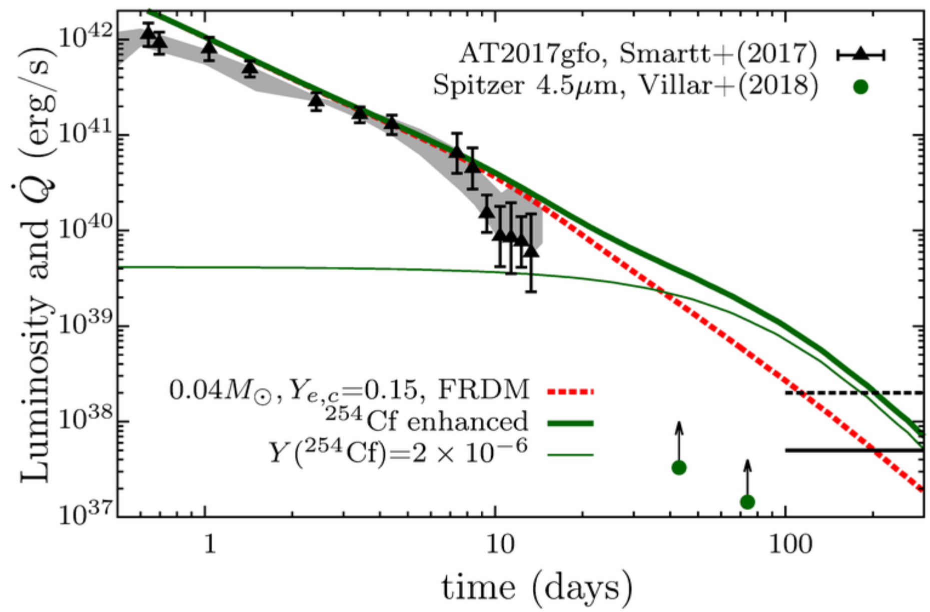

Decline observed light curve at 10 days suggest an upper limit of 0.01 $M_\odot$ of U and Th

Wu, Barnes, GMP, Metzger, arXiv:1808.10459

Sensitivity to solar abundances

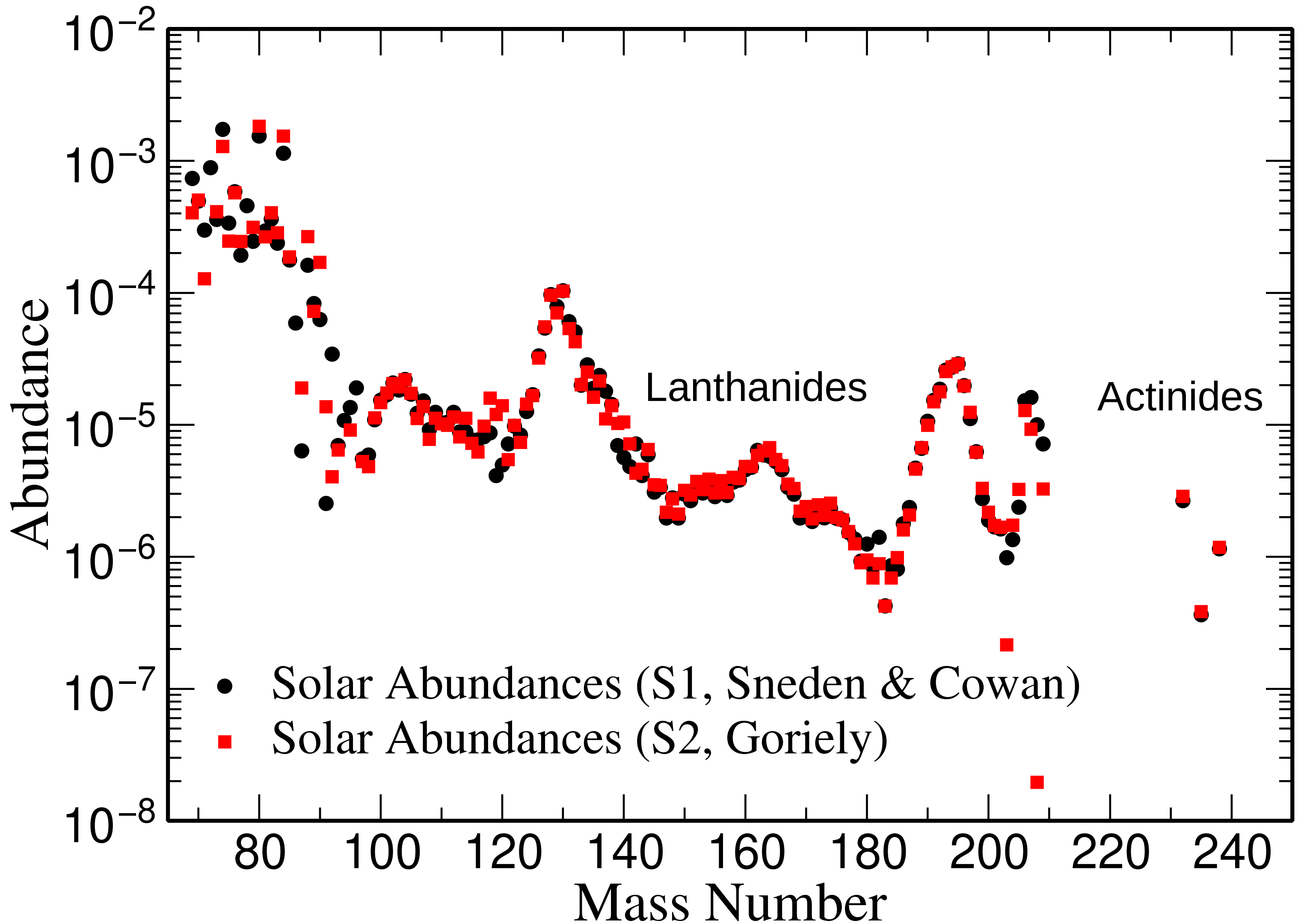

Consistency with solar r abundances

- Is the light curve consistent with the production of a Solar r-process abundance pattern?
- Large mass fraction of Lanthanides, $10^{-3} - 10^{-2}$, requires production of all r-process nuclei up to a minimum $A \sim 70$

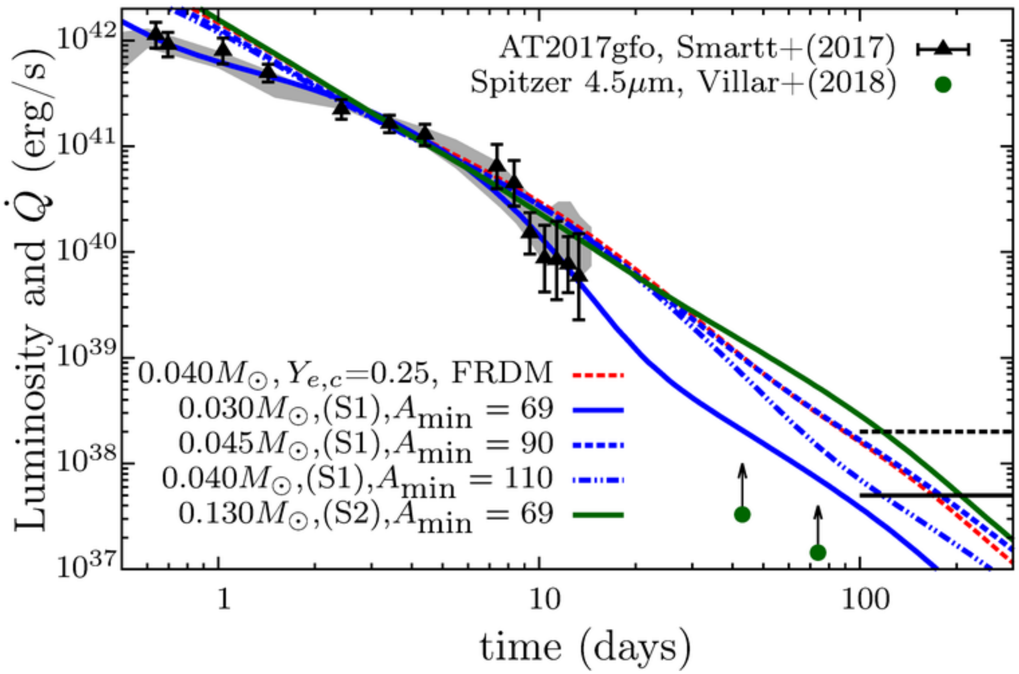

Light curve favors production all R-process nuclei down to A ~ 69

Sensitive to Solar abundance set S1 (Sneden & Cowan), S2 (Goriely)

Very different abundances of A=72 nuclei. ^{72}Zn half-life 1.92 days.

Wu, Barnes, GMP, Metzger, arXiv:1808.10459

Summary

- Kilonova from GW170817 originates from the radioactive decay of heavy elements
- Astrophysical site of the r process is identified
- Further observations necessary to confirm variability with respect to merging system and viewing angle
- Observations in time scale 10-100 days can provide signatures of individual nuclear decays
- Having identified the astrophysical site it becomes fundamental to reduce the nuclear physics uncertainties

GEFÖRDERT VOM

Bundesministerium für Bildung und Forschung

SFB 1245

DFG

Collaborators: J. Barnes (Columbia, USA), R. Fernandez (U Alberta, Canada), D. Kasen (UC Berkeley, USA), T. Marketin (U Zagreb, Croatia), B. Metzger (Columbia, USA), L. Robledo (UAM, Madrid), T. R. Rodriguez (UAM, Madrid), S. Giuliani (MSU, USA), M.-R. Wu (A Sinica, Taiwan)